



Study of different strategies of control for geostationary satellites

PROJECT REPORT

by

Angel Frutos Jurado

September 2012

Tutors: Diogo Silva Ribeiro (GMV)

Roberto Maurice Flores Le Roux (ETSEIAT)

ACKNOWLEDGEMENTS

Me gustaría agradecer a GMV la oportunidad brindada para realizar el proyecto final de carrera en el departamento de Flight Dynamics. En especial a Diogo Silva que siempre me ayudó y me hizo sentirme un ingeniero más.

Además, a nivel personal, recordar a todos los que durante 5 años han estado conmigo en los momentos difíciles.

Gracias.

Index

ACKNOWLEDGEMENTS.....	2
INDEX.....	3
List of figures.....	5
List of tables.....	7
List of diagrams.....	7
List of symbols.....	8
1. INTRODUCTION.....	9
1.1. Aim of the study.....	9
1.2. Problem statement: JUSTIFICATION.....	9
1.3. Scope of the study.....	10
1.4. Basic requirements.....	10
1.5. Code specifications.....	11
1.5.1. Inputs.....	13
1.6. BACKGROUND.....	14
1.6.1. Geostationary definition.....	14
1.6.2. Geostationary framework.....	17
1.6.3. Perturbed equations of motion.....	21
2. LONGITUDE CONTROL.....	23
2.1. Longitude requirements.....	23
2.2. Longitude considerations.....	24
2.2.1. Longitude evolution.....	24
2.2.2. Errors/Certification.....	27
2.2.3. Equilibrium points.....	28
2.3. Single manoeuvre.....	32
2.4. Symmetry control.....	34
2.4.1. Algorithm.....	37
2.4.2. Results.....	37
2.4.3. Problems to solve.....	48
2.5. Drift/Longitude strategy.....	51
2.5.1. Longitude trade off.....	52
2.5.2. Algorithm.....	55
2.5.3. Results.....	59

2.6.	Comparison/Enhancements.....	68
3.	ECCENTRICITY CONTROL.....	72
3.1.	Eccentricity requirements	72
3.2.	Eccentricity evolution.....	73
3.2.1.	Sun pressure perturbation	73
3.2.2.	Other perturbations.....	77
3.2.3.	Control circle	83
3.3.	Sun-pointing perigee.....	85
3.3.1.	Algorithm	87
3.3.2.	Results	89
3.4.	Fixed time with variations strategy	94
3.4.1.	Double manoeuvre	95
3.4.2.	Algorithm	97
3.4.3.	Results	98
4.	TRIPLE MANOEUVRES.....	104
5.	CROSS COUPLING CONTROL.....	107
5.1.	Results	109
5.2.	Final algorithm.....	111
6.	PLANNING	112
7.	TECHNICAL AND ECONOMICAL VIABILITY OF THE PROPOSAL	116
8.	LIFE CYCLE ENVIRONMENT EFFECT OF THE PROPOSAL.....	116
9.	CONCLUSIONS	117
10.	BIBLIOGRAPHY	119
10.1.	Books.....	119
10.2.	Websites.....	119
11.	ANNEXES.....	120
	ANNEX A- Table of acceleration tesseral elements.....	120

List of figures

Figure 1- focusgeo diagram.....	11
Figure 2- Relationship between the propagator and the manoeuvre algorithm ...	13
Figure 3- Deadbands.....	15
Figure 4-Classical elements	16
Figure 5- ToD representation	17
Figure 6- Free motion simulation at a stable point ($\lambda = 75.1^{\circ}E$) over several cycles	29
Figure 7- Free motion simulation at a stable point ($\lambda = 75.1^{\circ}E$) over a ten-year period	30
Figure 8- Free motion of an unstable point ($\lambda = 11.5^{\circ}W$)	31
Figure 9- Evolution of the semimajor axis vs mean longitude.....	33
Figure 10- Envelope longitude with symmetry control during one year ($\lambda = 300E$).....	38
Figure 11- Zoom on real longitude ($30^{\circ}E$) with symmetry strategy	39
Figure 12- Drift rate vs mean longitude ($\lambda = 300E$)	40
Figure 13- Thrust evolution throughout a year at $\lambda = 300E$	41
Figure 14- Longitude evolution with symmetry control ($\lambda = 75.10E$)	42
Figure 15- Drift rate vs mean longitude ($\lambda = 75.10E$).....	43
Figure 16- Thrust evolution throughout a year at $\lambda = 75.10E$	44
Figure 17- Longitude evolution vs symmetry strategy ($\lambda = 11.50W$).....	45
Figure 18- Drift rate vs mean longitude with symmetry strategy ($\lambda = 11.50W$)....	45
Figure 19- Thrust evolution throughout a year at $\lambda = 11.50W$	46
Figure 20- Thrust evolution throughout a year at $\lambda = 76.50E$	47
Figure 21- Drift rate vs mean longitude ($\lambda = 76.50E$).....	47
Figure 22- Zoom on drift rate vs mean longitude ($\lambda = 76.50E$).....	48
Figure 23- Mean longitude ($30^{\circ}E$) with symmetry strategy.....	49
Figure 24- Drift rate with a bad initial state vector.....	50
Figure 25- Longitude evolution with a bad initial state vector	51
Figure 26- Effects of increasing or reducing the first thrust.....	54
Figure 27- Envelope longitude with drift/longitude control during one year ($\lambda = 300E$).....	60
Figure 28- Drift rate vs mean longitude with longitude/drift control ($\lambda = 300E$) ...	61
Figure 29- Thrust evolution throughout a year at $\lambda = 300E$ with drift/longitude strategy	62
Figure 30- Thrust evolution throughout a year at $\lambda = 75.10E$ with drift/longitude strategy	63
Figure 31- Drift rate vs the mean longitude with longitude/drift control ($\lambda = 75.10E$).....	64
Figure 32- Zoom on drift rate vs the mean longitude with longitude/drift control ($\lambda = 75.10E$).....	64

Figure 33- Semimajor axis evolution with longitude/drift control ($\lambda = 75.10E$).....	65
Figure 34- Drift rate vs mean longitude with longitude/drift control ($\lambda = 11.50W$)	66
Figure 35- Drift rate vs mean longitude with longitude/drift control ($\lambda = 76.50E$)	67
Figure 36- Thrust evolution throughout a year at $\lambda = 76.50E$ with drift/longitude strategy	68
Figure 37- Comparison between symmetry strategy and longitude/drift strategy in longitude	69
Figure 38- Zoom on the comparison in longitude.....	69
Figure 39- Comparison between symmetry and drift/longitude strategy in drift rate with mean longitude.....	70
Figure 40- Zoom on the comparison of drift rate with mean longitude	71
Figure 41- Comparison between the thrusts of both strategies at $\lambda = 300E$	71
Figure 42 –Representation of the right ascension of the Sun, and its eccentricity perturbation	75
Figure 43-Eccentricity circles in one year varying the initial epoch.....	76
Figure 44-cpsm evolution in one year	77
Figure 45- Loops produced by the synodic period of the Moon.....	81
Figure 46-Free evolution of the Mean eccentricity in one year	82
Figure 47- Intersatellite distance between two satellites placed at same longitude	83
Figure 48- Angular separation between two satellites placed at same longitude	84
Figure 49- Pair of satellites in the intersection of their orbit planes.....	84
Figure 50- Pair of satellites 90^0 after the intersection of their orbit planes.....	85
Figure 51- Eccentricity change when the manoeuvre is tangential.....	86
Figure 52- Mean eccentricity with sun-pointing perigee strategy	90
Figure 53- Drift rate vs mean longitude with sun-pointing perigee strategy.....	91
Figure 54- Eccentricity evolution with sun pointing perigee strategy at an equilibrium point	93
Figure 55- Double manoeuvre	95
Figure 56- Eccentricity evolution with fixed time with variations strategy.....	99
Figure 57- Drift rate vs mean longitude with fixed time with variations strategy	100
Figure 58- Variation of the direction of the thrust to compensate Moon's effect	101
Figure 61- Mean eccentricity with the variation of the fixed time strategy.....	102
Figure 60- Three manoeuvres to reach the perfect point	105
Figure 61- Eccentricity vector with three manoeuvres	106
Figure 62-Zoom of the initial and final eccentricity vector.....	107
Figure 63- Interference between the thrust and the solar arrays.....	108
Figure 64- Longitude with cross-coupling effect.....	109
Figure 65- Drift rate vs mean longitude with cross-coupling effect.....	110
Figure 66- Gantt chart of the planning	114
Figure 67- Gantt chart of the reality tasks	115

List of tables

Table - 1- Initial state vector	13
Table - 2- Solution of Legendre's polynomials	26
Table - 3– List of manoeuvres with sun pointing and longitude/drift strategy ($\lambda = 300E$)	92
Table - 4– List of manoeuvres with fixed time with variations and longitude/drift strategy ($\lambda = 300E$)	103
Table - 5- Cross coupling effect	109
Table - 6- Planning	112
Table - 7- Reality tasks	113
Table - 8- Tangential acceleration due to tesseral Earth's terms.	120

List of diagrams

Diagram 1- Code scheme	12
Diagram 2- Algorithm of the strategy of symmetry control.....	36
Diagram 3- Algorithm of the strategy drift/longitude control	55
Diagram 4- Algorithm of the initialization process	57
Diagram 5- Algorithm of the drift symmetry.....	59
Diagram 6 – Algorithm of the eccentricity strategy of sun-pointing	88
Diagram 7 – Algorithm of fixed time eccentricity strategy	97
Diagram 8 – Final algorithm	111

List of symbols

a	Semimajor axis
A	Theoretical semimajor axis of a geostationary orbit
δa	Difference between a and A
e	Eccentricity
i	Inclination
λ_T	Longitude target
$\delta\lambda$	Longitude deadband
ΔV	Impulsive change of velocity
t_b	Time when the manoeuvre is applied
r	Orbital radius
ω	Argument to perigee
Ω	Right ascension of ascending node
ψ	Earth's angular velocity
s	Right ascension of the satellite
s_s	Right ascension of the Sun
s_b	Right ascension of the satellite when the manoeuvre is applied
T	Periodic time between two consecutive operations (control cycle)
δ	Declination
$D/\dot{\lambda}$	Drift rate
λ_0	Mean longitude at epoch
ν	True anomaly
c_{psm}	Cross pressure section by mass
σ	Effective cross-section to mass ratio

1. INTRODUCTION

1.1. Aim of the study

The aim of the study is to determine the required maneuvers to control geostationary satellites within a delimited **control window**. It will be done defining different strategies of control for the calculation of impulsive maneuvers to obtain optimal values which will minimize the fuel consumption and will provide an automatic control for any situation.

For each implemented strategy, an algorithm will be developed. These algorithms will be applied to some relevant longitudes in order to prove that they could be used for any longitude yielding good results.

The geostationary control will only implement in-plane maneuvers (East/West). This means that only the longitude and the radial direction will be controlled, ignoring changes in inclination.

1.2. Problem statement: JUSTIFICATION

This work has been developed for the company GMV Aerospace, and the algorithm will be implemented in **focusgeo**, a product of the **focussuite** family developed by the Flight Dynamics division.

The ancient strategies in **focussuite** did not accomplish all the desirable requirements. They produced the following problems

- The old control in the former strategy did not enforce a symmetric evolution.
- The longitude was not centered in the control window.
- The time for applying the maneuver was not optimized.

Thereby, the new code will have to address these shortcomings.

The inclination maneuvers (North/South) are considered independent from the in-plane maneuvers (East/West). The inclination maneuvers will not be studied in this study.

This study will take into account all the necessary elements to assure a good control of orbit plane components.

1.3. Scope of the study

This study pursues a new strategy of **longitude and eccentricity control**. Although the total control of a geostationary satellite includes the inclination control, this document does not include the strategies of the North/South maneuvers, because the inclination evolution will be considered independent from the other parameters. Nevertheless, in order to consider the cross-coupling perturbations that the inclination maneuver could introduce, a typical inclination maneuver will be simulated periodically.

The different strategies will be presented following the temporal order that were created, starting with the longitude and drift rate control, and following with the eccentricity control. The motivation behind the strategies will be discussed, presenting a flow diagram and a detailed explication of the code.

The actual code will not be included because it has been implemented in the GMV software **focusgeo**. Its internal structure is outlined in the block diagrams used during the description of the code. All the results presented in this report have been obtained with the newly developed software.

1.4. Basic requirements

- The station keeping strategy shall schedule the maneuvers in periodic cycles (control cycles).
- The maneuvers shall be applied at beginning of the control cycle.
- The longitude deadband ($\delta\lambda$) shall be of 0.1°
- The eccentricity evolution shall follow the control circle with a maximum of a 5% of tolerance.
- The longitude control shall be accomplished with only one burn impulse.

1.5. Code specifications

The algorithm has been coded in FORTRAN 77, using the platform Eclipse. Once the code has been compiled the new binary files are integrated into the **focussuite** framework. The figure 1 shows the diagram of the **focussuite** framework.

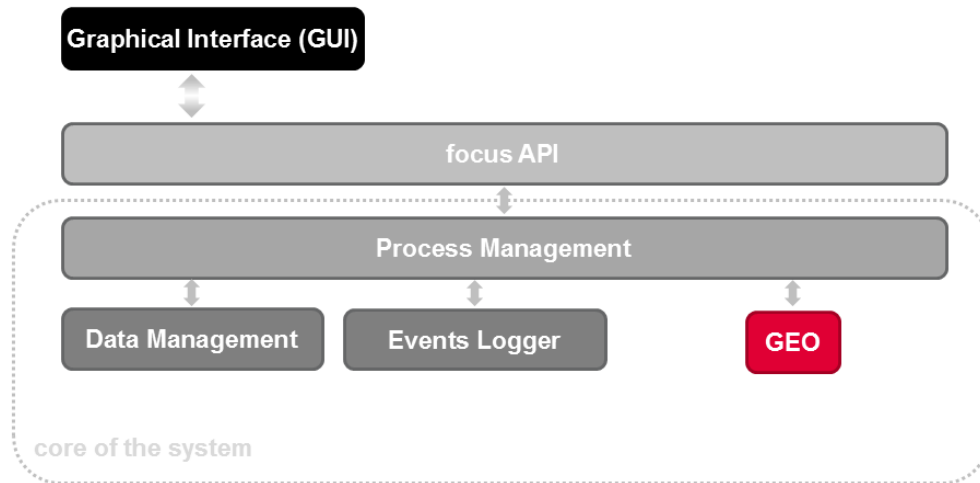


Figure 1- focusgeo diagram

The **focusgeo** client acts as the graphical interface through which the operator can modify the inputs of the different programs and control their execution. These modifications and actions are communicated to the **focusgeo** server through an application programming interface.

The **focusgeo** server is a set of three servers (process, data and events logger) that will:

- i. manage code execution and user requests (process management);
- ii. manage the data access and keep a repository of the modifications (data management);
- iii. keep track of the server events and user requests (events logger).

Each time the user requests a change to existing data or the execution of a module, the data management component locks the files susceptible of modification, and the process management spans the new process using the compiled binary to perform the computations and update the output files.

Different programs may be called sequentially in order to build an arbitrary solution strategy. The outline of the process is represented in the **diagram 1**

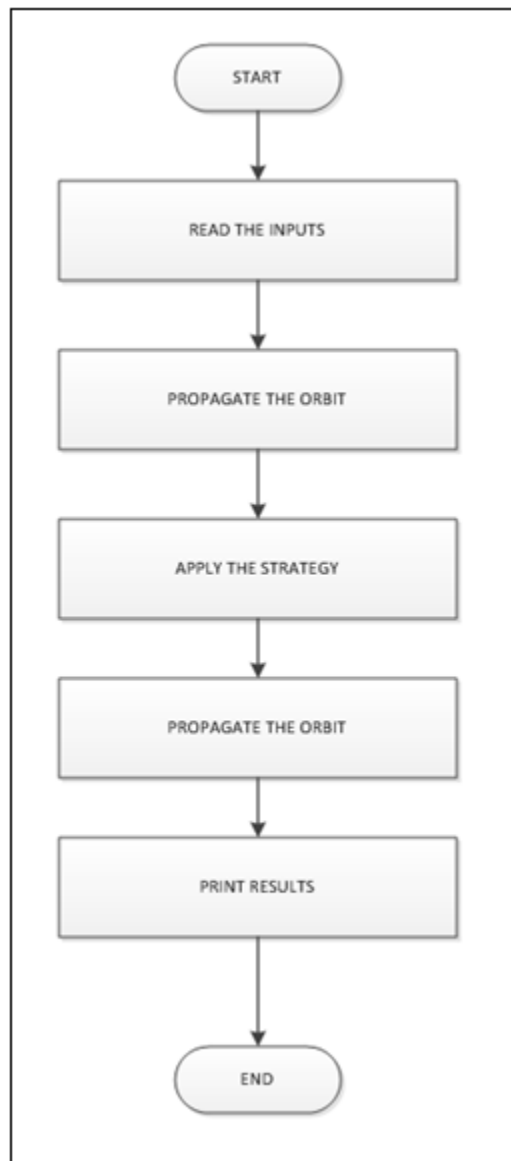


Diagram 1- Code scheme

First of all, the code must read the inputs that the Operator has chosen using the graphical interface.

Later the orbit will be propagated one cycle (T) into the future. The code scheme will run from the beginning to the end of every cycle. If the operator wants to see the strategy applied during one year, it should run the code the number of cycles necessary for that amount of time.

The propagation immediately after reading the inputs is necessary to obtain the evolution of the orbital elements across a complete cycle. The initial orbital

elements are inputs for the code. The propagation before printing the results is necessary to observe the final result.

Furthermore, within the control strategy, internal propagations are needed for the iterative solution of the problem. These are handled with additional calls to the orbit propagator.

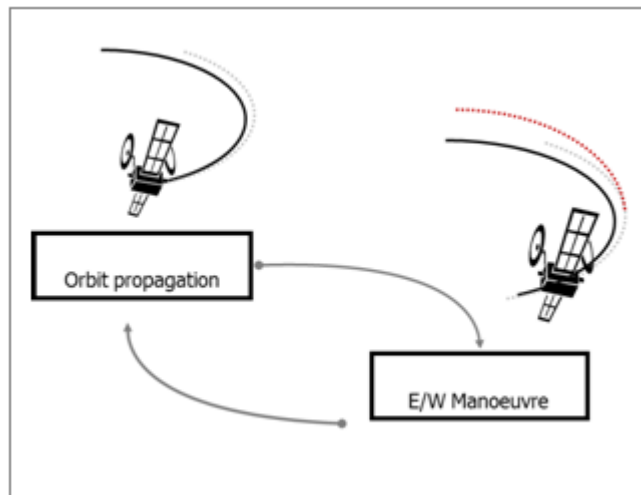


Figure 2- Relationship between the propagator and the manoeuvre algorithm

1.5.1. Inputs

To run the simulations a set of parameters belonging to a generic satellite has been chosen. The values are as follows:

- Initial epoch

The initial epoch to start all the simulations will be at epoch 2012/01/01 at 00.00.00h UTC.

- Initial state vector

a(Km)	42164.5
e	0.0002538524597
$i(^{\circ})$	0.0600019446588
$\omega(^{\circ})$	350.02955984800
$\Omega(^{\circ})$	297.02955984800
$\lambda(^{\circ})$	λ_T

Table - 1- Initial state vector

The only free parameter in the state vector is the longitude.

- Duration of the cycle of propagation.

$$T = 14 \text{ days}$$

The cycle is a constraint imposed by the operator that has the control of the station keeping. Performing the station keeping manoeuvre according to a regular schedule with a cycle of two weeks simplifies the planning of working hours for the Operator. The cycle is kept constant across the satellite lifetime. This time is adopted by current Operators because fourteen days fixes one day in a week during one year, and it is practical to know exactly which day in the week the operation should occur.

- Initial satellite mass at the initial epoch is 2000Kg
- The effective cross-section to mass ratio $\sigma = 0.01 \frac{m^2}{kg}$

1.6. BACKGROUND

1.6.1. Geostationary definition

A geostationary orbit (GEO) is a circular orbit which is placed at the equator and has the same rotation period of the Earth. Thus, a satellite placed in this orbit has a fixed position in the sky for an Earth-bound observer.

A perfectly geostationary orbit is a mathematical abstraction that could be achieved only if the Earth were perfectly symmetric with no forces acting other than Earth's gravity.

As the gravitational forces from other bodies (Sun and Moon) are small compared with Earth's attraction, it is the non-spherical nature of Earth's gravity potential which causes the main deviation from the ideal GEO.

The theoretical parameters of the geostationary can be calculated establishing a balance between the centrifugal force acting on the satellite and the gravitational attraction.

$$m\psi^2 r = \frac{m\mu}{r^2} \quad (1)$$

The Earth's rotation rate for a mean sidereal day is

$$\psi = 360.985647 \text{ deg/day} = 0.729211585 \cdot 10^{-4} \text{ rad/s}$$

Thus, the orbital radius for an ideal geostationary orbit is $r = 42164.2 \text{ Km}$

And the velocity $v_{geo} = \psi r = 3.075 \text{ Km/s}$

Because of the definition of geostationary orbit, all the orbital parameters are fixed except one. This parameter will be the **subsattellite longitude** that can be arbitrarily selected by the Operator.

In practice, a geostationary orbit can only exist instantaneously. The spacecraft will never stay at the same position in relation to the Earth, due to the asymmetry of the Earth's gravitational field and the perturbations created by other forces.

The geostationary region is defined as the region which is near to the theoretical geostationary orbit. This region is very small and placing a satellite inside it offers many advantages for communications, Earth observation, etc. For this reason, the region is split into several bands, and inside each one there is a limited deadband (zone where the spacecraft must be confined) limiting the number of satellites placed in geostationary orbit.

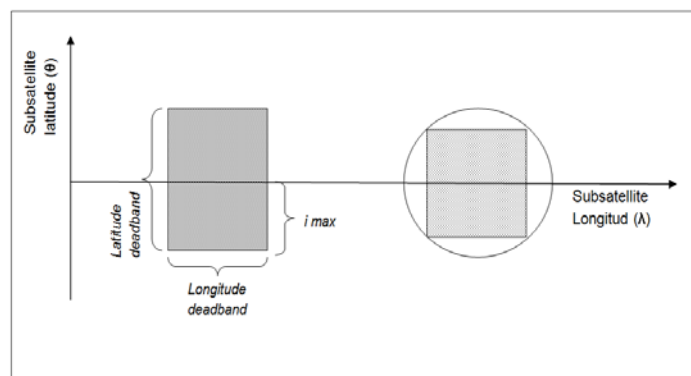


Figure 3- Deadbands.

In order to keep analysing the geostationary orbit, the classical orbital elements will be defined. They are consequence of the orbit geometry.

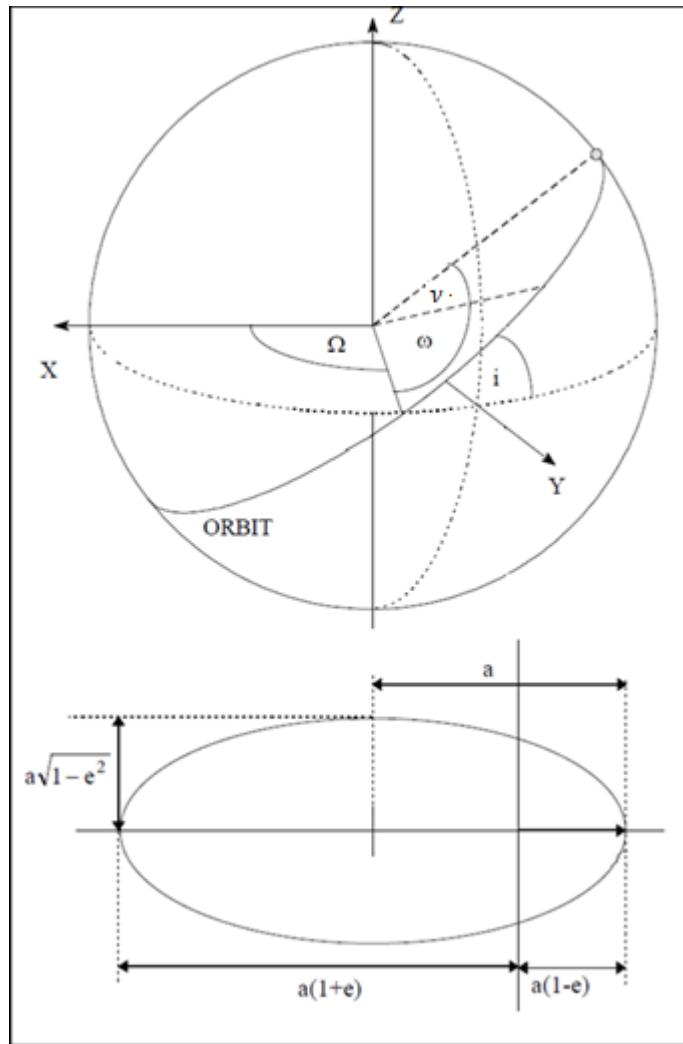


Figure 4-Classical elements

a – semimajor axis

e – Eccentricity

i – Inclination

Ω – Right ascension of the ascending node

ω – Argument of perigee

ν – True anomaly

Sometimes, the true anomaly can be replaced by the mean anomaly, $M=nt$, where n is the mean motion, $n = \frac{2\pi}{P}$ where P is the orbital period.

1.6.2. Geostationary framework

The time standard scale used is UTC (Universal Time Coordinated). UTC is uniform and continuous except when the leap-second is inserted.

The coordinate system used will be **ToD** (True of Date), a quasi-inertial reference system used for the geostationary orbits, which takes into account both precession and nutation. This system is referenced to the Modified Julian Date (MJD2000). **MJD2000** is the time measured in days from 12:00:00 UTC on January 2000.

The formula which defines the MJD2000 in UTC is

$$MJD2000 = JD - 2451544.5$$

$$JD = 367yr - INT \left\{ \frac{7 \left(yr + INT \left(\frac{mo+9}{12} \right) \right)}{4} \right\} + INT \left(\frac{275mo}{9} \right) + d + 1721013.5 + \frac{\frac{s}{60} + \frac{min}{60} + h}{24} \quad (2)$$

Where yr is the year, mo the month, d the day, min the minutes and s the seconds of the epoch.

The x-y plan is the equatorial of the Earth. The x-direction points out the Vernal Equinox(γ). The y-direction is displaced 90° following the rotation of the Earth and the z-direction is normal to the x and y-direction and directly positive.

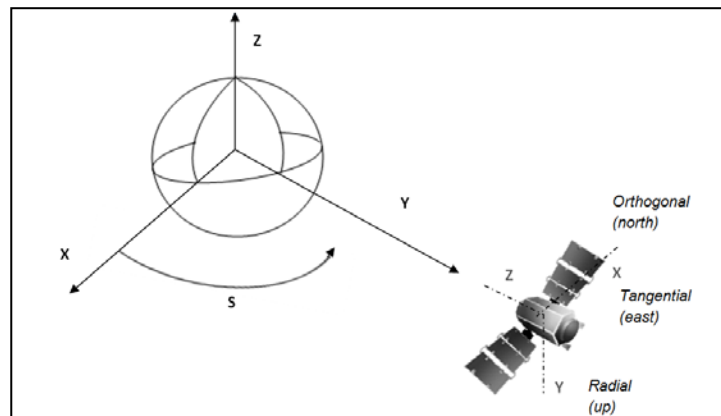


Figure 5- ToD representation

The distance from the centre of the Earth to the satellite in rectangular coordinates of the spacecraft in ToD is

$$\mathbf{r} = \begin{bmatrix} x \\ y \\ z \end{bmatrix} = \begin{bmatrix} r \cos \delta \cos s \\ r \cos \delta \sin s \\ r \sin \delta \end{bmatrix} \quad (3)$$

Where δ is the declination, s the right ascension and r the radial distance from the Earth's centre to the satellite.

The right ascension for a geostationary satellite can be expressed as

$$s = G_0 + \psi(t - t_0) + \lambda = \Omega + \omega + \nu \quad (4)$$

G_0 is the sidereal time in Greenwich for a determinate year, that is tabulated. ψ is the Earth's angular velocity. $t - t_0$ is the time elapsed since the beginning of the year under consideration, and λ is the longitude of the satellite. The longitudes are measured from the Greenwich Meridian, ranging from 0° to $+180^\circ$ (eastward) or -180° (westward). Longitudes traditionally have been written using "E" or "W" instead of "+" or "-" to indicate if they are counted following the Earth's angular velocity.

The instantaneous distance from The Earth to the satellite can be expressed as a function of the orbital elements ($a, e, i, \Omega, \omega, \nu$).

$$r = \frac{a(1-e^2)}{1+e \cos \nu} \quad (5)$$

However, the standard orbital elements are not suitable for equatorial orbits because the values of Ω, ω and ν are become undefined.

Thus, to study a perturbed geostationary orbit, a different set if parameters will be chosen. To this effect, the equations of motion will be linearized and two-dimensional vectors will be defined.

$$\mathbf{i} = (i_x, i_y) = (i \sin \Omega, -i \cos \Omega) \quad (6)$$

$$\mathbf{e} = (e_x, e_y) = (e \sin(\Omega + \omega), -e \cos(\Omega + \omega)) \quad (7)$$

Both vectors are projected in the equator plane. The vector \mathbf{i} points in the direction normal to the ascending node Ω . The vector \mathbf{e} points in the direction normal to the perigee.

Linearizing the **equation (5)**

$$r \approx a(1 - e \cos \nu) \approx A + \delta a - A e \cos \nu \quad (8)$$

Where δa is the difference between the theoretical semimajor axis (A) from the semimajor axis of the real orbit $\delta a = a - A$

The true anomaly satisfies the following differential equation

$$\frac{dv}{dt} = \frac{\sqrt{\mu a(1-e^2)}}{r^2} \quad (9)$$

And introducing **equation (8)** in **equation (9)**, yields

$$\frac{dv}{dt} = \sqrt{\frac{\mu}{a^3(1-e^2)^3}} (1 + e \cos v)^2 \quad (10)$$

Now, inserting Third Kepler's Law $\mu = \psi^2 A^3$, and linearizing the expression

$$\frac{dv}{dt} \approx \psi \left(\frac{A}{a}\right)^{\frac{3}{2}} (1 + e \cos v)^2 \approx \psi \left(1 - \frac{1.5\delta a}{A} + 2e \cos v\right) \quad (11)$$

The integration of **equation (11)** is simple and the integration constant is taken as the time of perigee passage t_p

$$v = \psi(t - t_p) \left(1 - 1.5 \frac{\delta a}{A}\right) + 2e \sin \psi(t - t_p) \quad (12)$$

Now, following the definition of the right ascension and substituting **equation (12)** in **equation (4)**

$$\lambda = s - G = \Omega + \omega + v - G_0 - \psi(t - t_0) \quad (13)$$

$$\lambda = \Omega + \omega - G_0 + \psi(t_0 - t_p) - 1.5 \frac{\delta a}{A} \psi(t - t_p) + 2e \sin \psi(t - t_p) \quad (14)$$

This new definition of the longitude contains two new parameters.

$$\lambda_0 = \Omega + \omega - G_0 + \psi(t_0 - t_p) \quad (15)$$

λ_0 is called the mean longitude at epoch.

The second parameter $(1.5 \frac{\delta a}{A} \psi)$ is the mean longitude drift rate that from now on, will be shortened as "**drift rate**". The drift rate measures the deviation between the orbital period and the rotation of the Earth.

For the particular case when no gravitational perturbations are considered, the drift rate takes the expression

$$D = \frac{d\lambda}{dt} = \dot{\lambda} = -1.5 \frac{\delta a}{A} \psi \quad (16)$$

The new set of parameters $(\lambda_0, D, e_x, e_y, i_x, i_y)$ is called the synchronous elements. The **synchronous elements** are defined as osculating elements for perturbed orbits in a manner analogous to the classical elements.

Now, the latitude, the longitude and the radius can be expressed as functions of these new parameters, linearizing the components of **equation (3)**. A full treatment is given in Soop [1].

$$\frac{x}{r} = \cos\delta \cos s \approx \cos(\Omega + \omega + \nu)$$

$$\frac{y}{r} = \cos\delta \sin s \approx \sin(\Omega + \omega + \nu)$$

$$\frac{z}{r} = \sin\delta \approx i \sin(\omega + \nu)$$

Adding the expressions of eccentricity and inclination vectors (**equation (6)** and **equation (7)**).

$$\delta = i \sin(s - \Omega) = -i_x \cos s - i_y \sin s$$

$$r = A + \delta a - A e \cos(s - \Omega - \omega) = A + \delta a - A(e_x \cos s + e_y \sin s)$$

The declination, the longitude and the radial distance yield

$$\delta = -(i_x \cos s + i_y \sin s) \quad (17)$$

$$r - A = -A \left(\frac{D}{\psi} + e_x \cos s + e_y \sin s \right) \quad (18)$$

$$\lambda = \lambda_0 + \frac{D}{\psi}(s - s_0) + 2(e_x \sin s - e_y \cos s) \quad (19)$$

The declination variation is equal to the inclination magnitude.

The **real longitude** will be longitude expressed by the equation (19), whereas the **mean longitude** will be the average of the real longitude in one sidereal day.

Now, it will be presented how these linear approximations change with the time. The following expressions give the radial, tangential and orthogonal components of the satellite velocity relative the Earth's angular velocity.

$$V_r = \frac{dr}{dt} = V(e_x \sin s - e_y \cos s) \quad (20)$$

$$V_t = A \frac{d\lambda}{dt} = V \left(\frac{D}{\psi} + 2e_x \cos s + 2e_y \sin s \right) \quad (21)$$

$$V_o = A \frac{d\theta}{dt} = V(i_x \sin s - i_y \cos s) \quad (22)$$

V_r is the radial velocity, V_t is the tangential velocity and V_o is the normal velocity relative to the geostationary orbit.

1.6.3. Perturbed equations of motion

The orbital perturbations can be classified as conservative or non-conservative forces. Conservative forces depend only on the position of the satellite; while non-conservative depend on both position and velocity.

In this report, the conservative perturbations (F) will be only considered, such as, the non-symmetry of the gravity field of the Earth, the gravity of the Sun and the Moon and the solar pressure.

At any instant, the situation of a satellite can be described by the rectangular components of position $x_i = \{x, y, z\}$ and velocity $\dot{x}_i = \{\dot{x}, \dot{y}, \dot{z}\}$. In place of these numbers, it is more useful to use the six orbit elements $\{a, e, i, M, \omega, \Omega\}$

Following the development of Kaula [7], the equations of the six elements with conservative perturbations that are known as Lagrange equations yield

$$\frac{da}{dt} = \frac{2}{na} \frac{\partial F}{\partial M} \quad (23)$$

$$\frac{de}{dt} = \frac{1-e^2}{na^2e} \frac{\partial F}{\partial M} - \frac{(1-e^2)^{\frac{1}{2}}}{na^2e} \frac{\partial F}{\partial \omega} \quad (24)$$

$$\frac{d\omega}{dt} = - \frac{\cos i}{na^2(1-e^2)^{\frac{1}{2}} \sin i} \frac{\partial F}{\partial i} + \frac{(1-e^2)^{\frac{1}{2}}}{na^2e} \frac{\partial F}{\partial e} \quad (25)$$

$$\frac{di}{dt} = \frac{\cos i}{na^2(1-e^2)^{\frac{1}{2}} \sin i} \frac{\partial F}{\partial \omega} - \frac{1}{na^2(1-e^2)^{\frac{1}{2}} \sin i} \frac{\partial F}{\partial \Omega} \quad (26)$$

$$\frac{d\Omega}{dt} = \frac{1}{na^2(1-e^2)^{\frac{1}{2}} \sin i} \frac{\partial F}{\partial i} \quad (27)$$

$$\frac{dM}{dt} = n - \frac{1-e^2}{na^2e} \frac{\partial F}{\partial e} - \frac{2}{na} \frac{\partial F}{\partial a} \quad (28)$$

However, for geostationary satellites, it is more useful the variation of the six synchronous elements. According to P.Legendre [8], the six synchronous elements yield.

$$\frac{da}{dt} = \frac{2}{na} \frac{\partial F}{\partial \lambda} \quad (29)$$

$$\frac{d\lambda}{dt} = \mathbf{n} - \dot{\mathbf{s}} - \frac{2}{na} \frac{\partial F}{\partial \mathbf{a}} \quad (30)$$

$$\frac{de_x}{dt} = -\frac{1}{na^2} \frac{\partial F}{\partial e_y} \quad (31)$$

$$\frac{de_y}{dt} = \frac{1}{na^2} \frac{\partial F}{\partial e_x} \quad (32)$$

$$\frac{di_x}{dt} = -\frac{1}{na^2} \frac{\partial F}{\partial i_y} \quad (33)$$

$$\frac{di_y}{dt} = \frac{1}{na^2} \frac{\partial F}{\partial i_x} \quad (34)$$

The drift rate is proportional to the semimajor axis, so variations in the semimajor axis will produce the same effect in the drift rate.

2. LONGITUDE CONTROL

The longitude control consists of maintaining always the real longitude the closest from the longitude target (λ_T). Because of the perturbations, the satellite will only reach instantly this longitude. The maximum longitude the satellite could reach is the longitude deadband ($\delta\lambda$).

To assure the good behaviour of the algorithm, the longitude control must accomplish the following requirements.

2.1. Longitude requirements

- The real longitude shall always be confined inside a deadband, except if a change of strategy has been accorded (longitude shift), in this case another longitude target will be the centre of the deadband, λ_T .

$$\lambda_T - \delta\lambda \leq \lambda(t) \leq \lambda_T + \delta\lambda$$

The complexity of station keeping operations increases when the deadband decreases.

- The algorithm shall predict the longitude evolution during the whole cycle.

The simplest strategy of longitude would be to wait until the day before the longitude exceeds the deadband and applying a ΔV to distance the longitude from the boundary. However, it is unsatisfactory, because the longitude is not controlled and the ΔV would not be optimized.

- The algorithm shall be compatible for all the longitudes.

Equilibrium positions and near equilibrium positions present very different characteristics in comparison with the rest of longitudes. Thereby, the objective is to create an algorithm which does not distinguish between equilibrium regions (near to the equilibrium points) and other longitudes.

- The manoeuvres and the longitude evolution shall be the most similar possible throughout the cycles.

This requirement is as a summary of the rest. If the longitude evolution were approximately the same in each control cycle during the satellite lifetime, the algorithm would be autonomous.

A general line of development in space operations is the trend to perform more and more functions on-board in automatic mode, including orbit determination and manoeuvre planning. The purpose of automation is to reduce the manual workload for current operations. Thus, when the algorithm produces similar manoeuvres, the automation is most easy and more efficient.

2.2. Longitude considerations

2.2.1. Longitude evolution

The longitude is perturbed practically only by the non-symmetry of the gravity field. Thereby, the next section will explain with details the effect of the gravitational potential.

The gravity acceleration can be expressed as function of a potential V

$$\mathbf{g} = \nabla V \quad (35)$$

The potential V must accomplish the Laplace's equation

$$\nabla^2 V = \frac{\partial^2 V}{\partial x^2} + \frac{\partial^2 V}{\partial y^2} + \frac{\partial^2 V}{\partial z^2} = 0 \quad (36)$$

Writing the Laplace's equation in **spherical coordinates** (r, λ, θ) Where r is the radial distance, λ the longitude and θ the latitude.

$$r^2 \nabla^2 V = \frac{\partial}{\partial r} \left(r^2 \frac{\partial V}{\partial r} \right) + \frac{1}{\cos \theta} \frac{\partial}{\partial \theta} \left(\cos \theta \frac{\partial V}{\partial \theta} \right) + \frac{1}{\cos^2 \theta} \frac{\partial^2 V}{\partial \lambda^2} = 0 \quad (37)$$

A possible solution for the Laplace's equation has the form

$$V = R(r) \Phi(\theta) \Lambda(\lambda) \quad (38)$$

Substituting **equation (37)** into **equation (38)**

$$\frac{1}{R} \frac{d}{dr} \left(r^2 \frac{dR}{dr} \right) + \frac{1}{\Phi \cos \theta} \frac{d}{d\theta} \left(\cos \theta \frac{d\Phi}{d\theta} \right) + \frac{1}{\Lambda \cos^2 \theta} \frac{d^2 \Lambda}{d\lambda^2} = 0 \quad (39)$$

Because the first term of **equation (39)** is the only term that is function of r , it must be constant ($l(l+1) = ct$),

$$r^2 \frac{d^2 R}{dr^2} + 2r \frac{dR}{dr} = l(l+1)R \quad (40)$$

The choice of this constant is because **equation (45)** is the Euler differential equation, and the series solution is

$$R = \sum_{n=0}^{\infty} a_n r^{n+c}$$

Then,

$$r^2 \sum_{n=0}^{\infty} (n+c)(n+c-1)a_n r^{n+c-2} + 2r \sum_{n=0}^{\infty} (n+c)a_n r^{n+c-1} - l(l+1) \sum_{n=0}^{\infty} a_n r^{n+c} = 0$$

$$\sum_{n=0}^{\infty} [(n+c)(n+c+1) - l(l+1)]a_n r^{n+c} = 0$$

This must hold true for all power of r. With n=0, r^c

$$c(c+1) = l(l+1)$$

Which is only true when $c = l, -l - 1$. And $a_n = 0$ for $n \neq l, -l - 1$. Therefore, the solution of R is given by

$$R_l(r) = A_l r^l + B_l r^{-l-1} \quad (41)$$

Where A_l and B_l are arbitrary constants.

Substituting the solution of R in **equation (39)** and multiplying by $\cos^2 \theta$

$$l(l-1) \cos^2 \theta + \frac{\cos \theta}{\Phi} \frac{d}{d\theta} \left(\cos \theta \frac{\partial \Phi}{\partial \theta} \right) + \frac{1}{\Lambda} \frac{d^2 \Lambda}{d\lambda^2} = 0$$

The last term is the only one which is function of λ , so it must be constant. Making this constant equal to $-m^2$

$$\Lambda = C_m \cos m\lambda + S_m \sin m\lambda \quad (42)$$

Where C_m and S_m are arbitrary constants.

Substituting the solution of Λ in **equation (39)** and multiplying by $\Phi / \cos^2 \theta$, the solution of the equation which yields is only function of θ

$$\frac{1}{\cos \theta} \frac{d}{d\theta} \left(\cos \theta \frac{d\Phi}{d\theta} \right) + \left(l(l+1) - \frac{m^2}{\cos^2 \theta} \right) \Phi = 0$$

Which is similar to

$$\sin \theta \frac{d}{d\theta} \left(\sin \theta \frac{d\Phi}{d\theta} \right) + (l(l+1) \sin^2 \theta - m^2) \Phi = 0 \quad (43)$$

This equation is the associated Legendre function.

Substituting $\mu = \cos \theta$ is possible to find Legendre's polynomials that are solution of Φ

$$\Phi = P_{lm}(\mu) = \frac{1}{2^l l!} (1 - \mu^2)^{\frac{m}{2}} \frac{d^{l+m}}{d\mu^{l+m}} (\mu^2 - 1)^l \quad (44)$$

In the **table 2** are written the first Legendre's polynomials

l	$P_l(\mu)$
0	1
1	μ
2	$\frac{1}{2}(3\mu^2 - 1)$
3	$\frac{1}{2}(5\mu^3 - 3\mu)$

Table - 2- Solution of Legendre's polynomials

The complete real solution of the Laplace equation, setting $A_l=0$ and $B_l=1$ is

$$V(r, \theta, \lambda) = \sum_{l=0}^{\infty} \sum_{m=0}^{\infty} \frac{1}{r^{(l+1)}} P_{lm} \cos \theta (C_{lm} \cos m\lambda + S_{lm} \sin m\lambda) \quad (45)$$

Thus, the potential of gravity yields

$$U(r, \theta, \lambda) = \frac{\mu}{r} + \mu \sum_{l=2}^L \sum_{m=0}^l \frac{R_E^l}{r^{(l+1)}} P_{lm} \sin \theta (C_{lm} \cos m\lambda + S_{lm} \sin m\lambda) \quad (46)$$

The radial force

$$F(r) = \frac{\partial U}{\partial r} = -\frac{\mu}{r^2} \sum_{n=0}^{\infty} (n+1) \left(\frac{R_E}{r}\right)^n \sum_{m=0}^n P_{nm}(\sin \phi) [C_{nm} \cos m\lambda + S_{nm} \sin m\lambda] \quad (47)$$

The three coefficients with $l=1$ (C_{10}, C_{11}, S_{11}) are zero by definition because the origin of the coordinate system is placed at the centre of mass of the Earth.

The zonal terms with $m=0$ are rotationally symmetric, so they are independent from the longitude. However, they affect the radial direction, and consequently the drift.

The sectorial terms ($|m| = l$) have no zero-lines parallel to the equator, but they have a variation in the meridional direction.

The tesseral terms ($m \neq l$) are caused by the unsymmetrical mass distribution inside the Earth. In spite of having a small value, the tangential components have a great importance in the drift evolution.

Because the tangential acceleration is dominated by the two coefficients with $l=m=2$ its longitude dependence becomes approximately sinusoidal with four nodes. Two of these are stable equilibrium points since any small longitude

deviation from the node would induce a drift back towards the node. The other nodes are unstable; the spacecraft will drift away in either direction.

When a geostationary satellite is kept by a narrow deadband of less than 1° , the tesseral acceleration can be considered constant for the mean longitude. Its tangential component ($\ddot{\lambda}$) cause a change of the semimajor axis and drift rate, which is the same effect of a weak continuous thrust. Because of the rotational symmetry, the eccentricity does not change. Thus,

$$\frac{d^2\lambda}{dt^2} = c t = \ddot{\lambda} \quad (48)$$

The tangential accelerations for every longitude slot are tabulated in the **ANNEX-A**. If the longitude is not near one of the four nodes, the mean variation of longitude as a function of time describes a parabola. The expression of this parabola comes from integration the **equation (48)**

$$\lambda(t) = \lambda_0 + \dot{\lambda}(t - t_0) + \frac{1}{2} \ddot{\lambda}(t - t_0)^2 \quad (49)$$

Where t_0 is the initial epoch.

2.2.2. Errors/Certification

The longitude control must be ready to support any adversity. The adversities could be errors in calculations, changes of strategies or any other cause. The causes of these problems mainly arise from:

- Orbit determination

There are errors due to the accuracy of the orbit determination program.

The orbit determination program is used to calculate the orbital elements and auxiliary parameters for an epoch. This program should be run regularly. In this study, this program is totally independent from the program which calculates the manoeuvres for the station keeping.

- Longitude station keeping

These are the errors associated to the expression of longitude. By analysing the free motion of the satellite, it is possible to detect the errors that will be the cause of the total longitude error.

$$\epsilon_\lambda = \epsilon_{\lambda_0} + \epsilon_D \psi(t - t_0) + 2\epsilon_e \quad (50)$$

The error ϵ_D of the drift rate stays approximately constant in time, whereas the factor $(\epsilon_D \psi(t - t_0))$ increases linearly in time.

The error ϵ_{λ_0} is a constant error in the longitude expression; however, this error can be high, because this error represents the precision of a shift longitude manoeuvre.

The error interval for the eccentricity vector can be expressed as a circle with radius ϵ_e around the measured element e_0 . The reason will be analyzed in the eccentricity strategy.

$$|e - e_0| \leq \epsilon_e \quad (51)$$

Both \bar{e}_0 and ϵ_e are constant in time.

- Real manoeuvres

The manoeuvre must have an excellent precision. Normally, the manoeuvres are of the order from 0.5 to 0.001m/s, so small changes in the impulse produce large changes in the drift rate.

If the thrust error is such that the window control is left, the manoeuvre must be performed with a corrective thrust to slow down the drift. The thrust error influences more the drift rate than the other parameters.

- Iteration thresholds

The manoeuvres are calculated with an iterative process. The thresholds limit the accuracy of the solution, but it is necessary to pay attention because a tiny threshold could prevent the iteration from converging. Normally, the value of the thresholds will be chosen based on experience.

2.2.3. Equilibrium points

According to the perturbations caused by the tesseral elements, there are four longitudes where the tangential acceleration disappears. Two are stable and two unstable.

Stable = **75.1° E** and **105.3° W**

Unstable = **11.5°W** and **161.9° E**

Station keeping at these longitudes should have a drift rate equal to zero, but because of the Moon and the Sun, there are small perturbations which result in the longitude going outside of the deadband.

In these cases, the longitude drifts slowly. As shown in the **figure 6** where the longitude at $\lambda = 75.1^{\circ}E$ drifts free.

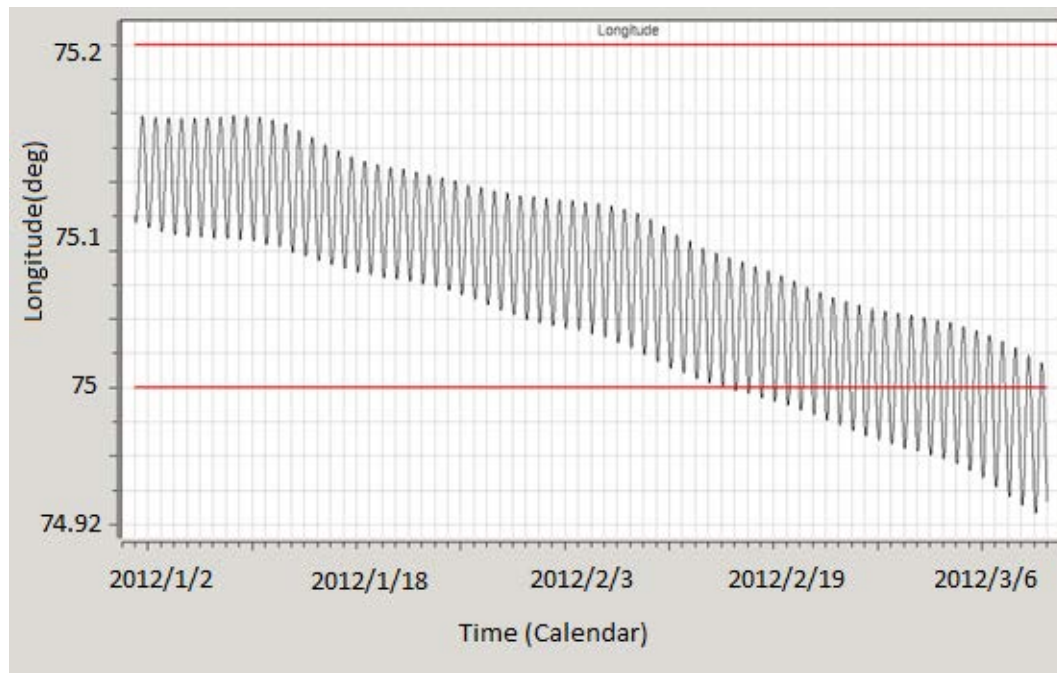


Figure 6- Free motion simulation at a stable point ($\lambda = 75.1^{\circ}E$) over several cycles

In this equilibrium stable point is necessary to wait until 2012/02/12 (3 control cycles) to have the longitude out the deadband. The drift rate is extremely small and it is really different from the rest of longitudes because the other perturbations (Moon, Sun, etc.) are higher than the perturbations produced by the tesseral terms.

Near these longitudes, the situation is similar because the drift rate is small in comparison with any other longitude. Thus, the treatment of the equilibrium points will be applied for all the regions where the drift rate is very small, they will be called equilibrium regions.

The free drift motion of the mean longitude around a **stable point** is that of a harmonic oscillator with a period of more than two years and no damping, always that the initial drift rate is zero.

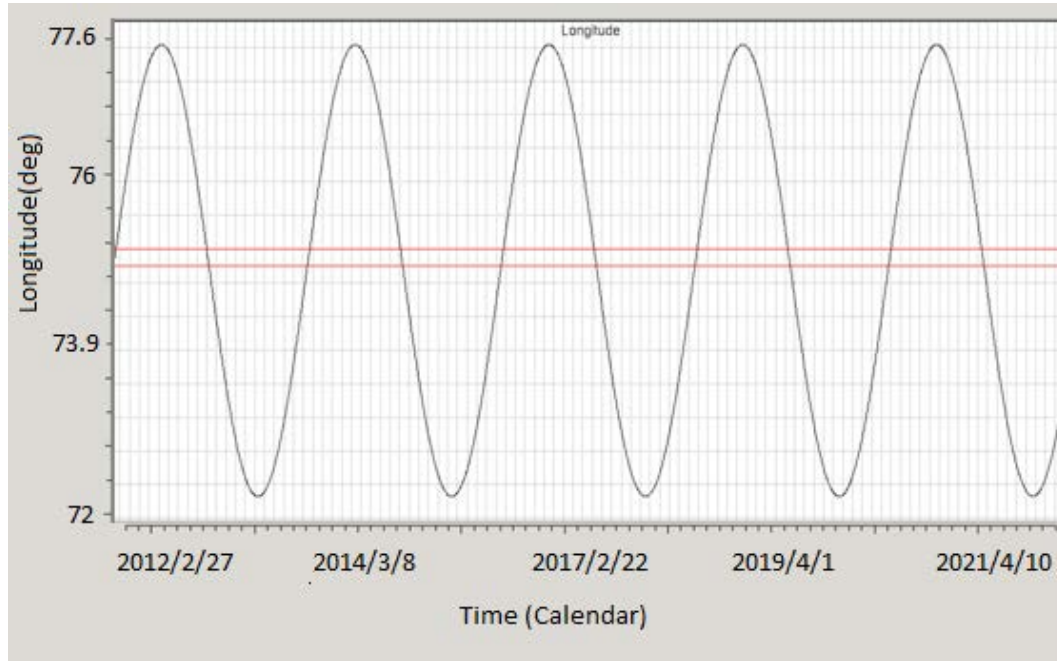


Figure 7- Free motion simulation at a stable point ($\lambda = 75.1^{\circ}\text{E}$) over a ten-year period

The simulation of the free motion at a stable point could be represented as a sinusoidal function, with a period of two year. Normally, the errors produced by the thrusts of the station keeping are the main problem to correct the orbit.

The task of station keeping for an **unstable point** is similar to that of balancing a ball on the top of a hill, without any friction. The acceleration of the mean longitude in the vicinity of an equilibrium point (λ_0) can be approximated by a linear function in λ with the proportionality constant (p^2)

$$\frac{d^2\lambda}{dt^2} = p^2(\lambda - \lambda_0) \quad (52)$$

The differential **equation (52)** has two partial solutions, one convergent and one divergent.

The convergent solution

$$\lambda = \lambda_0 + C_1 e^{-pt} \quad (53)$$

$$\dot{\lambda} = -p(\lambda - \lambda_0) \quad (54)$$

The divergent solution

$$\lambda = \lambda_0 + C_2 e^{+kt} \quad (55)$$

$$\dot{\lambda} = p(\lambda - \lambda_0) \quad (56)$$

Whatever the starting conditions are, the longitude evolution will be dominated by the divergent solution. Longitude station keeping can be described as manoeuvring the mean longitude to the convergent solution, but a small error will bring it back again to the divergent solution.

The **figure 8** shows the free evolution of the mean longitude around a divergent point 11.5°W with the drift rate.

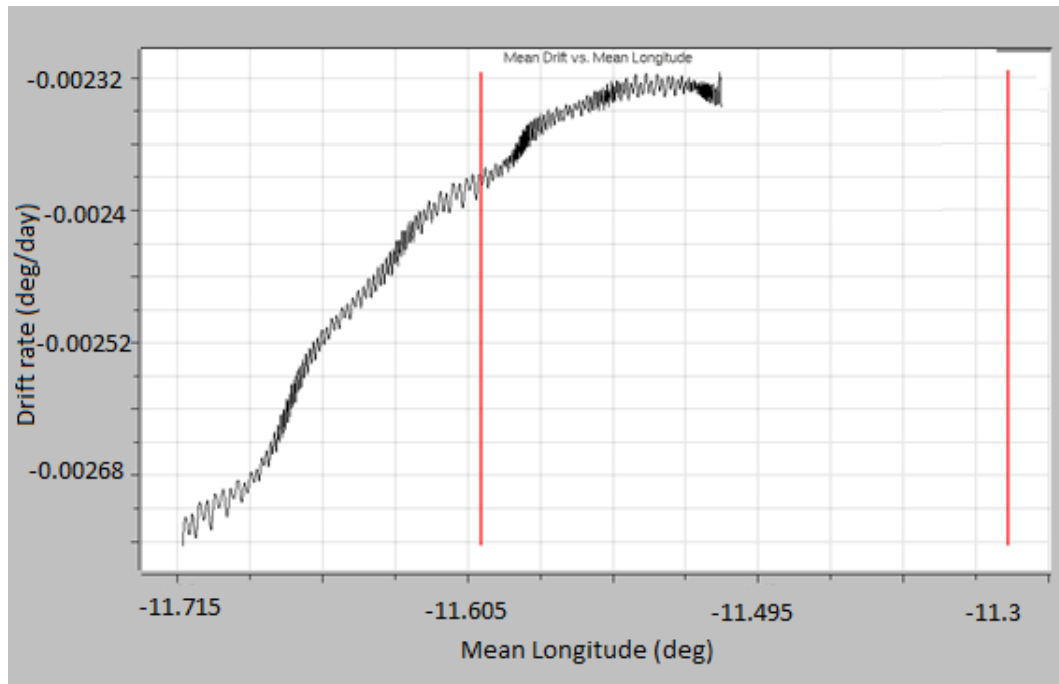


Figure 8- Free motion of an unstable point ($\lambda = 11.5^{\circ}\text{W}$)

In both cases, (stable and unstable points) the drift rate near the points is almost zero. For this reason they will be considered as being similar, because the control cycle is fourteen days, during which the drift rate has not evolved appreciably.

Thus, station keeping at an equilibrium region always needs active manoeuvring, although the fuel needed to correct it was very small.

2.3. Single manoeuvre

As mentioned in the requirements, for the longitude control, only one manoeuvre will be considered. An East/West thrust or a tangential manoeuvre changes the longitude, the drift rate and the eccentricity vector (e_x, e_y) .

A single tangential thrust can be considered as an instantaneous impulse that changes instantaneously the flight velocity of the satellite, but not its position. The new orbit will keep the original height at this point and the perigee will be located there.

The fact that the instantaneous spacecraft position does not change at the instant of the impulsive thrust imposes the following conditions on the change in the synchronous elements. According to **equations (18)** and **(19)**

$$\Delta \mathbf{r} = \mathbf{0} = -A \left(\frac{\Delta D}{1.5} + \Delta e_x \cos s_b + \Delta e_y \sin s_b \right) \quad (57)$$

$$\Delta \lambda = \mathbf{0} = \Delta \lambda_0 + \Delta D (s_b - s_0) + 2(\Delta e_x \sin s_b - \Delta e_y \cos s_b) \quad (58)$$

Being s_0 the initial right ascension of the satellite, and s_b the right ascension of the satellite when the manoeuvre will be applied.

And adding the change in the spacecraft velocity from the **equation (20)** and the **equation (21)**

$$\Delta V_r = V(\Delta e_x \sin s_b - \Delta e_y \cos s_b) \quad (59)$$

$$\Delta V_t = V(\Delta D + 2\Delta e_x \cos s_b + 2\Delta e_y \sin s_b) \quad (60)$$

There are four linear equations and four parameters. This a linear system where the exact solutions are

$$\Delta \lambda_0 = \frac{3\Delta V}{V} (s_b - s_0) \quad (61)$$

$$\Delta D = -\frac{3\Delta V}{V} \quad (62)$$

$$\Delta e_x = \frac{2\Delta V}{V} \cos s_b \quad (63)$$

$$\Delta e_y = \frac{2\Delta V}{V} \sin s_b \quad (64)$$

The change $\Delta \lambda_0$ is only a mathematical result of extrapolating the new drift rate back to the original epoch. The expression for the change of the semimajor axis becomes

$$\Delta a = -\frac{2A}{3} \Delta D = \frac{2}{\psi} \Delta V \quad (65)$$

The drift rate changes in the opposite direction of the direction of the manoeuvre. An east thrust gives a west drift and a west thrust gives an east drift. This happens because, although an east thrust first increases the flight velocity and causes a short initial east move, the main effect is to raise the semimajor axis of the orbit. This increases the orbital period so the orbital velocity decreases, with a west drift as consequence.

For instance, a drift rate of 0.1°/sec gives a $\Delta V = 1.788875 \text{ m/s}$.

Following the linearized **equations (18)** and **(19)**, for a manoeuvre at time t_b , the radius and longitude variations are

$$\Delta r = \frac{2\Delta V}{\psi} [1 - \cos((t - t_b)\psi)] \quad (66)$$

$$\Delta \lambda = \frac{\Delta V}{V} [4 \sin((t - t_b)\psi) - 3((t - t_b)\psi)] \quad (67)$$

The longitude does not change instantaneously but changes in time as a result of the new drift rate.

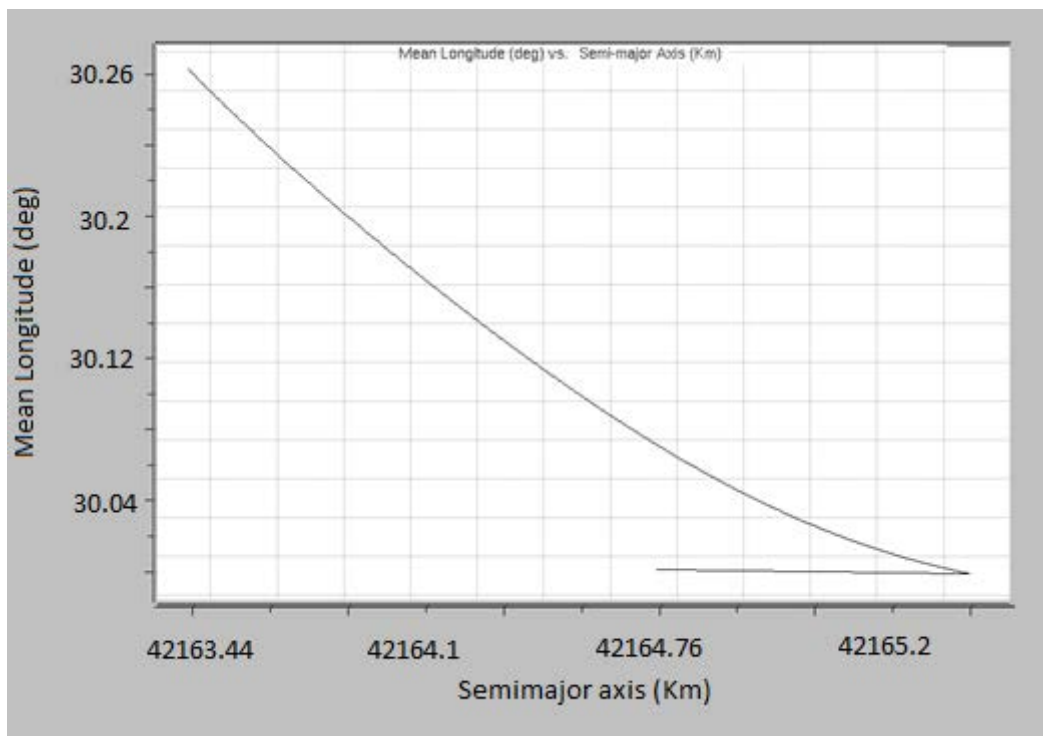


Figure 9- Evolution of the semimajor axis vs mean longitude

This figure shows the position in the radial direction with the longitude. The displacement along-track ($A\Delta\lambda$) goes from $A\lambda_1 = 42164.5 \cdot 30 \cdot \frac{\pi}{180} = 22077.28 \text{ Km}$ to

$A\lambda_2 = 42164.5 \cdot 30.28 \cdot \frac{\pi}{180} = 22283.34 \text{ Km}$, the difference $A\Delta\lambda = 206.055 \text{ Km}$ is really high in comparison with the displacement in the radial direction $\Delta r = 1.76 \text{ Km}$. This high sensitivity of the along-track position for a given ΔV compared to the radial position must be taken into account when assessing the effect of manoeuvres uncertainties.

2.4. Symmetry control

The symmetry control consists of giving the necessary ΔV to produce a symmetric parabola in one cycle of the mean longitude, in such a way that the difference between the maximum and the deadband is equal to the difference between the minimum and the deadband. The manoeuvres are applied at the maximum or at the minimum of the longitude evolution, in the interval of time between the initial time (t_0) and the end of the control cycle ($t_0 + T$)

$$\lambda_T - \min_{t_0 \leq t \leq t_0 + T} \lambda(t) = \max_{t_0 \leq t \leq t_0 + T} \lambda(t) - \lambda_T = W$$

This difference (W) is called the symmetry parameter.

The following conditions are valid when the parabola is positive (negative drift rate), whereas a negative value is dealt within an analogous way by swapping east and west and changing the signs. Following this assumption, the conditions to fulfil the symmetry in one cycle must be

$\lambda(t_0) = \lambda_T + W$ Start the cycle with the longitude near the east boundary

$\dot{\lambda}(t_0) = \dot{\lambda}_0$ Initial drift rate

$\lambda(t_0 + T/2) = \lambda_T - W$ Arrive to the value of the symmetry parameter

$\dot{\lambda}(t_0 + T/2) = 0$ Natural drift reversal at the west boundary.

The longitude centre of the deadband is the longitude target, the manoeuvre will be applied analysing the real longitude, not the mean longitude. Actually, this is the real longitude, so controlling the real longitude; the longitude will be always inside the deadband.

The objective is to obtain an expression which determines the necessary ΔV to get the conditions of symmetry.

$g(t)$ is an auxiliary function that represents the rate between the difference of longitudes with the manoeuvre of the **equation (68)**

$$g(t) = \frac{\Delta\lambda}{\Delta V} = \frac{3}{A} (t - t_b) - \frac{4}{V} \sin(\psi(t - t_b)) \quad (68)$$

The necessary thrusts to get symmetry in the maximum and in the minimum of the longitude are

$$U_A = \min_{t_0 \leq t \leq t_0 + T} \frac{\lambda(t) - \lambda_T + W}{g(t_A)} \quad (69)$$

$$U_B = \max_{t_0 \leq t \leq t_0 + T} \frac{\lambda(t) - \lambda_T - W}{g(t_B)} \quad (70)$$

The subscripts A and B represent the minimum and the maximum respectively.

In order to reach both maximum and minimum longitude separated by the parameter W , an iterative expression must be found.

In order to approach this symmetry during the iteration W_{n+1} is solved during the same step by requiring

$$\Delta V_{n+1} - \Delta V_n = \frac{\lambda(t_A) - \lambda_T + W_{n+1}}{g_n(t_A)} = \frac{\lambda(t_B) - \lambda_T - W_{n+1}}{g_n(t_B)}$$

The orbit is calculated by the propagator to the end of the control cycle with the manoeuvres from the latest iteration.

This leads to the following formula for each iteration step, using the accurate numerical integration of Soop [1]

$$\Delta V_{n+1} = \Delta V_n + \frac{g_n(t_A)U_{nA} + g_n(t_B)U_{nB}}{g_n(t_A) + g_n(t_B)} \quad (71)$$

$$W_{n+1} = W_n + \frac{(U_{nB} - U_{nA})g_n(t_A)g_n(t_B)}{g_n(t_A) + g_n(t_B)} \quad (72)$$

This process requires propagating the orbit every iteration in order to obtain the maximum and the minimum longitude updated. Normally, in a few iterations the solution converges.

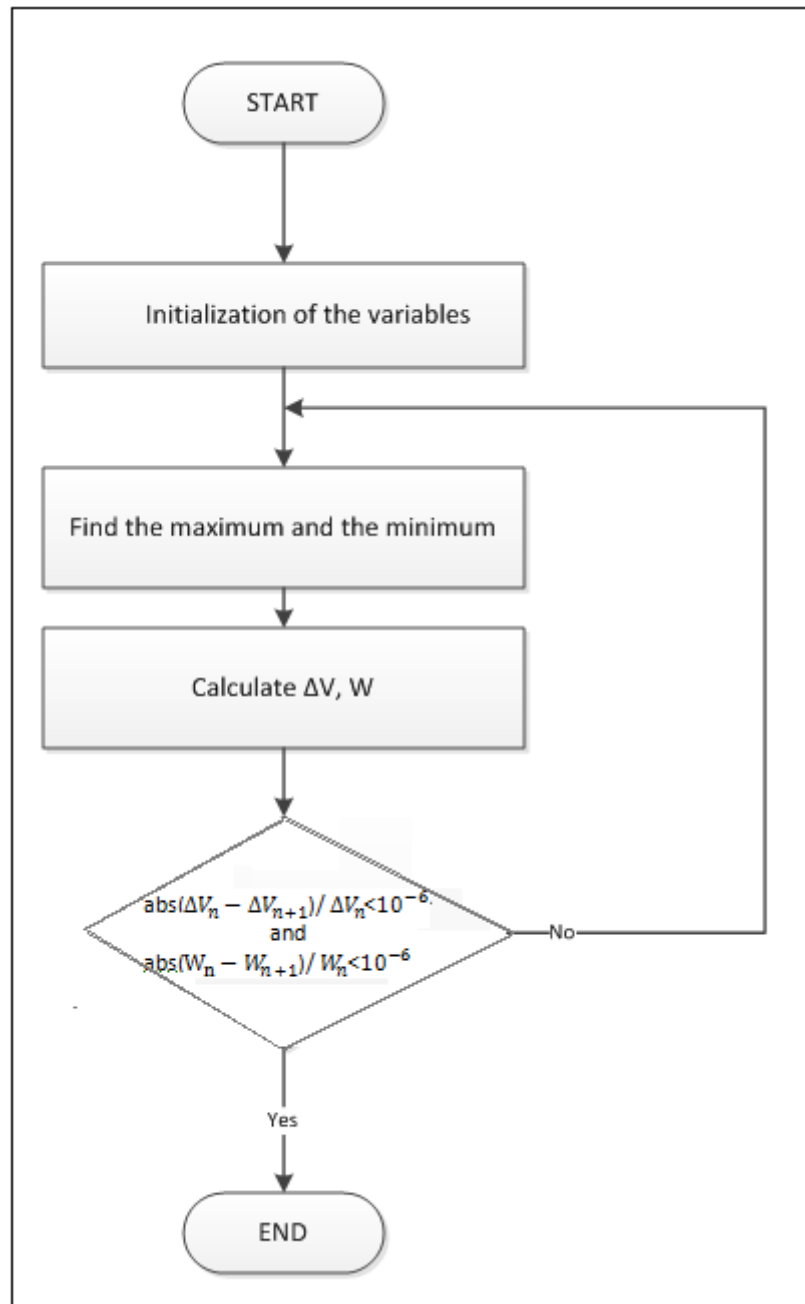


Diagram 2- Algorithm of the strategy of symmetry control

2.4.1. Algorithm

- Initialization of variables.

At the start of the first iteration the initial values are $W_0 = \frac{\delta\lambda}{4}$ and ΔV_0 the necessary because the longitude arrives to the boundary of the control window, $\delta\lambda$ (just the first step of the first control cycle), later these values will be these of the ancient control cycle.

- Find the maximum and the minimum

This function searches the maximum and the minimum real longitude and the time when the maximum and the minimum are obtained.

This function is called every time that a new ΔV is obtained, because each time the ΔV changes, the maximum and the minimum will be different, and so will be the times when the maximum and the minimum are placed.

- Calculation of the ΔV and W

Following the expressions calculated above, **equations (71)** and **(72)**, both ΔV and W will not be considered accurate enough unless the following criteria are met

$$\epsilon_r(\Delta V) = \frac{(\Delta V_{n+1} - \Delta V_n)}{\Delta V_n} < 10^{-6} \quad (73)$$

$$\epsilon_r(W) = \frac{(W_{n+1} - W_n)}{W_n} < 10^{-6} \quad (74)$$

These values have been chosen because are the minimum tolerance that can be tolerated by the computer process.

2.4.2. Results

As explained before, the only free parameters that the Operator could choose in a geostationary satellite are the longitudes and its respective deadbands. The others will be consequence of the strategy to follow and they will depend on the initial conditions.

The algorithm works for all the range of longitudes, but for obvious reasons, it is impossible to show the solutions in all the longitudes. The simulations will be done showing the most representative cases.

The longitudes chosen are: a typical longitude ($\lambda = 30^\circ\text{E}$), a stable equilibrium point ($\lambda = 75.1^\circ\text{E}$), an unstable equilibrium point ($\lambda = 11.5^\circ\text{W}$), and a longitude near to the stable equilibrium point ($\lambda = 76.5^\circ\text{E}$).

All the simulations will start with the specified inputs from the **section 1.6.1** where $\lambda_0 = \lambda_T$

Actually, the only requirement to choose adequate initial values is that they must be close to the real geostationary orbit ($e=0$; $i=0$; $a=42164.5\text{Km}$)

2.4.2.1. Longitude 30° E

The plot of the real longitude throughout one year is aliased. Because to have a good representation, the sample must be each half hour, and the resolution of the format does not allow so much precision. However, the envelope longitude will be presented, showing where the maximum and minimum longitudes are.

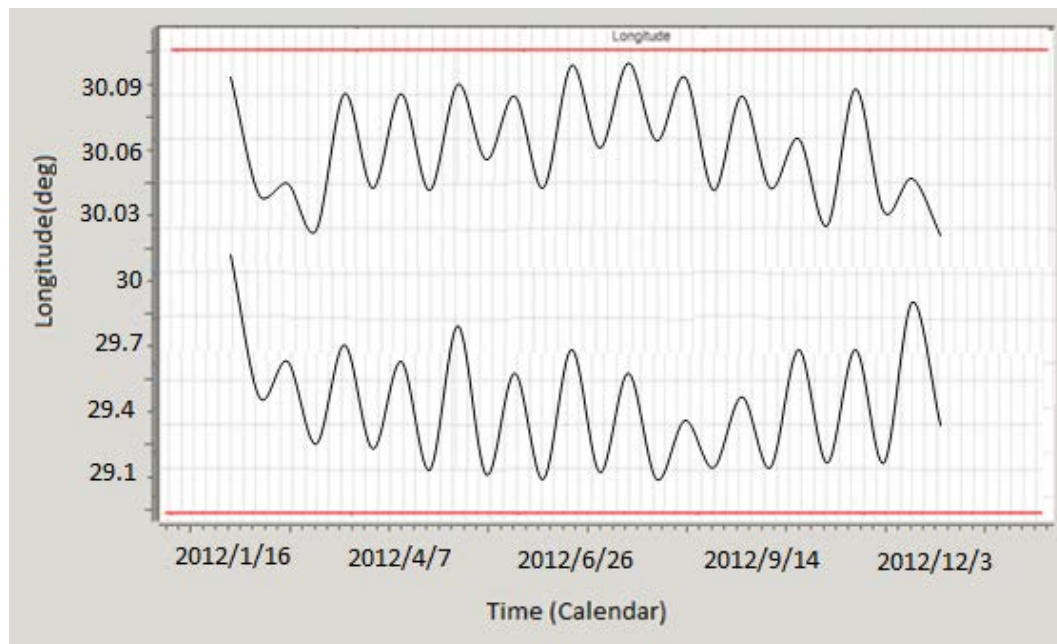


Figure 10- Envelope longitude with symmetry control during one year ($\lambda = 30^\circ\text{E}$)

The first observation is that the real longitude is inside the deadband, so the main objective is accomplished. However, throughout the year the maximum and the minimum do not have similar values, this is due to the eccentricity, but also to the mean longitude.

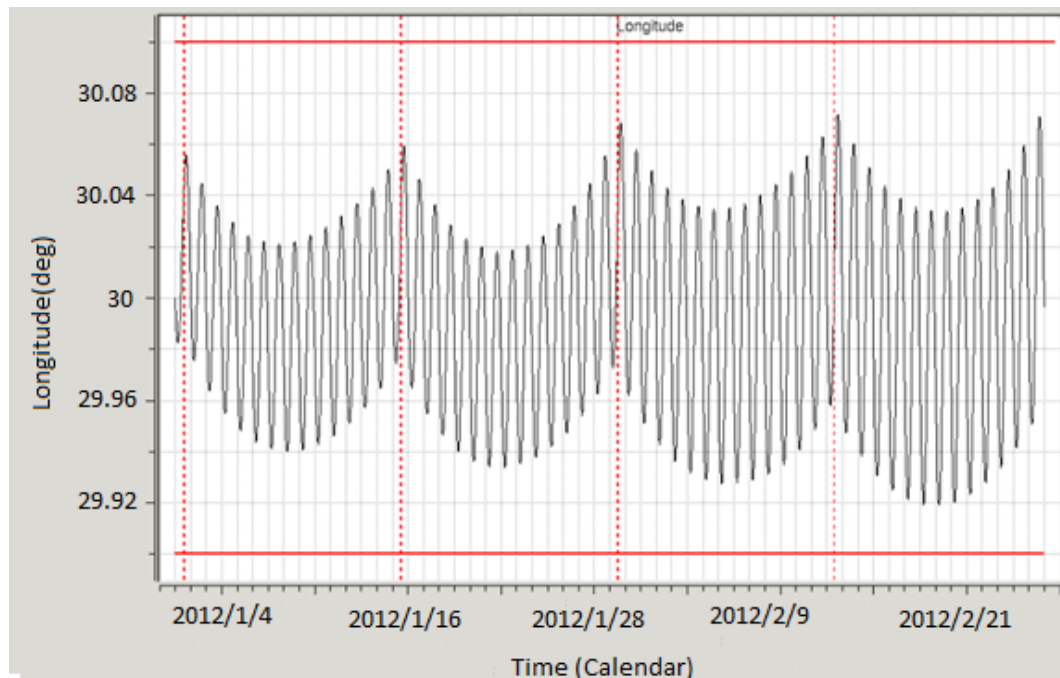


Figure 11- Zoom on real longitude (30⁰E) with symmetry strategy

The **figure 11** shows the symmetry strategy of the real longitude in four control cycles. The minimum is always near the middle of the control cycles and the maximum can be at the beginning or at the end of the cycle, according to the eccentricity evolution.

Although the objective is to control the mean longitude and assure that the real longitude is inside the control window, the maximum and minimum (time or longitude) found in every control cycle belong to the real longitude, and tge manoeuvres are applied to the real longitude, so the mean longitude is not entirely controlled.

This effect means that the longitude evolution in one control cycle will not be centred, so if an unexpected error could produce the satellite would move outside the control window.

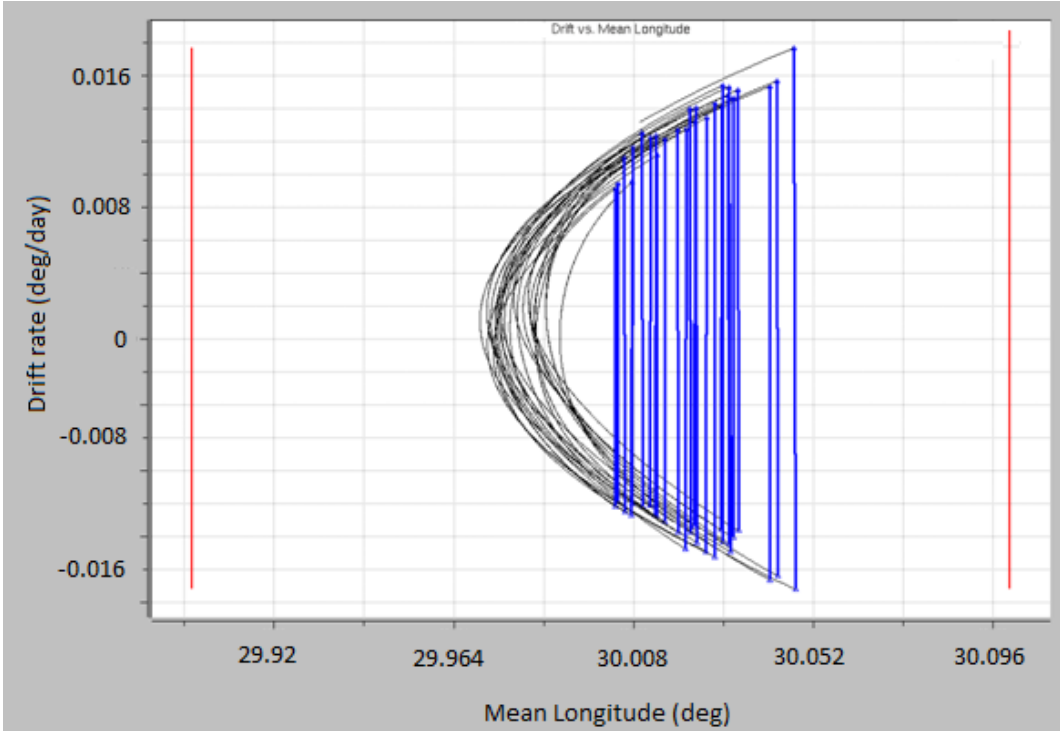


Figure 12- Drift rate vs mean longitude ($\lambda = 30^{\circ}E$)

Actually, the symmetry is not perfect because the eccentricity changes with the time. An eccentricity strategy will be necessary to control the longitude.

Figure 13 shows the thrust evolution throughout a year.

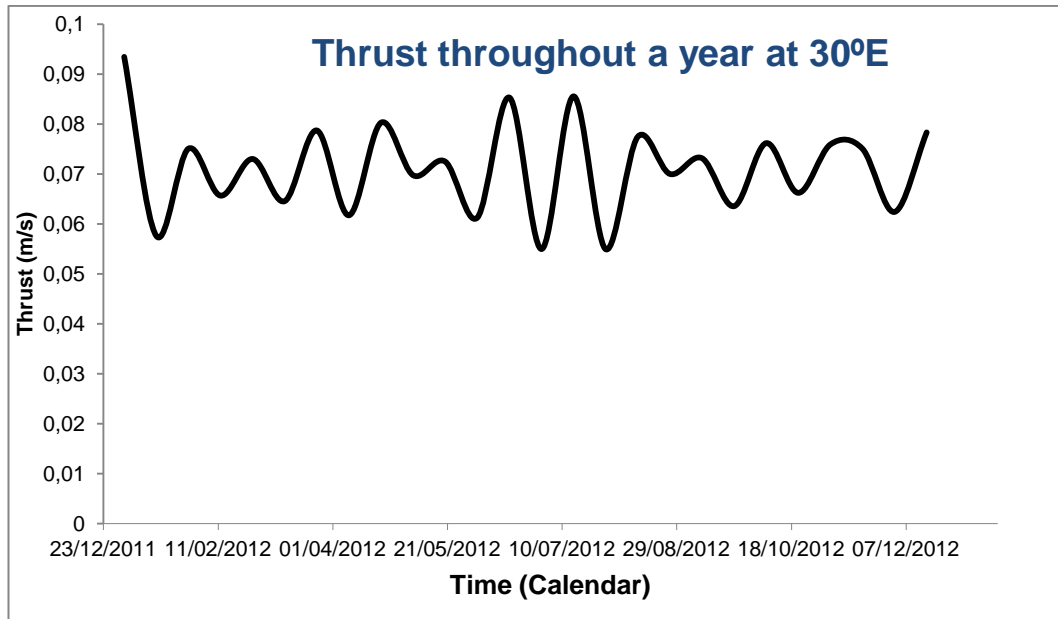


Figure 13- Thrust evolution throughout a year at $\lambda = 30^{\circ}E$

The ΔV do not have the same size, and there is no obvious tendency for one value. For this reason, the drift evolution will be different every cycle.

In the course of one year, it will be impossible to control the longitude and the drift with only one manoeuvre; because a change of ΔV has implicit a change of drift rate, and consequently, the next real longitude cycle will be different from the previous one.

2.4.2.2. Longitude 75.1°E

This is an equilibrium stable point. The strategy will try to ensure that the real longitude is symmetric, like in the longitude of 30°E. However, it is not possible because the drift rate is so small that having a control cycle fixed of 14 days, the longitude cannot evolve enough to have symmetry.

As mentioned before, the real longitude evolution in one year does not give important information; with a few of control cycles is enough to understand what happens with the stable equilibrium point.

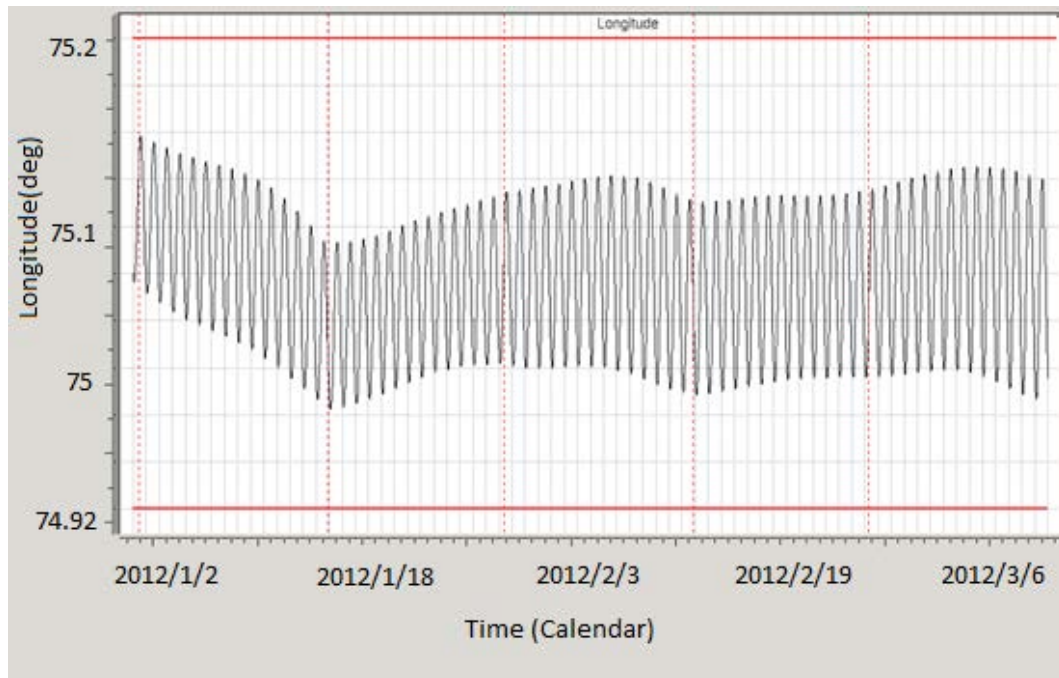


Figure 14- Longitude evolution with symmetry control ($\lambda = 75.1^{\circ}E$)

Figure 14 shows that the manoeuvres required are significantly small, and the longitude almost does not change.

Moreover, for the control cycle, the drift rate evolution is so slight that applying a manoeuvre is more probably to increase the perturbation and not to help to stabilize the longitude. This is an important point to consider, because if the manoeuvre must control the longitude, and it happens the contrary, there is no control.

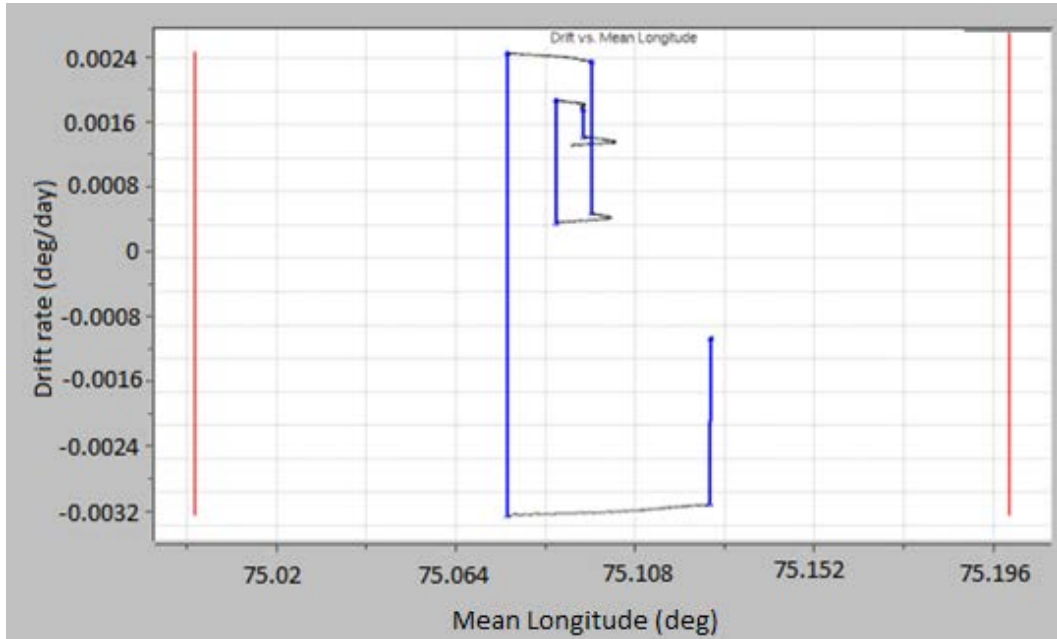


Figure 15- Drift rate vs mean longitude ($\lambda = 75.1^{\circ}E$)

Figure 16 shows that the thrusts throughout a year have a low order of magnitude. Actually, values that are smaller than 0.005 m/s cannot be considered by the satellite engine. The errors associated to the thrusts are higher than the thrust they can produce. Most of the values of the thrust are under this minimum value (0.005 m/s)

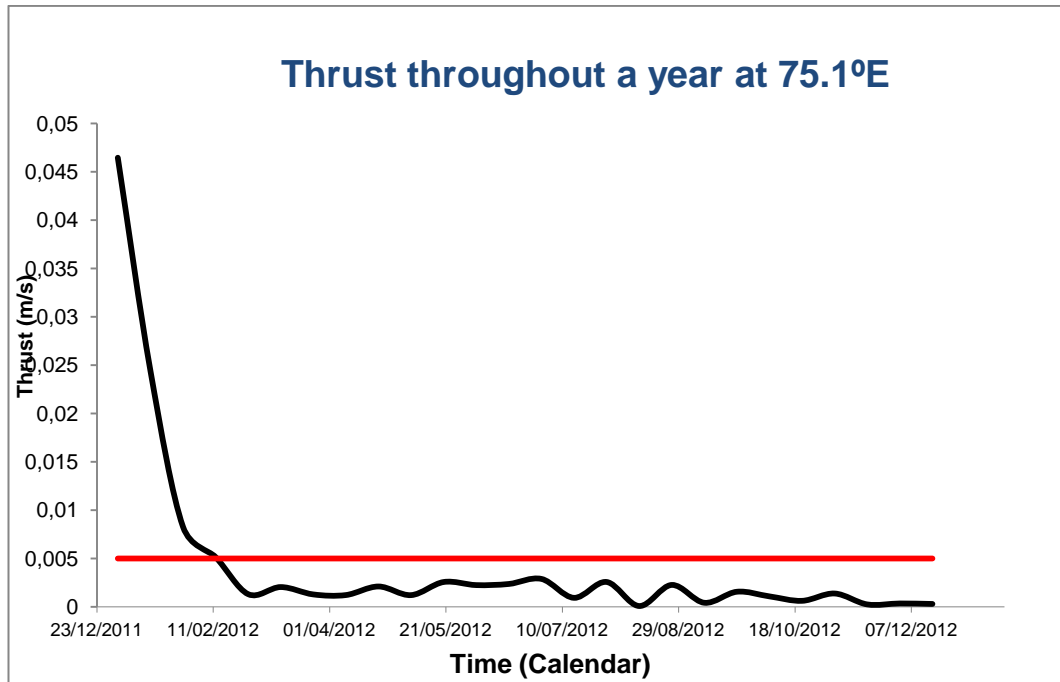


Figure 16- Thrust evolution throughout a year at $\lambda = 75.1^{\circ}E$

All the values of the thrusts are lower than the minimum thrust that the engine can detect.

This strategy cannot work for an equilibrium stable point having the control circle of 14 days. One possible solution to adapt this strategy to this point would be to change the control circle increasing the number of days, but the control cycle is an external requirement impossible to change.

2.4.2.3. Longitude 11.5°W

The longitude evolution is similar to the stable equilibrium point.

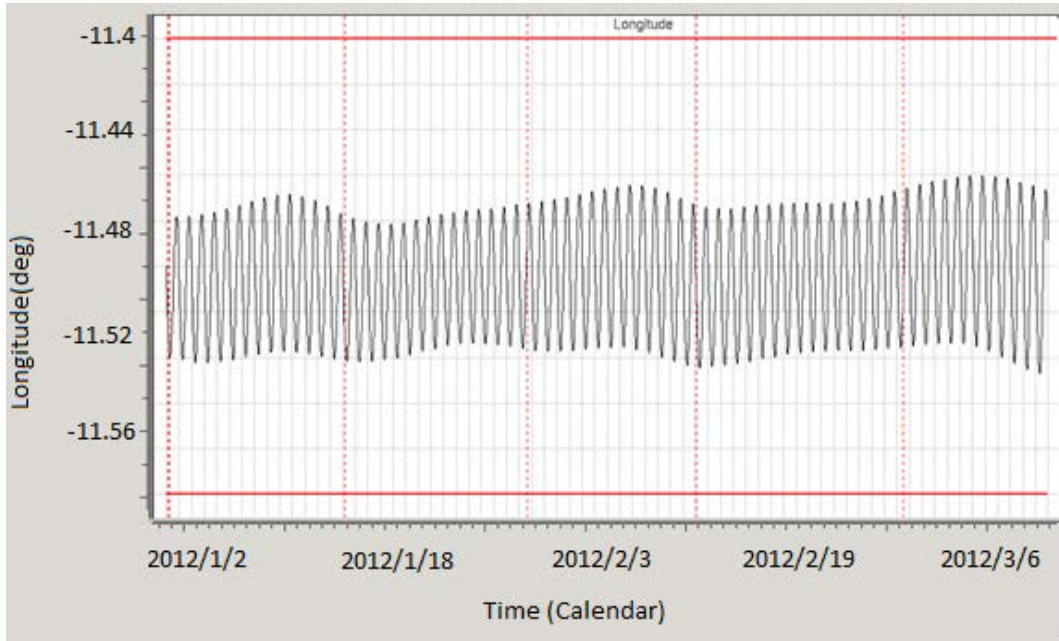


Figure 17- Longitude evolution vs symmetry strategy ($\lambda = 11.5^{\circ}W$)

Nevertheless, the drift rate evolution is quite different. The drift rate diverges (slightly) because is very sensible to any perturbation, even if the thrust is really small.

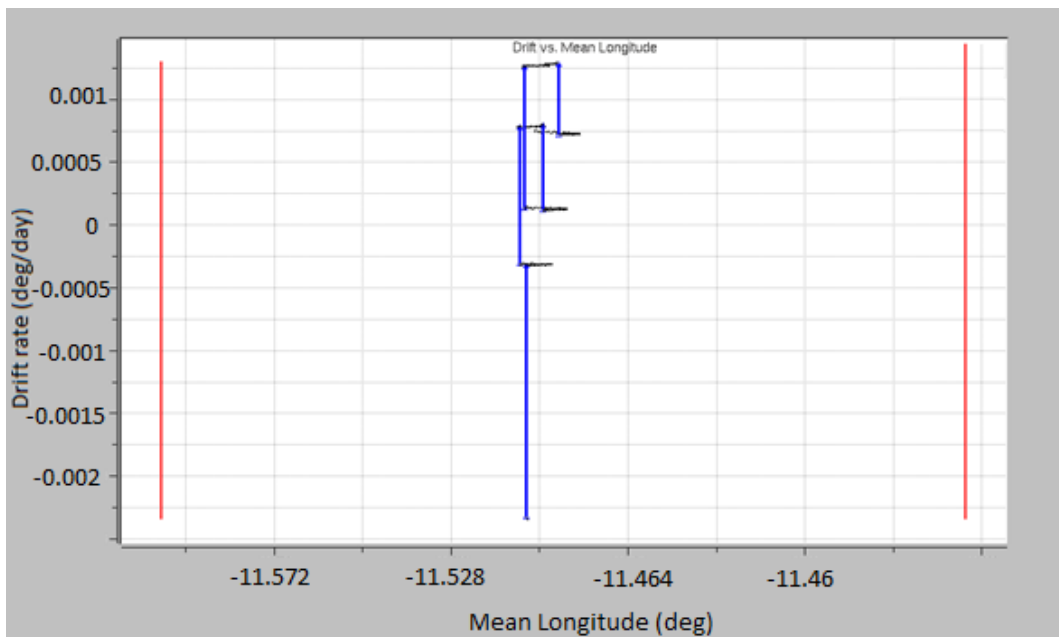


Figure 18- Drift rate vs mean longitude with symmetry strategy ($\lambda = 11.5^{\circ}W$)

ΔV applied in the equilibrium points are of the same order of magnitude. So the errors produced are similar. But, due to the instability of the drift, there are more manoeuvres are higher than the threshold value (0.005 m/s) indicated before.

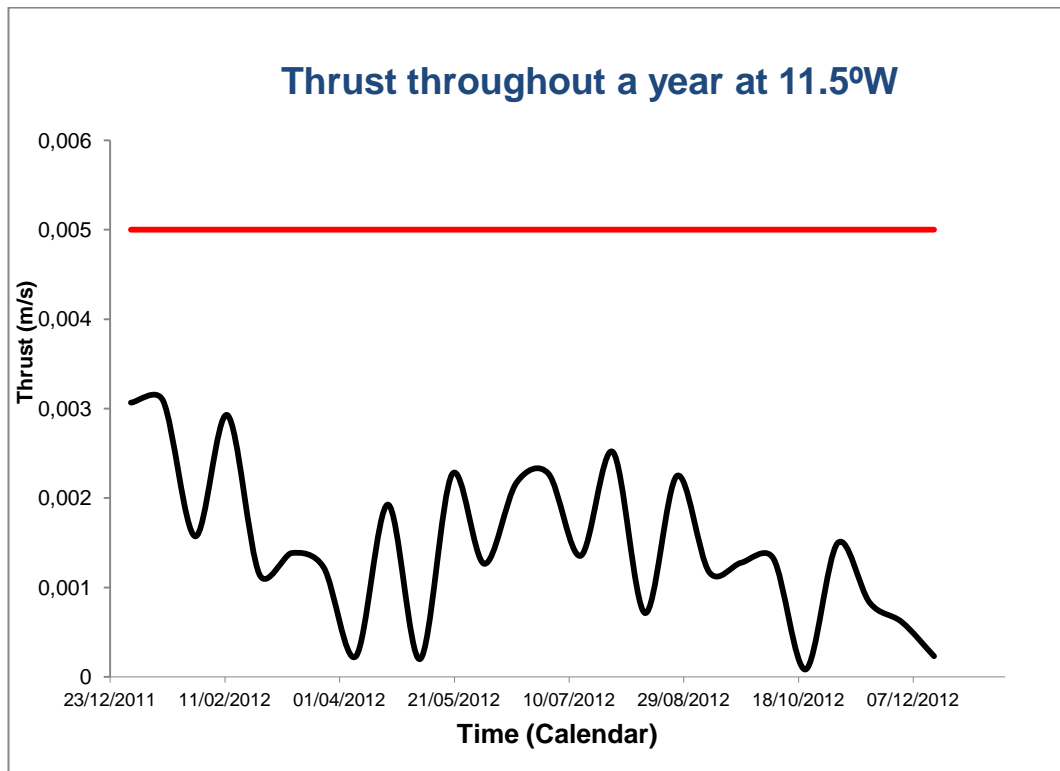


Figure 19- Thrust evolution throughout a year at $\lambda = 11.5^\circ W$

The fact of not having a controlled evolution in the drift rate evolution produces that the manoeuvres are unpredictable in the long-term (being low values)

2.4.2.4. Longitude 76.5°E

It is interesting to study a longitude near to an equilibrium point because it has characteristics of a typical point and of an equilibrium stable point.

The drift rate in the longitudes near to an equilibrium point is also small. Here, the tesseral elements and the other perturbations have the same importance.

The longitude evolution is similar to the longitude evolution of $\lambda = 30^\circ E$, but with ΔV small.

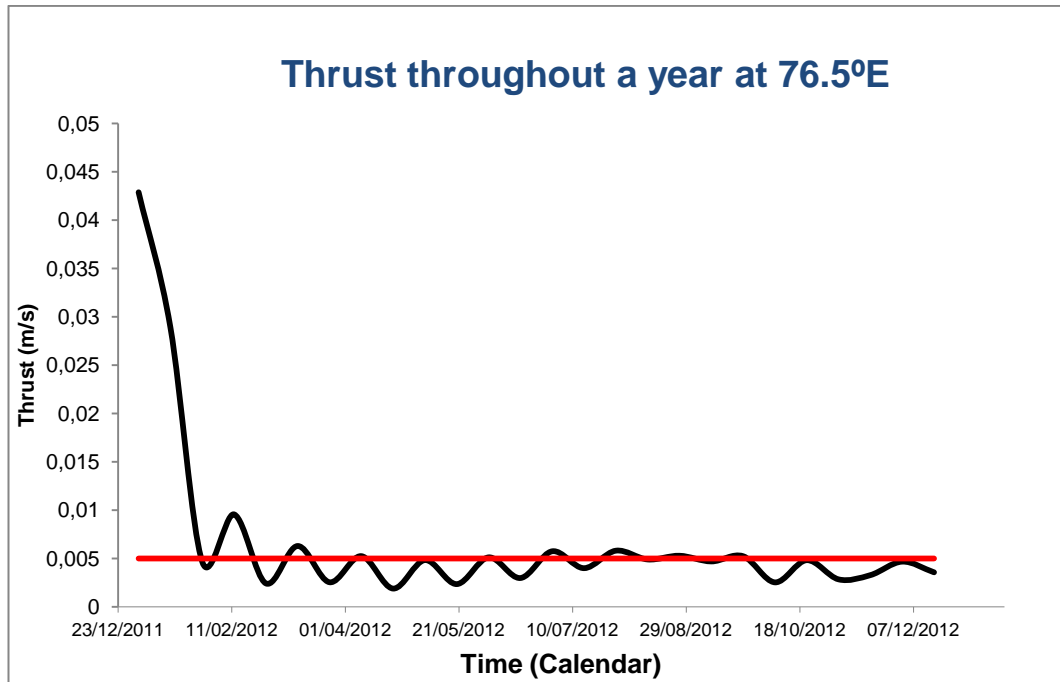


Figure 20- Thrust evolution throughout a year at $\lambda = 76.5^{\circ}E$

The thrust problem of the equilibrium points also appears in this longitude. Although the values are higher than on the equilibrium points, they are not enough to be significant.

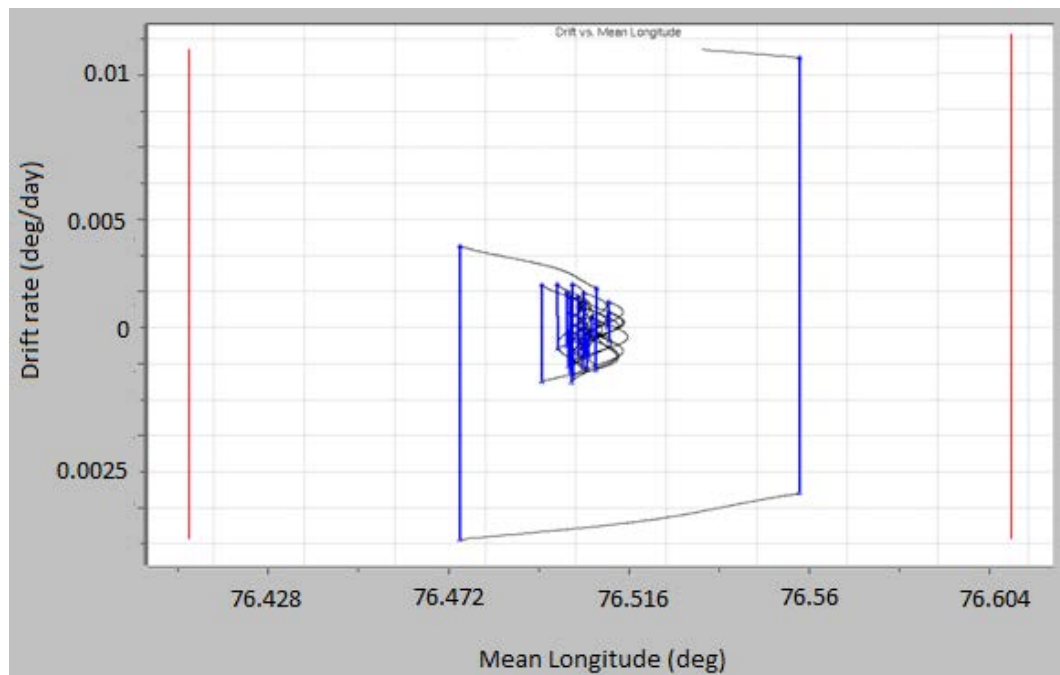


Figure 21- Drift rate vs mean longitude ($\lambda = 76.5^{\circ}E$)

The way that the parabolas are centred reminds the equilibrium points, but unlike them, the drift rate is enough to do a little parabola. This is how the “hybrid” point behaves.

Looking at the figure of the zoom in the drift rate, it can be observed that no parabola is centred in zero. Furthermore, they are placed arbitrarily in a delimited region inside the deadband.

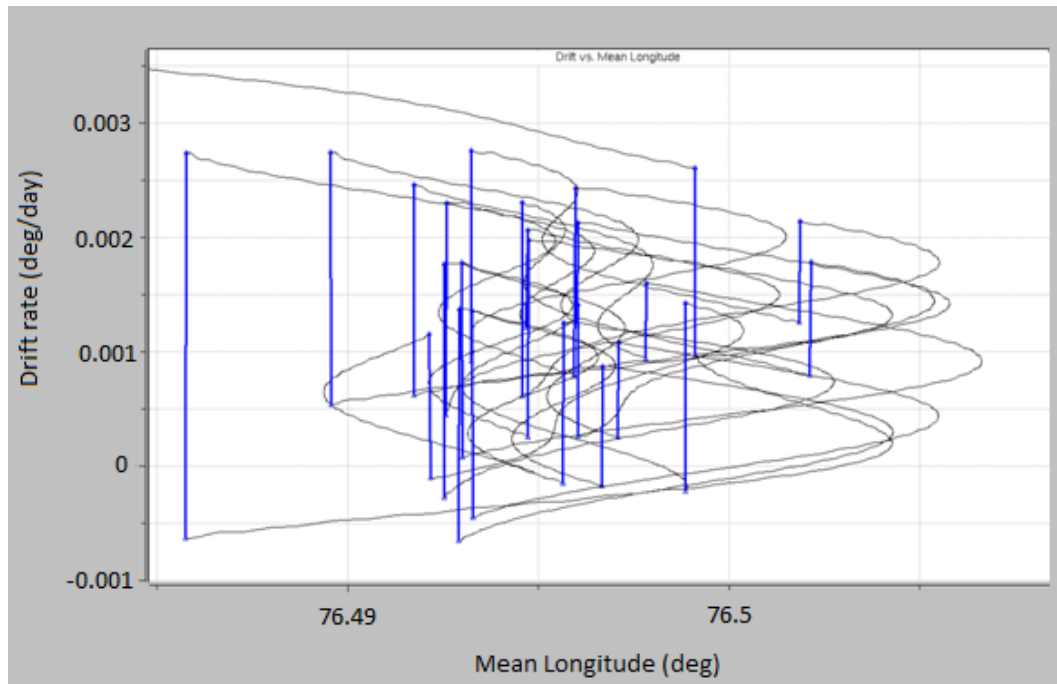


Figure 22- Zoom on drift rate vs mean longitude ($\lambda = 76.5^{\circ}E$)

2.4.3. Problems to solve

- **The value of the thrusts changes in every control cycle.**

The values do not seem to keep a trend; the difference between two consecutive values can be up to 20%.

The problem of the strategy is that the algorithm is only made according to one control cycle; there is no relation between a control cycle and the ancient control cycle.

The ΔV changes because the algorithm produces a thrust necessary to obtain a symmetric longitude in one cycle and if the maximum or minimum longitude vary, also the ΔV .

Thus, the initial longitude and the final longitude in one cycle are not the same. There is no capability to control the thrust in order to get more similar values.

This problem is more evident analyzing the mean longitude in a several cycles:

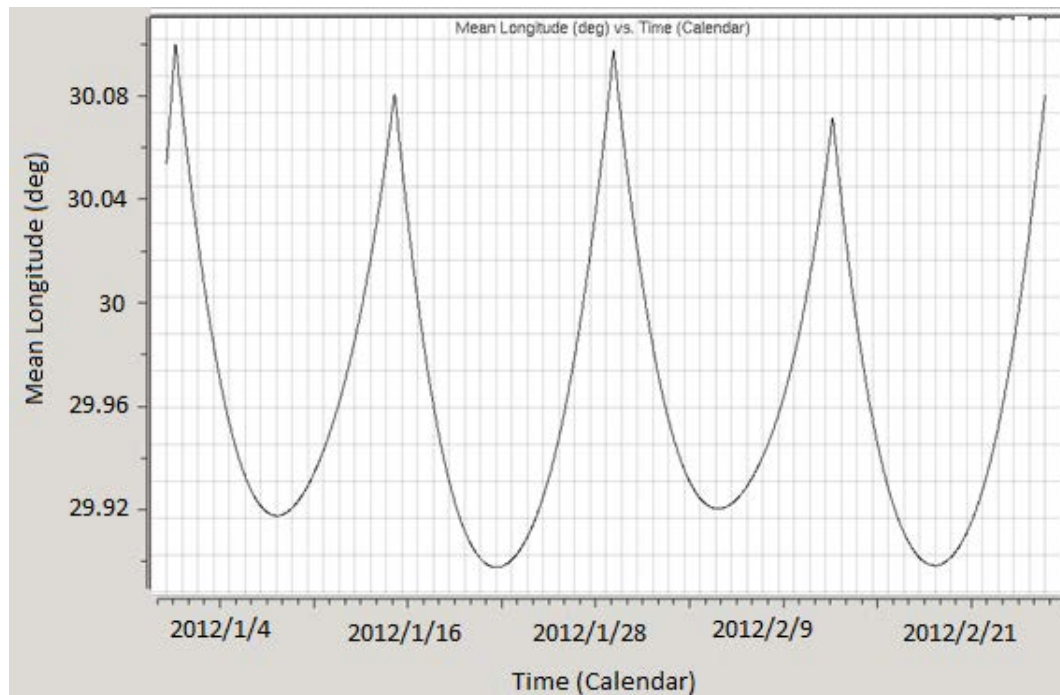


Figure 23- Mean longitude (30°E) with symmetry strategy

If the initial longitude and the final longitude are not levelled, the maximum and the minimum also, so the algorithm will not be automatic and it is one of the requirements.

One of the causes is that the code is based on the oscillatory eccentricity, so the maximum and the minimum could not coincide with the maximum amplitude. Furthermore, the eccentricity varies in one cycle.

- **This strategy does not work as desired in the equilibrium points.**

It is true that the longitude is confined in a small region and never escapes. However, this region has not been chosen, so it is not centred and not controlled.

Nevertheless, the weakest point of this strategy for the equilibrium points is that the ΔV applied in most of the cases is very small.

- **The initial state vector must be coherent.**

As mentioned in the introduction of this section, the rest of synchronous parameters could be chosen arbitrarily, but in case the drift is really different from zero or the mean longitude at epoch is far from the longitude target, the algorithm does not answer well.

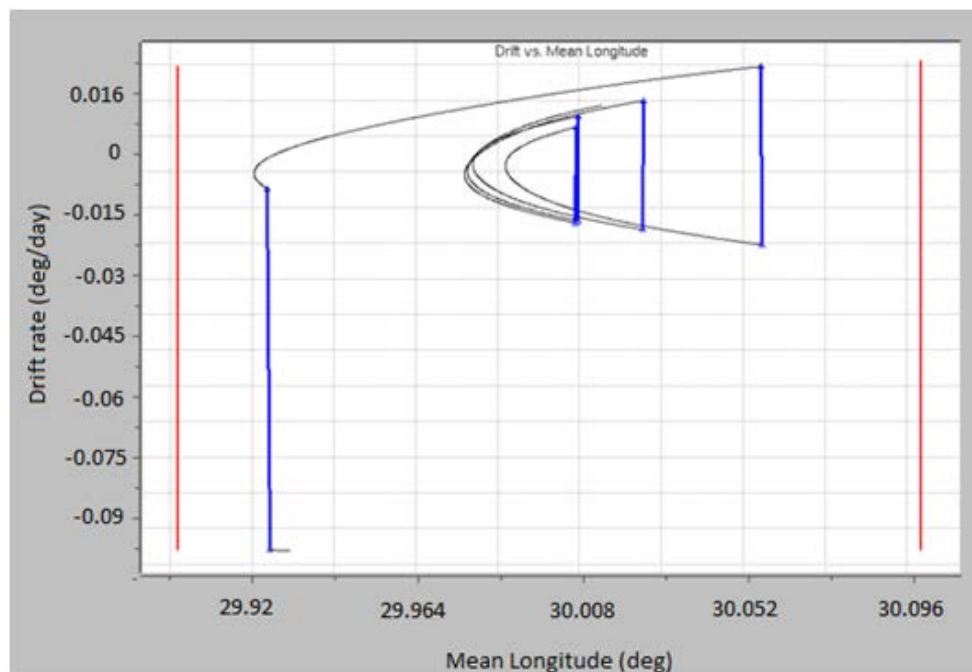


Figure 24- Drift rate with a bad initial state vector

Figure 24 shows that four control cycles are needed to obtain a right longitude. Four manoeuvres mean one month since the set in orbit. Thus, once the initial longitude is not well placed, the algorithm cannot stabilize the longitude in a region. The worst problem is that the real longitude goes away the control window, as shown in **figure 25**

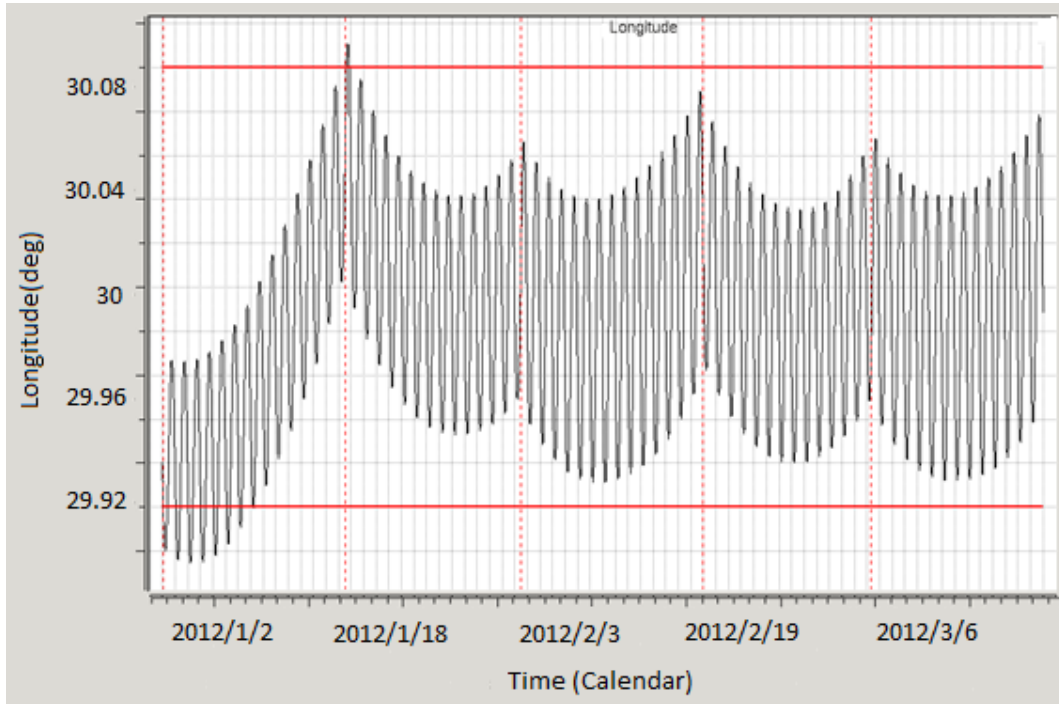


Figure 25- Longitude evolution with a bad initial state vector

In order to solve the problems before mentioned, a new strategy will be presented.

2.5. Drift/Longitude strategy

The free drift rate without perturbing forces relates the real semimajor axis (a) with the theoretical semimajor axis (A), **equation (16)**

However, in an environment where all the perturbing forces are considered, it is difficult to obtain an expression of the drift rate such as the mentioned before, where there are no perturbing forces, but is directly related with the semimajor axis.

The free drift rate and the drift rate considering all the disturbing forces represent the same concept.

Returning to the **equation (49)**, considering that at the beginning of the cycle $t_0 = 0$ and taking the derivative of the longitude

$$\dot{\lambda} = \frac{\partial \lambda(t)}{\partial t} = \dot{\lambda}_0 + \ddot{\lambda}t \quad (75)$$

Where $\dot{\lambda}_0$ is the initial drift rate which could be found analysing the initial conditions and $\ddot{\lambda}$ is the drift acceleration, which depends on the longitude that have been chosen These accelerations are tabulated and constant inside the deadband (**ANNEX A**).

The time can be expressed as

$$t = \frac{\lambda - \lambda_0}{\dot{\lambda}} \quad (76)$$

Thus,

$$\lambda(\dot{\lambda}) = \lambda_0 - \frac{1}{2} \frac{\dot{\lambda}_0}{\ddot{\lambda}} + \frac{\dot{\lambda}^2}{2\ddot{\lambda}} = D + E\dot{\lambda}^2 \quad (77)$$

The independent term D depends on the initial conditions $(\lambda_0, \dot{\lambda}_0)$ and the coefficient E is constant.

The term D is the longitude that will be reached when the drift rate was zero. The factor $k = \frac{\dot{\lambda}^2}{2\ddot{\lambda}}$ determines the maximum and minimum values that the mean longitude could reach in function of the drift rate.

The first condition that it must fulfil is that the parameter k is smaller than the deadband.

$$k < \delta\lambda \quad (78)$$

The second condition is to control the term k to produce symmetry in the mean longitude with the drift rate. However, this symmetry is only possible in a determinate longitude (λ_b) because the control cycle is fixed in fourteen days. Hence, the question here is whether there is a point where applying a thrust, after the cycle, the longitude would arrive to the same place thanks to the drift evolution. If this point exists, the strategy would be completed. The aim of the strategy is to find this point where the mean longitude will repeat for long term.

2.5.1. Longitude trade off

There are several questions to answer, such as, if this point exists, if it would be constant and if it is possible to reach it with only one manoeuvre.

- Does this point exist?

Obviously, the point where there will be longitude symmetry is not the longitude target because, in a determinate longitude, the drift rate will move the longitude to one side of the deadband, so the longitudes would be always displaced, not centred in the control window.

It is impossible to know where this point is with only one control cycle. Because in only one control cycle, the strategy does not have enough information about the longitude throughout the time, only consider the longitude information in this control cycle.

Thus, the strategy must take into account two cycles. The first one will find the point where in the next cycle, applying the symmetry strategy; the initial mean longitude and the final mean longitude will be at same place.

Thus, there will be an iterative process, where the thrust of the first control cycle will be varying in order to find when the second cycle will have the initial and final longitude at same place applying the symmetry strategy.

Normally, the ΔV of the second control cycle will not change throughout the iterative process.

In the **figure 26**, the longitude painted of black represents the normal propagation. The longitude painted of green is the propagation when the thrust of the first cycle is smaller, and the blue is the effect of doing higher the first thrust.

If the final longitude of the second cycle (λ_3) is higher than the initial longitude of the second cycle (λ_2), the velocity of the first manoeuvre increases. If it is the opposite case, the manoeuvre decreases.

$$\lambda_2 > \lambda_3 \rightarrow \Delta V_1 \uparrow$$

$$\lambda_2 < \lambda_3 \rightarrow \Delta V_1 \downarrow$$

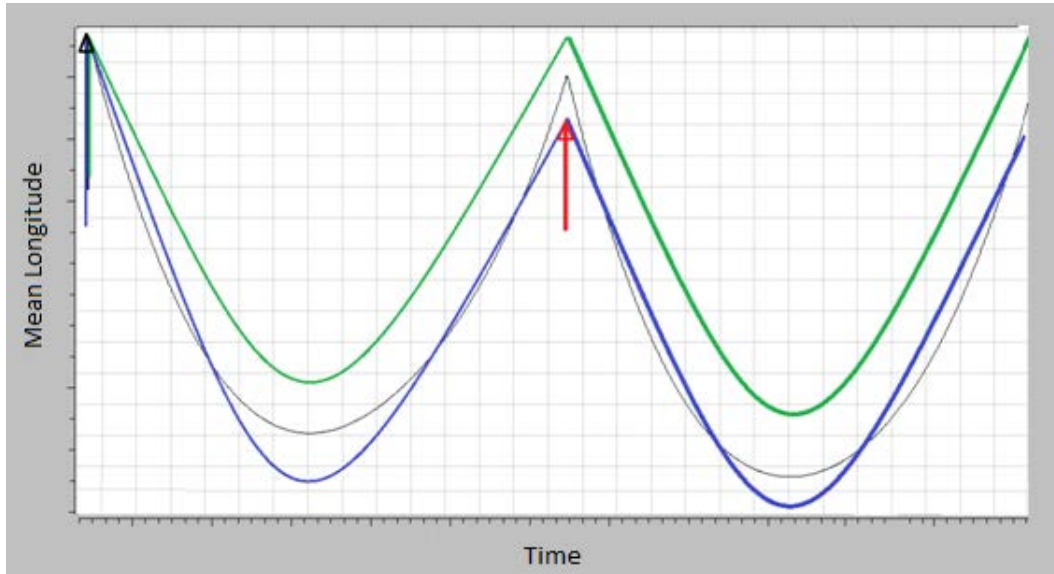


Figure 26- Effects of increasing or reducing the first thrust

- Will the point be constant throughout one year?

The first manoeuvre must be the necessary to set the second parabola in the point where the longitude and drift will be symmetric in the next cycles. For making sure that the next control cycle to the second parabola will be also similar, in every iteration a verification of the next cycle will be done.

This means that throughout the satellite lifetime, the strategy will consider two control cycles, and will vary the thrust of the first one in order to obtain symmetry in the second one. Thus, the symmetry will be always carried out.

With this process exists the assurance that one control cycle could not do a manoeuvre to destabilize the algorithm. By the way, if there was any perturbation that placed the longitude on an undesirable point, the algorithm will apply a manoeuvre to set the longitude at the end of the control cycle in order that the next cycle arrives at the point where all the iteration would repeat again.

- Is possible to reach the point with only one manoeuvre?

The theory says that it is not possible to control longitude and drift at same time, with only a single manoeuvre, but in reality, the only parameter that is controlled is the longitude, a **longitude based on the symmetry of the drift rate**. For this reason, the code must be ready to initialize each time that the drift rate has a big value.

2.5.2. Algorithm

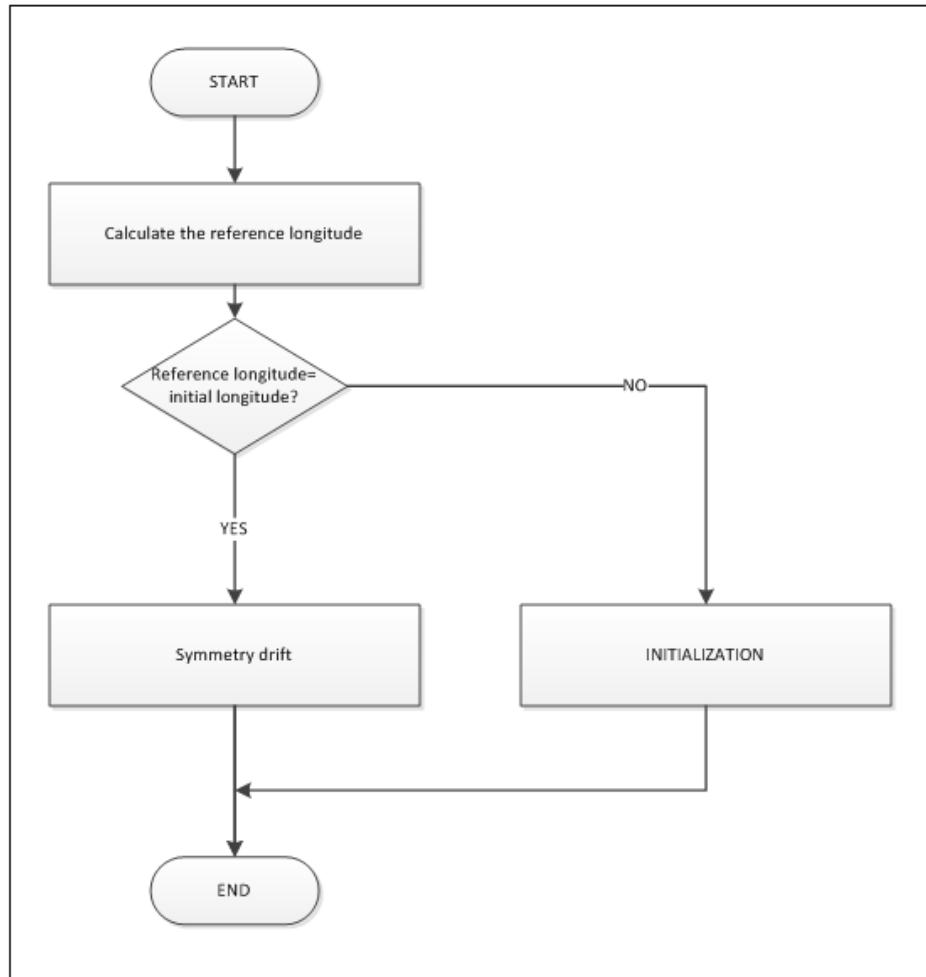


Diagram 3- Algorithm of the strategy drift/longitude control

- Calculate the reference longitude

According to the assumptions of section 2.4, the period of a cycle is fixed by the size of the deadband and by the tesseral acceleration.

$$T = 4\sqrt{\delta\lambda/\ddot{\lambda}} \quad (79)$$

Here, T represents the control cycle that is fixed. The cycle is fixed, where the $\delta\lambda$ will be the parameter k , from the **equation (78)**. The objective is to calculate this value, being the maximum of the mean longitude could reach. If the algorithm

could reach this value at the end of the longitude cycle, the longitude and the drift will be symmetrical for all the cycles.

The table of the tangential accelerations due to the tesseral elements, **ANNEX-A**, only contains the accelerations for integer values of longitudes, so for the other longitudes (between two integer longitudes) the tangential acceleration will be found by extrapolation.

In this way, the theoretical longitude is found as $\lambda_b = \lambda_T + k$

- According to the difference between the reference point and the mean initial point, two processes of determination of longitude can be chosen.

If the initial longitude is different than the theoretical longitude, the process chosen is (i), unless the process chosen is (ii).

i. INITIALIZATION

Case when the initial longitude is different with the reference longitude.

The algorithm of this method is

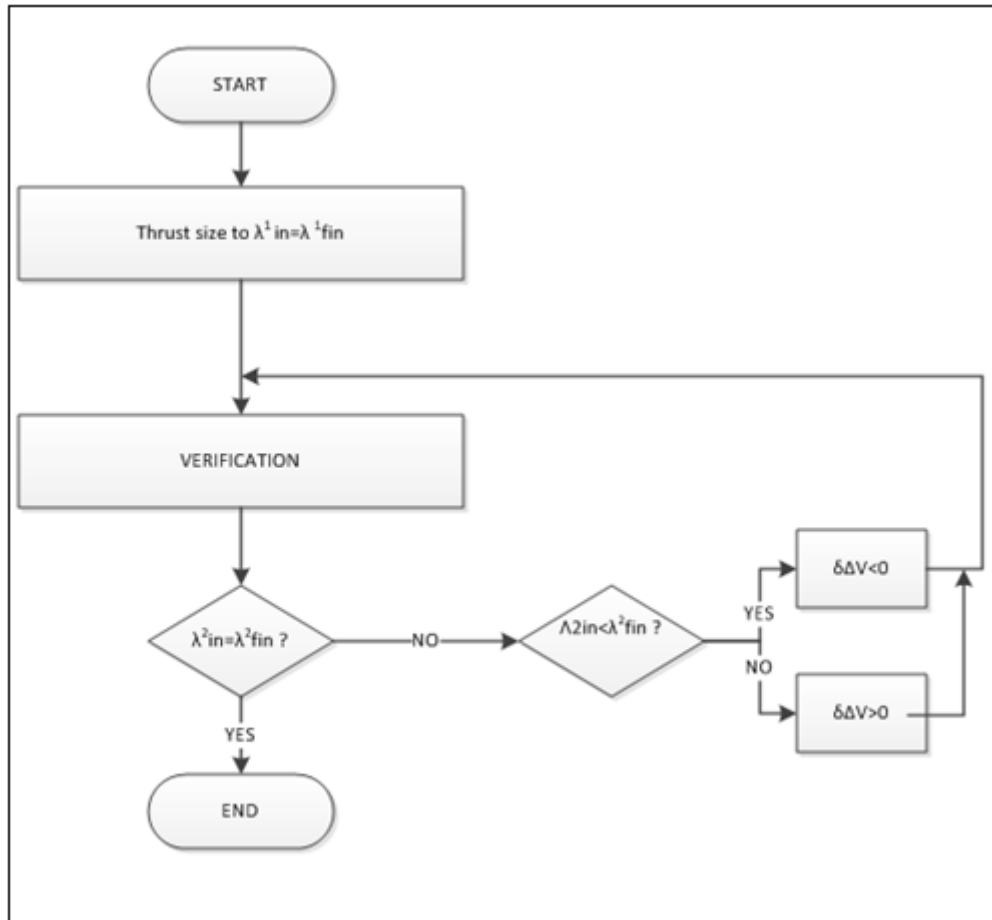


Diagram 4- Algorithm of the initialization process

- ΔV to achieve the reference longitude

Normally, the initial longitude of the first cycle will not be at the right point. Thus, the first cycle is called an **initialized cycle**. This cycle will not follow the drift or longitude symmetry, its only aim is to set the next longitude in drift and longitude symmetry.

As it was mentioned before, the reference longitude should not be so far than the optimal point, so the first approximation will be a manoeuvre where the reference point would be the final longitude point.

To do this by only considering the mean longitude, the required thrust comes from the equation

$$\Delta \lambda V = \Delta V \left(\frac{3}{A} (t_T - t_b) \right) \quad (80)$$

Where t_T would be the time when the longitude will be targeted and t_b the time when the manoeuvre should be done.

As the time of the manoeuvre is not yet controlled (it will be reserved for the eccentricity), $t_T - t_b = 14$ days

The iteration becomes

$$\Delta V_{n+1} = \Delta V_n + \frac{A \lambda_n(t_T) - \lambda_T}{3 \cdot (t_T - t_b)} \quad (81)$$

Starting with the ΔV used for the symmetry strategy.

- Verification

This function propagates the second control cycle, taking the final state vector as the initial state vector for the second cycle.

Now, in this second cycle, the strategy to follow is the symmetry longitude strategy. Applying the strategy of symmetry longitude the real longitude will be inside the deadband. Hence, in the first cycle, that is cycle which is really being controlled, the strategy is applied to the mean longitude. The second control cycle is only used to verify the thrust of the first cycle.

With the thrust found by the **equation (81)**, the initial longitude and the final are compared. If they do not have the same value, the thrust of the first control cycle will be changed.

it is necessary to pay attention in the order of magnitude of the different components of the **equation (81)**.

$$\Delta V_1 \sim 42164.5 \cdot \frac{\lambda_n(t_T) - \lambda_T}{3 \cdot 14 \cdot 86400} \approx 0.01162 (\lambda_n(t_T) - \lambda_T)$$

Taking accuracy between the longitudes of 0.01^0 the contribution in km/s is of $1.162E-4$. Thus, taking accuracy of 0.0001^0 the iteration is not possible to achieve these values.

Thus,

$$\text{If } \lambda_i^2 < \lambda_f^2 \text{ the } \Delta V_{2n+1} = \Delta V_n + \delta \Delta V$$

$$\text{If } \lambda_i^2 > \lambda_f^2 \text{ the } \Delta V_{2n+1} = \Delta V_n - \delta \Delta V$$

The $\delta \Delta V$ can take the precision that the User wants. Considering the smaller it is, the much better the precision is, but the time required to perform it is really will increase.

Finally, the program ends, calculating the size of the manoeuvre which will fulfil a symmetric parabola which will start and finish at the same longitude.

ii. DRIFT SYMMETRY

Once the initial longitude has been initialized, if the assumptions have been right, using the **equation (81)**, the initial and the final longitude will be the same, doing the drift rate a symmetric parabola.

Nevertheless, to make sure that the next cycle will follow also a symmetric parabola, there will also be verification and in the case that the initial and final longitude of the second cycle will not overcome the threshold, another increment will be applied as mentioned before for the other case.

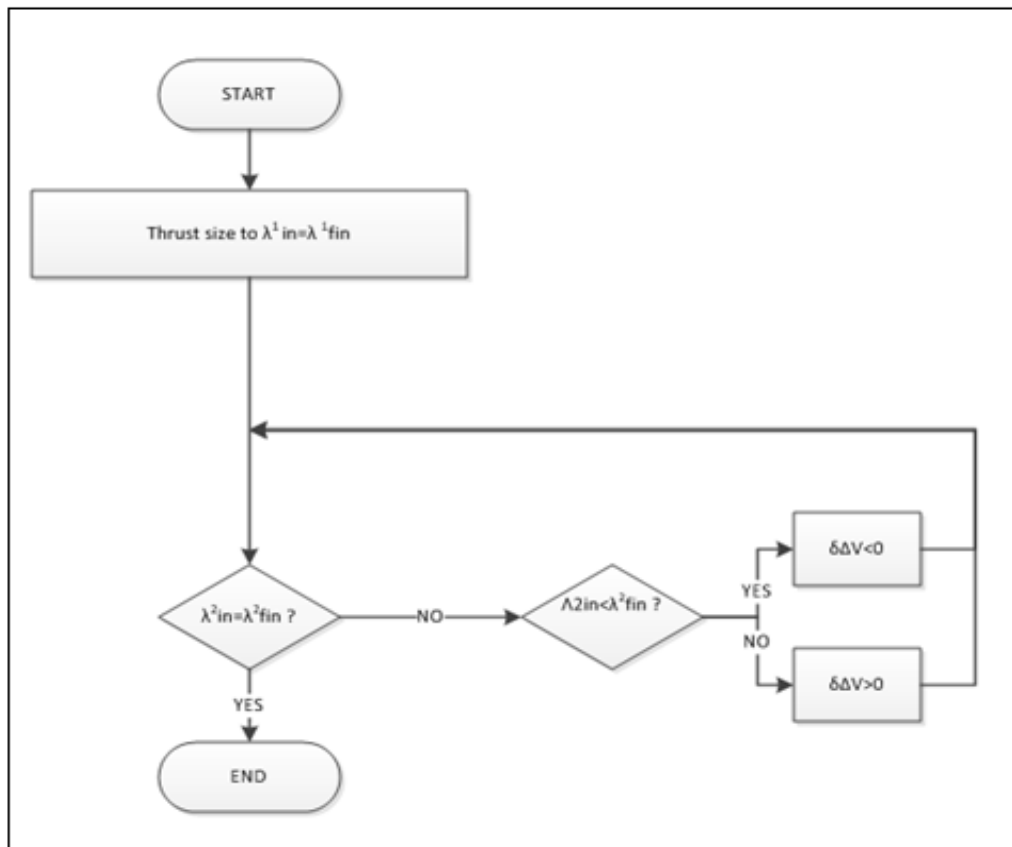


Diagram 5- Algorithm of the drift symmetry

2.5.3. Results

As in the symmetry strategy, the analyzed longitudes will be the same than before, because they are the most relevant.

In order to demonstrate that applying the strategy in the mean longitude, the real longitude will also have better results, the plots showed will be of the real longitude versus time and the drift rate versus mean longitude.

2.5.3.1. Longitude 30°E

The typical value of $\lambda_T = 30^\circ$ sets the real longitude inside the deadband with a margin of no more than the 20% of the total deadband. To show it, as done in the symmetry strategy, the envelope longitude will replace the real longitude in one year.

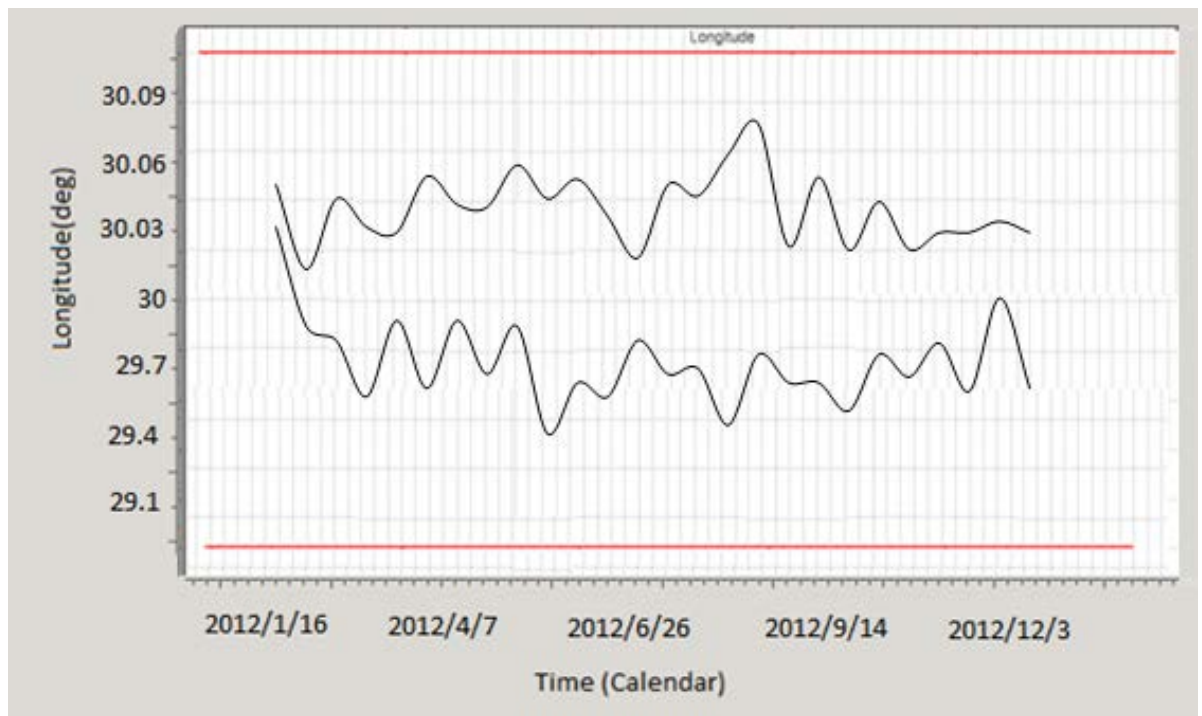


Figure 27- Envelope longitude with drift/longitude control during one year ($\lambda = 30^\circ E$)

Now, examining the drift rate, it is easy to watch where the optimum point is. Except the first longitude which comes from any point inside the deadband (initial state vector), the rest of longitudes are inside a really small range.

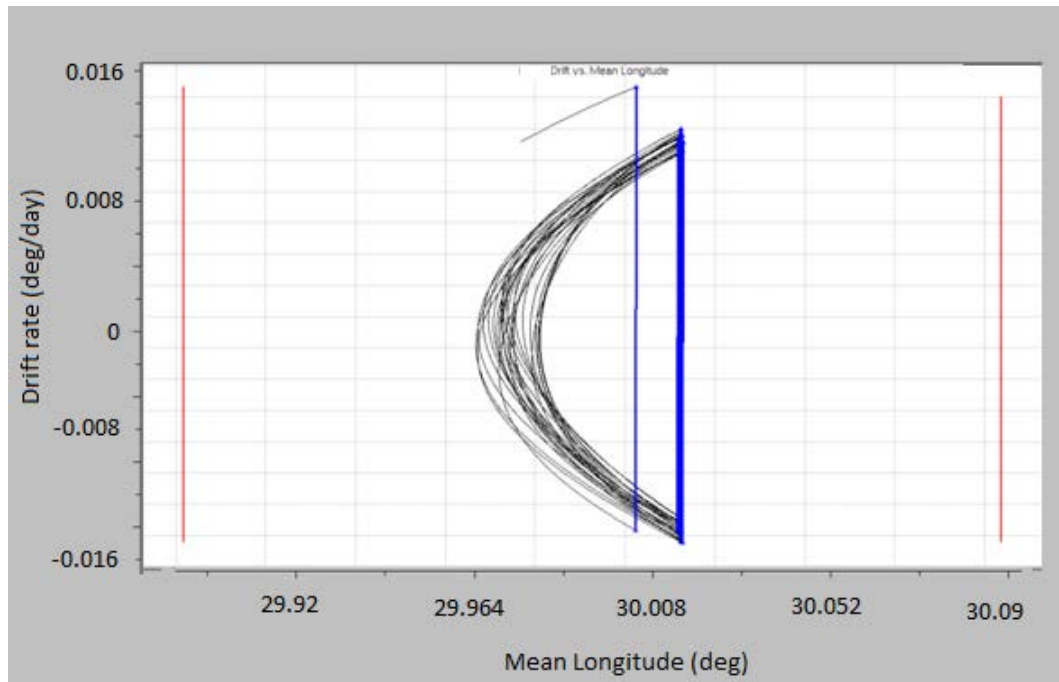


Figure 28- Drift rate vs mean longitude with longitude/drift control ($\lambda = 30^0E$)

It is true that the drift rate is not the same at the end of each control cycle. This is the influence of the other perturbing effects. These effects do not influence in the algorithm and neither in the choice of the optimum point. However, as mentioned in the **equation (50)**, the drift error is accumulated, so if the mission was for two or more years, a double manoeuvre would be necessary to reduce the drift rate towards the value obtained of the first control cycle.

These effects can be watched in the **figure 29**.

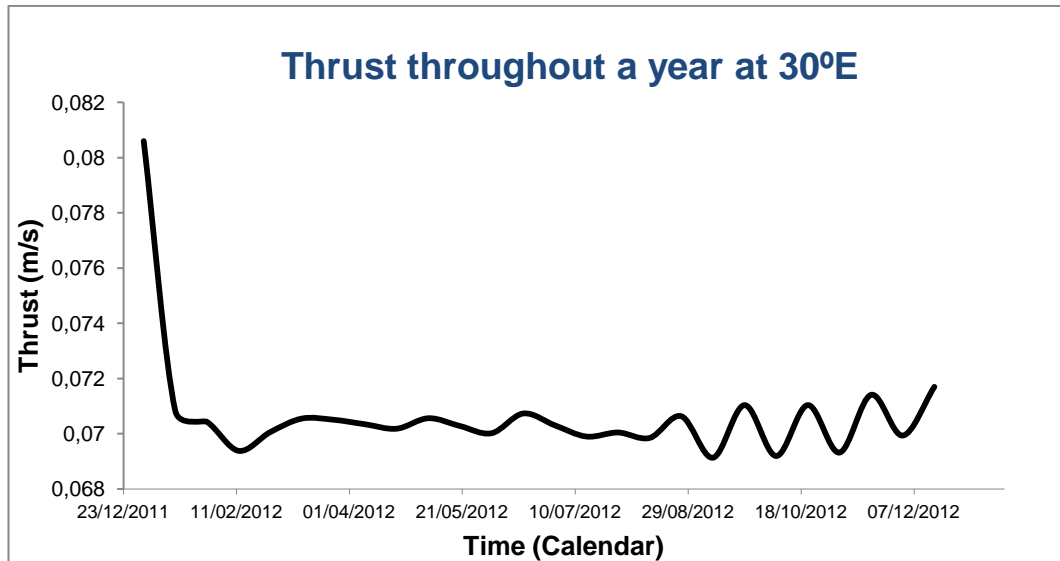


Figure 29- Thrust evolution throughout a year at $\lambda = 30^{\circ}E$ with drift/longitude strategy

The thrust evolution is constant during the first half year, later the drift error start to influence in the thrust. A second initialization should be necessary or a double manoeuvre if it was urgent.

2.5.3.2. Longitude 75.1°E

In the equilibrium points, the real longitude does not change so much with the time.

The main characteristics which define a longitude control in a stable point are the thrust evolution and the changes of drift rate between two control cycles.

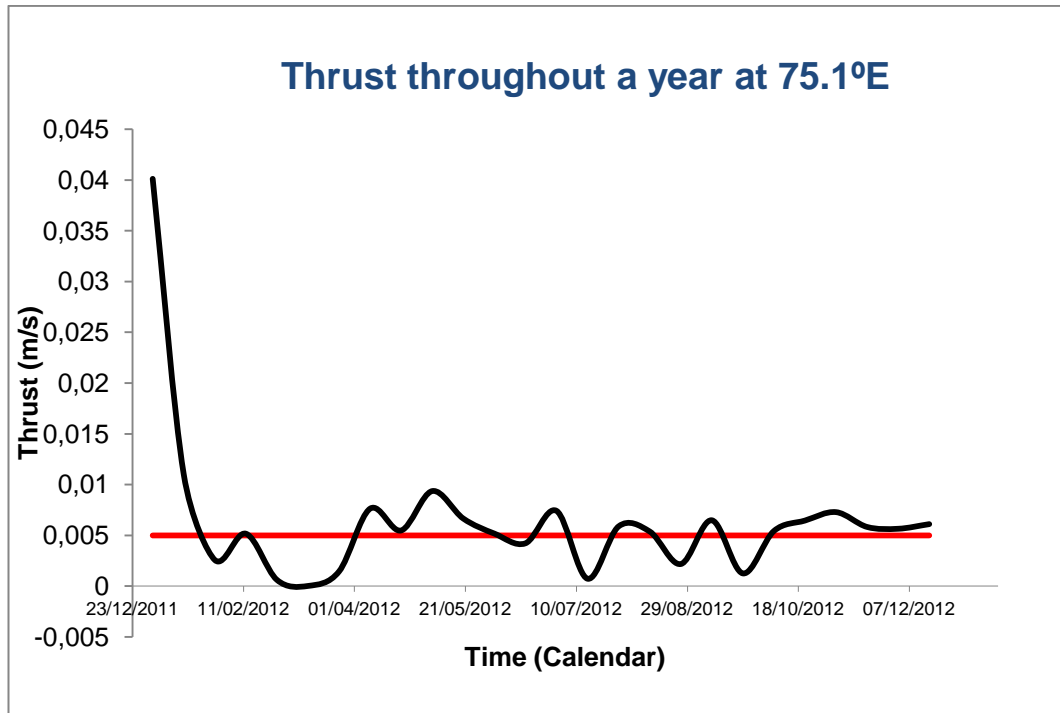


Figure 30- Thrust evolution throughout a year at $\lambda = 75.1^{\circ}E$ with drift/longitude strategy

Although the most of the values of the thrusts are upper the minimum, it exists a lot of values that would not be considered. These values could be neglected. A good strategy would be avoiding doing manoeuvre in this cycle, because there will not be consequences, and having a control cycle that changes with the time.

However, in comparison with the manoeuvres of this point with longitude symmetry, here, only a few of them are under the thrust threshold. In order to force the drift parabola, the thrust is higher.

The **figure 31** shows the drift rate, and the confirmation is done. This algorithm behaves correctly at equilibrium points.

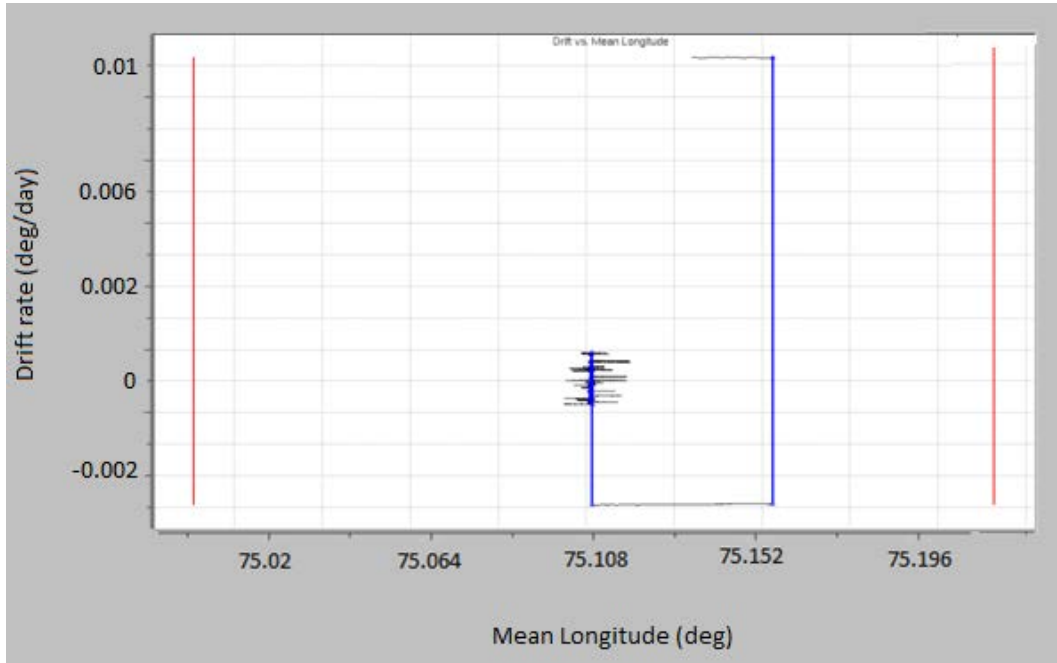


Figure 31- Drift rate vs the mean longitude with longitude/drift control ($\lambda = 75.1^0E$)

The mean longitude is centred in the middle of the control window. The next picture shows a zoom of the zone where the manoeuvres take place.

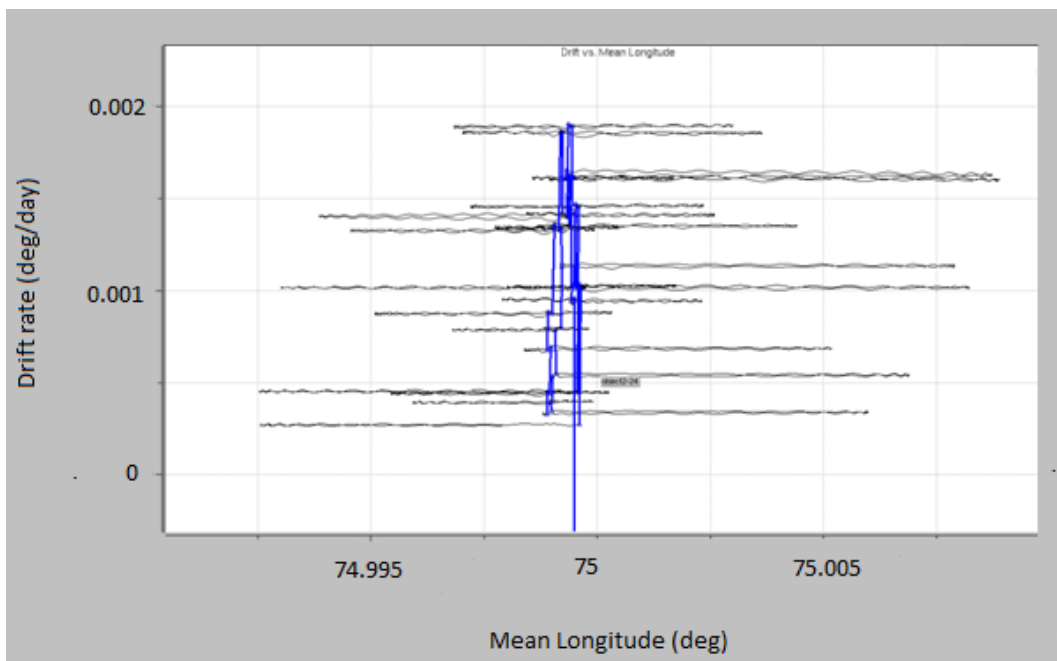


Figure 32- Zoom on drift rate vs the mean longitude with longitude/drift control ($\lambda = 75.1^0E$)

The drift varies more due to errors in thrusts than as a result of gravitational perturbations. To see better how the drift does not evolve along a manoeuvre.

Watching the evolution of the semimajor axis could help, because of the mean drift rate definition.

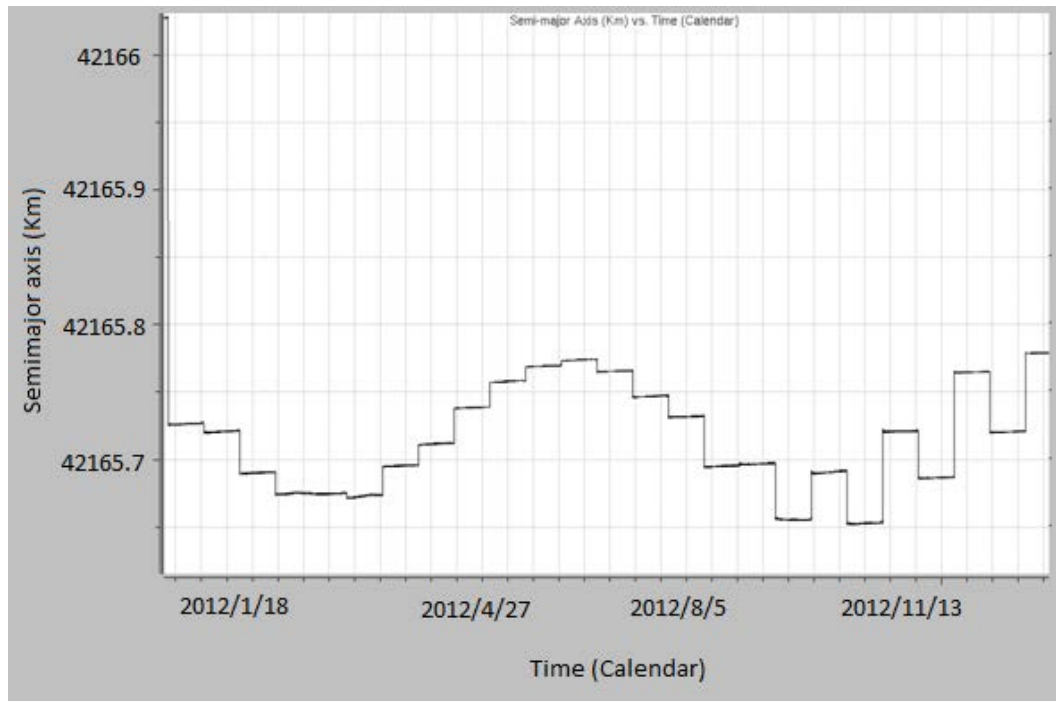


Figure 33- Semimajor axis evolution with longitude/drift control ($\lambda = 75.1^{\circ}E$)

The horizontal lines represent the moments when the satellite is drifting. The vertical lines take place when the manoeuvres are applied. There is not almost drift rate between two control cycles.

2.5.3.3. Longitude $11.5^{\circ}W$

The real longitude evolution is similar to that found for the stable equilibrium point.

The unstable point is the worst longitude to control. The solution obtained is not perfect but it shows some improvements with respect to the symmetry longitude strategy.

First of all, it is impossible to set the longitude in one region, because its drift is very small but very sensitive to any perturbation. However, the longitude fluctuation has been reduced in comparison with the symmetry longitude strategy.

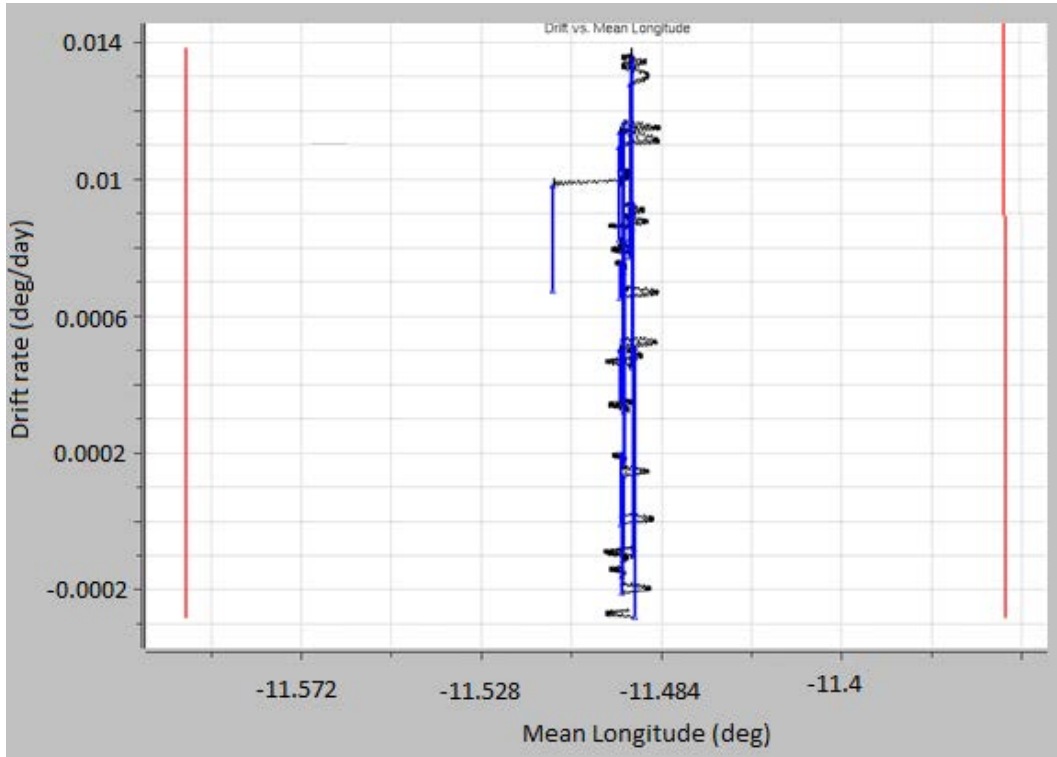


Figure 34- Drift rate vs mean longitude with longitude/drift control ($\lambda = 11.5^{\circ}W$)

The region the longitudes take place is at the middle of the control window. The difference of thrusts between two consecutive cycles is due to the impossibility of not having a drift rate constant. It is small, but sometimes with tendency to displace to the east and sometimes to the west.

2.5.3.4. Longitude 76.5°E

Only analyzing the drift rate with the mean longitude is enough to show the improvements.

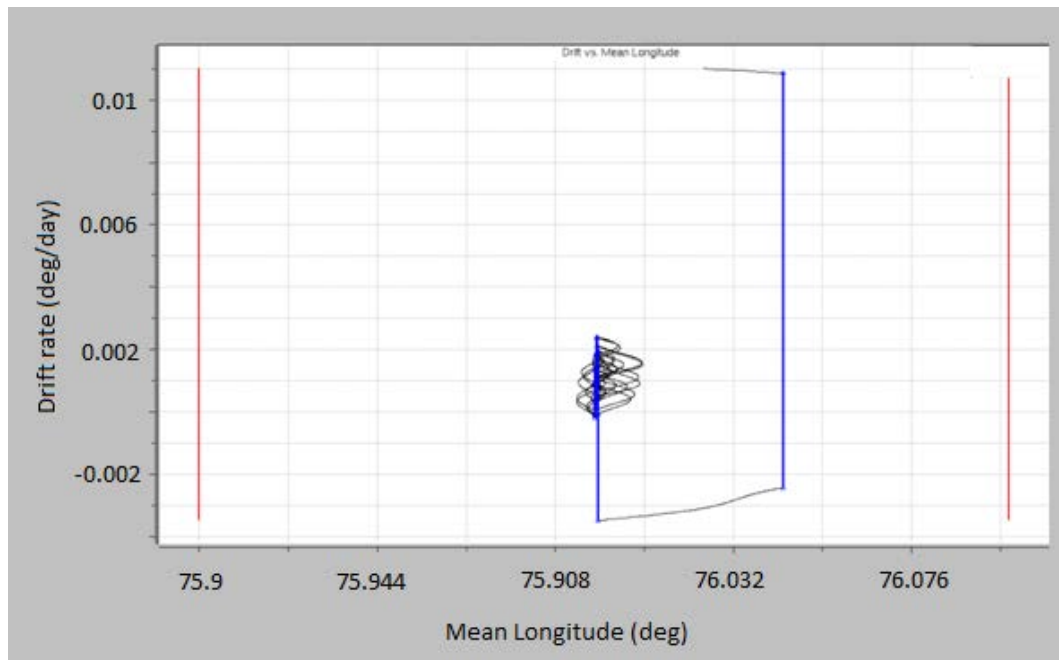


Figure 35- Drift rate vs mean longitude with longitude/drift control ($\lambda = 76.5^{\circ}E$)

The drift rate is enough to produce symmetry with the mean longitude. As the drift rate is so small, the error of the drift rate produces that the parabolas move changing the position.

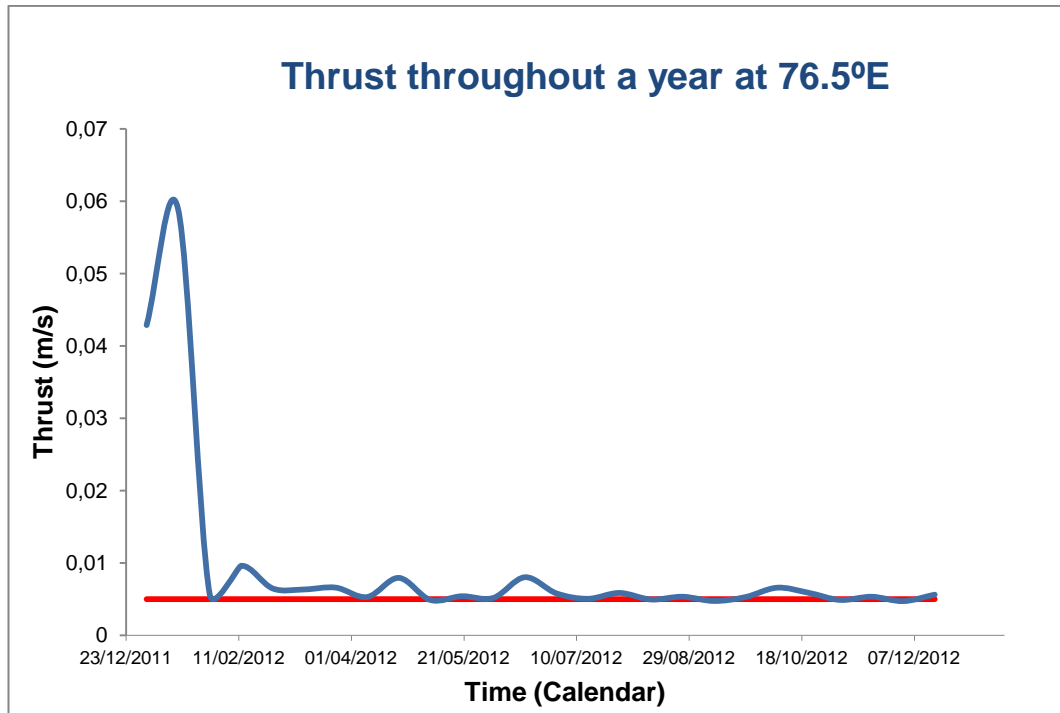


Figure 36- Thrust evolution throughout a year at $\lambda = 76.5^{\circ}E$ with drift/longitude strategy

Only several of the values are under thrust threshold. It is a very good result in comparison with the longitude symmetry control.

2.6. Comparison/Enhancements

The graphics will show both strategies together in one plot. The comparison will be between the longitude symmetry strategy and the longitude/drift strategy, analyzed previously, and for a longitude of $\lambda = 30^{\circ}E$.

Red colour represents the Drift/Longitude strategy and black denotes the symmetry longitude strategy.

The drift/longitude control represents a better strategy than the symmetry control. Actually, the second strategy was born from the first one, and in one of its functions used the strategy of symmetry longitude. So, the symmetry longitude is included in the strategy of drift/longitude control.

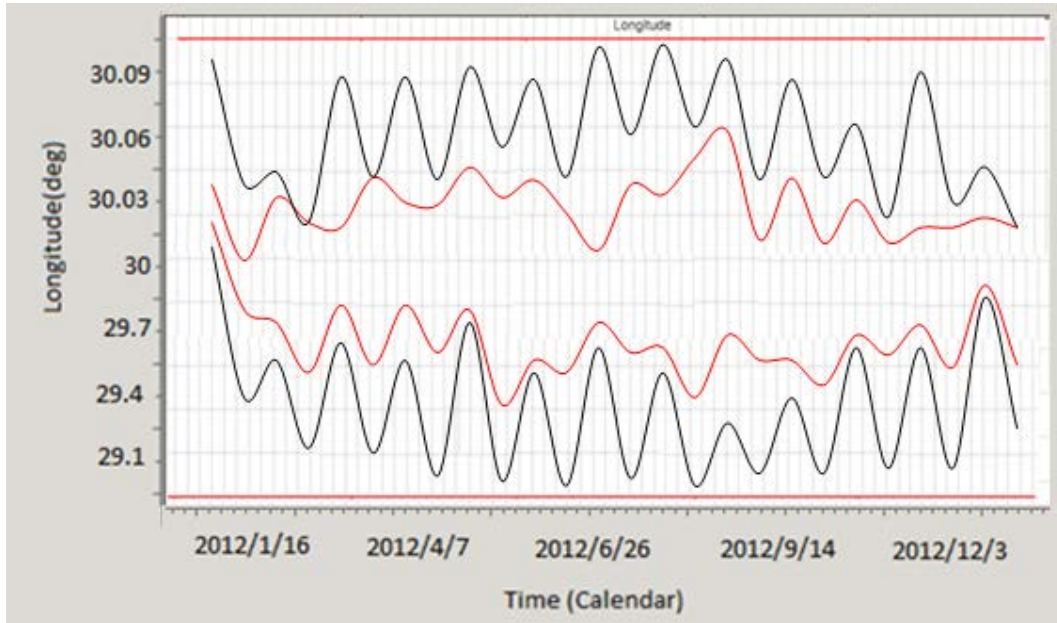


Figure 37- Comparison between symmetry strategy and longitude/drift strategy in longitude

The black grows more and is more irregular than the red one. The red is more delimited in one region.

To show better the differences, a zoom of the picture before is shown.

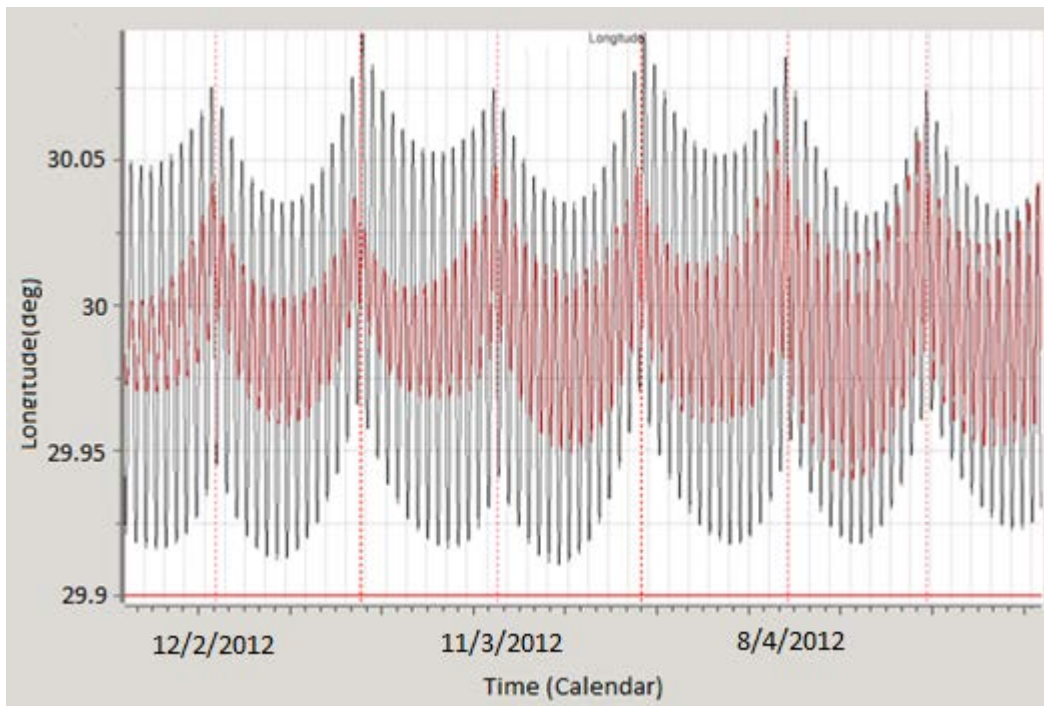


Figure 38- Zoom on the comparison in longitude

The drift rate shows better the improvements of the second strategy.

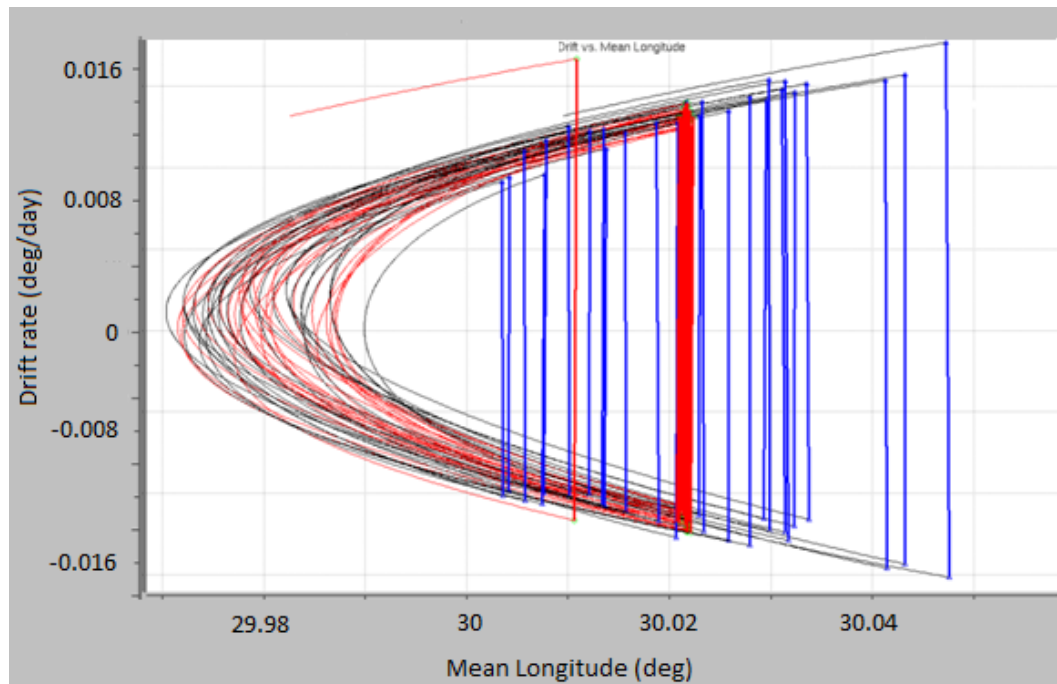


Figure 39- Comparison between symmetry and drift/longitude strategy in drift rate with mean longitude

The curves closely overlap and are confined inside a smaller region. If the threshold decreases, this region will be shrink. However this has a negative effect. If the threshold is too small, a lot of initializations will take place, because the difference between the initial mean longitude and the reference point will be higher than the threshold.

The drawback is that the time required calculating a process of initialization is much longer than the time to produce symmetry between the mean longitudes.

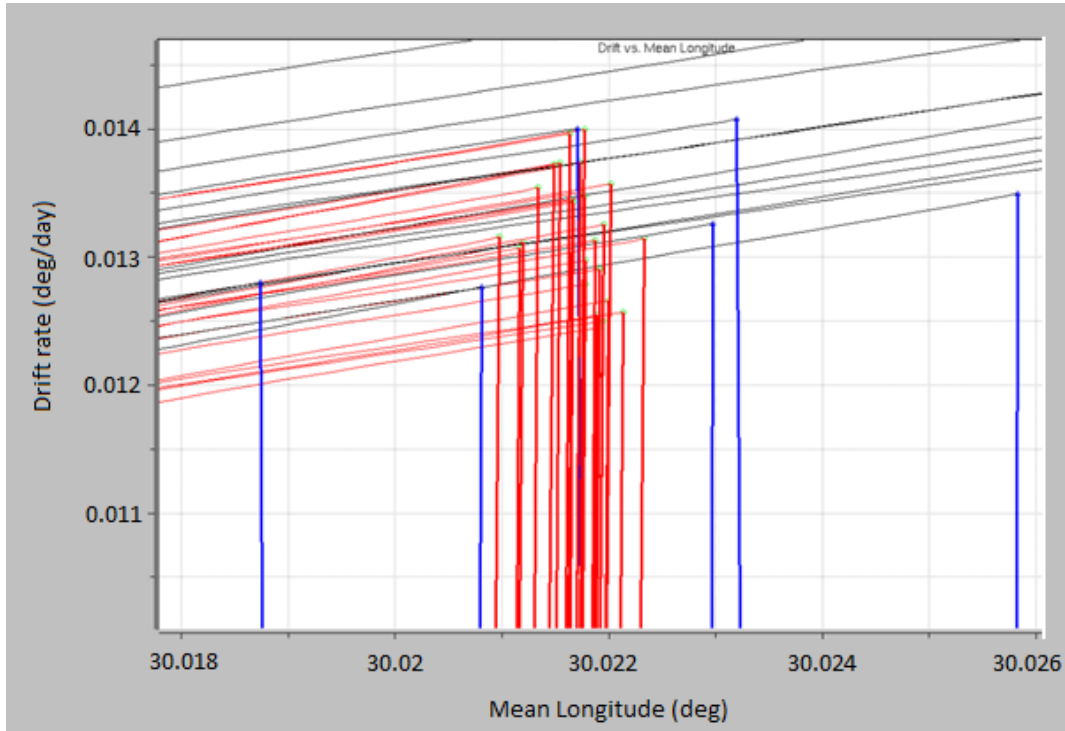


Figure 40- Zoom on the comparison of drift rate with mean longitude

The longitude objective is accomplished. The longitudes at the beginning of every control cycle are at the same region, with a low tolerance.

Figure 41 shows that the thrust applied in the Drift/longitude strategy is almost constant, except the first manoeuvre that is an initialization manoeuvre. At the end of the year, the ΔV starts to increase, if this growth continues the initialization process shall activate

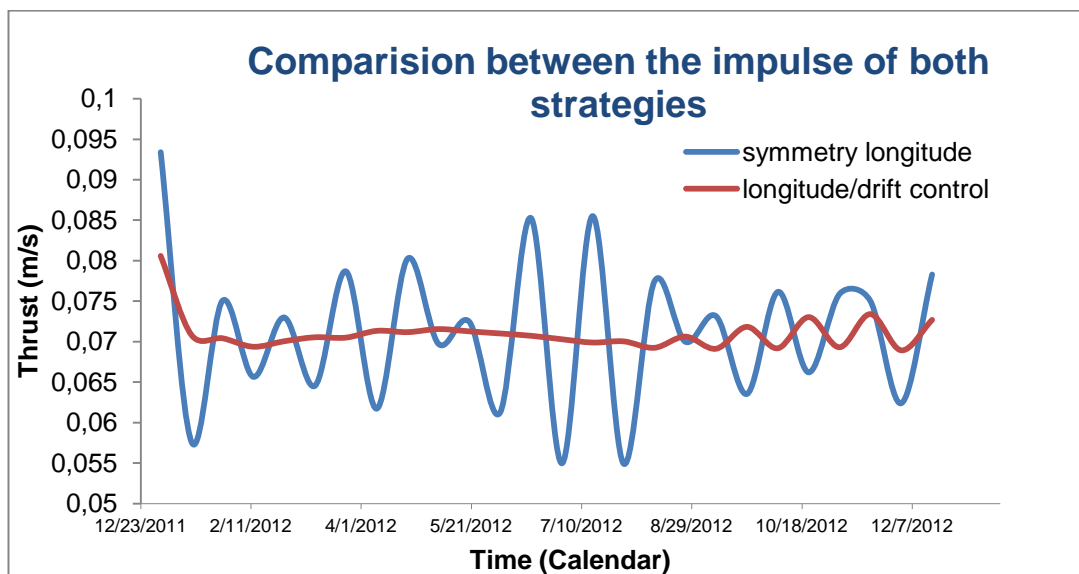


Figure 41- Comparison between the thrusts of both strategies at $\lambda = 30^{\circ}E$

3. ECCENTRICITY CONTROL

3.1. Eccentricity requirements

- The eccentricity strategy shall be complementary with the longitude strategy.

The amplitude of the longitude fluctuations depends on the eccentricity ($2e$), so enforcing a good eccentricity control; the longitude control will improve.

- The eccentricity control shall determine the time of the manoeuvre.

The time of the manoeuvre is a free parameter that has not been treated in the longitude control, because it has been reserved for the eccentricity control. The ΔV is calculated by the longitude control, but the time when the manoeuvre will be realized will only depend on the eccentricity.

- The eccentricity control shall follow any control circle.

The control circle is imposed by the Operators which take care of different satellites which are placed at the same longitudes. The radius and the position of the circle are chosen at the beginning of the mission, and the eccentricity must follow the circle as close as possible.

The control circle will only change in case that the mission changes.

- Double manoeuvres shall be allowed in cases where the eccentricity vector is too far from the control circle sought.

In case that the direction of a single manoeuvre was pointing directly to the control circle and it did not reach it, a double manoeuvre will be necessary. They will be realized only in a strictly necessary case because the aim of the algorithm is to get the right control using the minimum manoeuvres possible.

- The time of the manoeuvre shall be in the first day of a cycle.

The eccentricity vector points to any direction throughout a day, so the choice of the first day is to constrain the problem.

However, not all the hours of a day are good because the thrusters in geostationary orbit use normally three axis controller to be pointing always to the Earth. If the thrusters are burning when the nozzle is pointing to the Sun, the temperature could reach a maximum and an undesirable effect could happen.

3.2. Eccentricity evolution

3.2.1. Sun pressure perturbation

The main contribution to the eccentricity evolution is **the solar radiation pressure**. The solar pressure constant is the power that the Sun produces in the form of electromagnetic radiation. The mean radiation intensity (I) near the Earth is 1.4kW/m^2 . The solar radiation pressure is defined by the radiation intensity divided by the light velocity ($c = 3 \cdot 10^8 \text{ m/s}$), Agrawal [3]

$$\frac{I}{c} = P = 4.56 \text{ N/m}^2 \quad (82)$$

The electromagnetic radiation pressure exerts a force on the spacecraft proportional to its cross-section (C) which points to the Sun.

$$F = PC(1 + \epsilon) \quad (83)$$

Where ϵ is the reflectivity coefficient of the surface, which could take a value between $0 < \epsilon < 1$ according the surface materials.

The acceleration caused by the solar pressure is

$$\frac{dv}{dt} = \frac{PC(1+\epsilon)}{m} \quad (84)$$

The acceleration depends on the cross-section to mass ratio (C/m) of the spacecraft.

The cross-section (C) is defined to be the area of the silhouette of the spacecraft, projected onto a plane perpendicular to the incoming Sun rays, so its value depends on the surface of the spacecraft which points to the Sun.

Accurate modelling of the solar radiation acceleration is difficult because different surfaces with different reflectivity are often exposed to the sunlight. Furthermore, the different types of reflectivity, diffuse or specular, contribute by deflecting the incoming rays. However, for most geostationary satellites it is sufficient to model the radiation acceleration with only one single parameter σ , which is called the effective cross-section to mass ratio.

$$\sigma = \frac{C(1+\epsilon)}{m} \quad (85)$$

This yields the acceleration

$$\frac{dv}{dt} = P\sigma \quad (86)$$

Not considering the declination of the Sun with the Earth (that would give a normal component to be studied in the inclination control); the acceleration produced by the sun radiation pressure could be interpreted as a tangential and radial acceleration. The two components in the tangential and radial directions of the velocity differential (dV_t, dV_r) from the radiation pressure become,

$$dV_t = \sin(s - s_s)dV$$

$$dV_r = \cos(s - s_s)dV$$

And from **equations (63)** and **(64)**, the variation of the eccentricity produced by the Sun pressure

$$\frac{de}{dt} = \begin{pmatrix} \frac{de_x}{dt} \\ \frac{de_y}{dt} \end{pmatrix} = \frac{2}{v} \begin{pmatrix} \cos s \\ \sin s \end{pmatrix} \frac{dV_t}{dt} + \frac{1}{v} \begin{pmatrix} \sin s \\ -\cos s \end{pmatrix} \frac{dV_r}{dt} \quad (87)$$

Integrating **equation (87)** and replacing $dt = ds/\psi$

$$\frac{de}{dt} = \frac{P\sigma}{2\pi V} \int_0^{2\pi} \left[2\sin(s - s_s) \begin{pmatrix} \cos s \\ \sin s \end{pmatrix} \frac{dV_t}{dt} - \begin{pmatrix} \sin s \\ -\cos s \end{pmatrix} \cos(s - s_s) \right] ds = \frac{3P\sigma}{2V} \begin{pmatrix} -\sin s_s \\ \cos s_s \end{pmatrix}$$

$$e(t) = e_0 + \frac{3P\sigma Y}{4\pi V} \begin{pmatrix} \cos s_s \\ \sin s_s \end{pmatrix} \quad (88)$$

Here, e_0 is the constant of integration, Y is the angular velocity of the Earth around the Sun (in 1 sidereal year) with respect to fixed stars and s_s is the right ascension of the Sun that can be approximated by

$$s_s \approx s_0 + Y(t - t_0)$$

Being s_0 the initial position of the Sun with respect to the Vernal point.

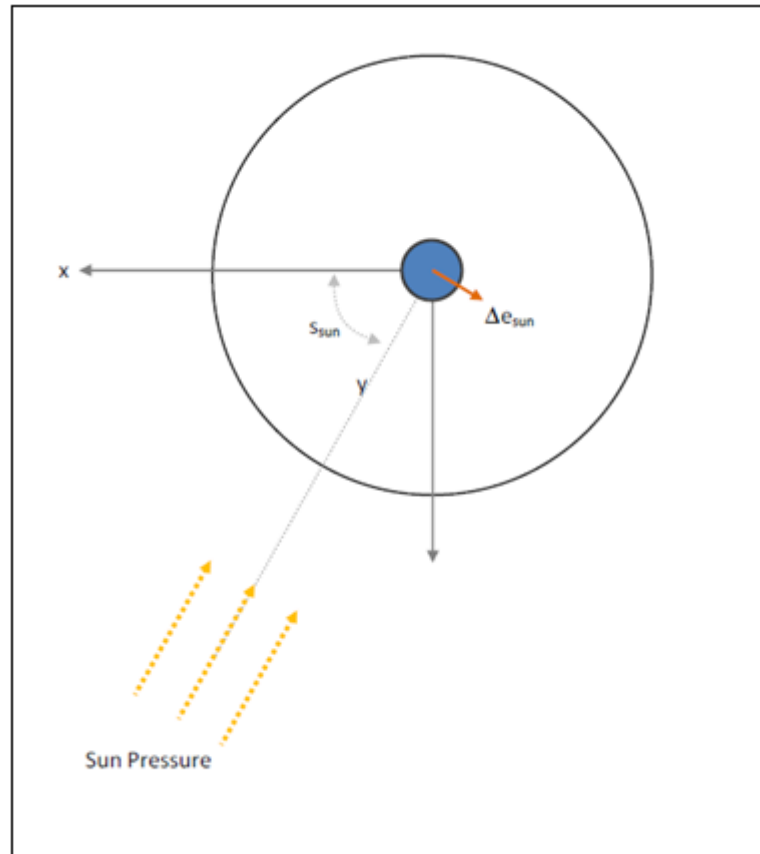


Figure 42 –Representation of the right ascension of the Sun, and its eccentricity perturbation

Because the velocity of the Earth around the Sun is not constant ($Y \neq ct$), the geometrical solution is a ellipse that can be approximated by a circle with the initial point e_0 .

The right ascension of the Sun is independent of the position of the satellite. The cross-section defines the radius of the circle, the constant of integration defines the starting point of the eccentricity evolution and the initial epoch defines the orientation of the circle. In one year, the initial and the final point would be the same.

Now, fixing e_0 in zero, fixing the effective cross-section to mass ratio and varying the initial epoch, the circles take these forms

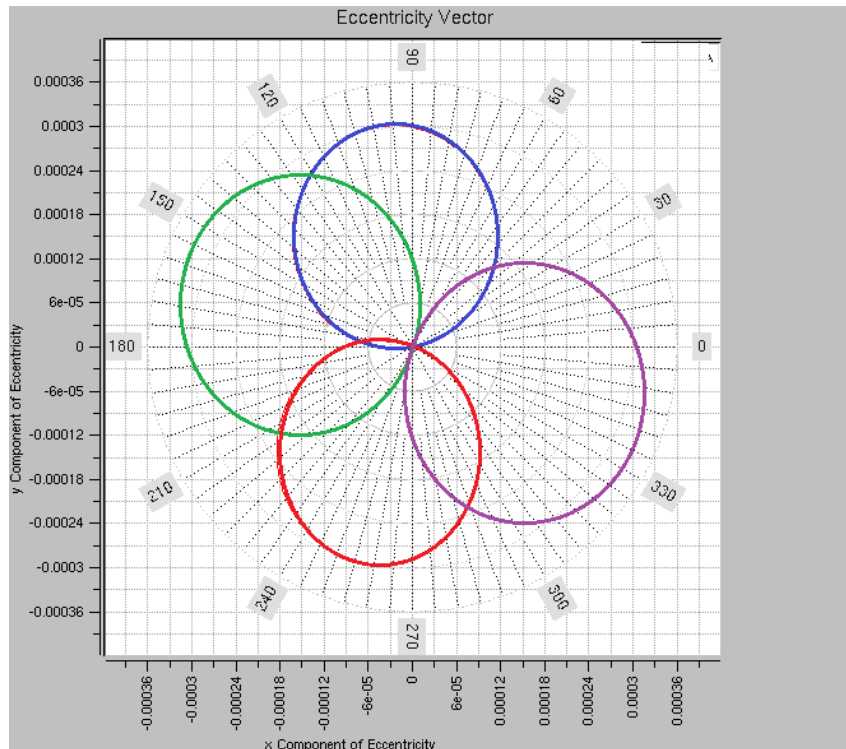


Figure 43-Eccentricity circles in one year varying the initial epoch

The blue circle starts on the date 2012/01/01, the green on 2012/03/01, the red on 2012/06/01, and the fuchsia on 2012/09/01.

The initial eccentricity (e_0) and the initial epoch do not affect to the size of the circle, only in the orientation that will follow.

However, the initial epoch was fixed in the initial inputs (2012/01/01 at 00.00.00h UTC), the cross-section is fixed by the mass and satellite surface lighted by the Sun, and the initial eccentricity vector was also fixed in the inputs. Hence the solar pressure evolution is predetermined.

Just like the velocity of the Earth around the Sun (Y), the solar radiation pressure (P) also depends on the distance from the satellite to the Sun. To understand better the effect of these factors, the coefficient $\frac{3P\sigma Y}{4\pi V} = \alpha$, also called cpsm (cross pressure section by mass) throughout a year is represented in **figure 44**

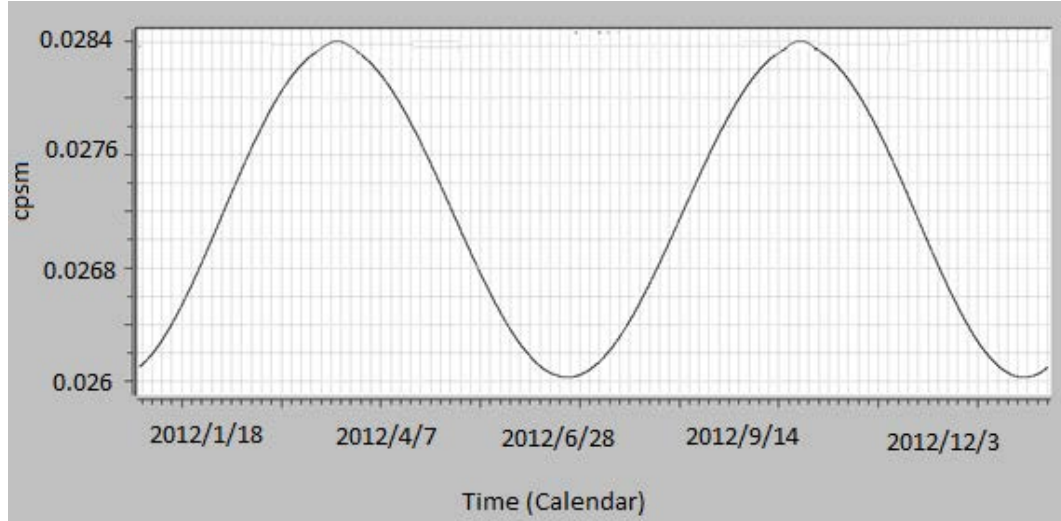


Figure 44-cpsm evolution in one year

The time evolution of the coefficient is sinusoidal. The peaks of the curve have the same height, because the fuel consumption caused by East/West manoeuvres in one year is negligible.

3.2.2. Other perturbations

The eccentricity control must be more accurate than the longitude control because of its order of magnitude. For this reason, the gravitational field of the Moon and Sun must be analysed.

The gravity potential of a third body is expressed

$$\frac{d^2 r_{sat}}{dt^2} = -\mu_* \left(\frac{(r_* - r_{sat})}{|r_* - r_{sat}|^3} - \frac{r_*}{r_*^3} \right) \quad (89)$$

In which the subscript * designates either the Moon or the Sun. So, the r_* designs the position vector from the Earth to the third body, and r_{sat} the position vector from the Earth to the satellite.

The positions of the Moon and Sun are derived from Brown theories (for the Moon) and Meeus theories (for the Sun), that are described in Vallado [6]

To calculate the Sun position vector, the mean longitude of the Sun (λ_{MS}) is calculated considering the nutation and the equinox precession.

$$\lambda_{MS} = 280.4606184^0 + 36000.77005361T_{UT1}$$

Where T_{UT1} is the number of Julian centuries, calculated with the expression

$$T_{UT1} = \frac{JD2000 - 2451545}{36525}$$

The mean anomaly of the Sun (M_S) is calculated by means of

$$M_S = 357.5277233^0 + 35999.05T_{UT1}$$

Because the Earth's orbit is approximately circular, it is possible to assume that the true anomaly is close to the longitude to express the ecliptic longitude (λ_{eclS}) as

$$\lambda_{eclS} = \lambda_{MS} + 1.914666 \sin M_S + 0.019994 \sin 2M_S + \dots$$

The distance in AU from the Earth to the Sun using an expansion of elliptic motion, Taff [10]

$$r_S = a_e \left[1 + \frac{e_e^2}{2} + \left\{ e_e + \frac{3e_e}{8} - \frac{5e_e^5}{192} + \dots \right\} \cos M_S + \left\{ -\frac{e_e^2}{2} + \frac{e_e^4}{3} - \frac{e_e^6}{16} + \dots \right\} \cos 2M_S \right]$$

By using the solar constants from Seidelmann [9], the value for the semimajor axis is $a_e = 1.00000100178 AU$ and for the eccentricity $e_e = 0.016708617$

Thus, it yields

$$r_S = 1.00014 - 0.016708 \cos M_S - 0.000139589 \cos 2M_S$$

And taking into account the obliquity of the ecliptic.

$$\epsilon_S = 23.439^0 - 0.013004T_{UT1}$$

The Sun position vector yields

$$r_S = \begin{bmatrix} r_S \cos \lambda_{ecl} \\ r_S \cos \epsilon \sin \lambda_{eclS} \\ r_S \sin \epsilon \sin \lambda_{eclS} \end{bmatrix}$$

The Moon's motion is very complex. Ernest Brown developed one of the best numerical theories to determine the position of the Moon. The longitude (λ_{eclM}), latitude (ϕ_{eclM}) and parallax (φ) are expressed following the series expansion, where M_M is the mean anomaly of the Moon,

$$\lambda_{eclM} = 218.32^0 + 48126708813T_{UT1} + 6.29 \sin M_M - 1.27 \sin(M_M - 2D_S) + 0.66 \sin 2D_S + 0.21 \sin 2M_M - 0.19 \sin M_S - 0.11 \sin 2u_M(90)$$

$$\phi_{eclM} = 5.13 \sin u_M + 0.28 \sin(M_M + u_M) - 0.28 \sin(u_M - M_M) - 0.17 \sin(u_M - 2D_S) (91)$$

$$\begin{aligned} \varphi = & \\ & 0.9508^0 + 0.0518 \cos M_M 0.0095 \cos(M_M - 2D_S) + \\ & 0.0078 \cos 2D_S 0.0028 \cos 2M_M \quad (92) \end{aligned}$$

$$r_M = \frac{1}{p(\sin\varphi)} \quad (93)$$

Where the p in the **equation 93** means that is measured in parsecs, and D_S, u_M, M_M are auxiliary values that are calculated following the next formulas
 $D_S = 297.85027^0 + 445267.111^0 T_{UT1}$, $M_M = 357.52543^0 + 35999.04944 T_{UT1}$,
 $u_M = 134.96292^0 + 477198.86753 T_{UT1}$

$$r_M = \begin{bmatrix} r_M \cos \lambda_{ecl} \cos \phi_{eclM} \\ r_M [\cos \epsilon \sin \lambda_{eclS} \cos \phi_{eclM} - \sin \epsilon \sin \phi_{eclM}] \\ r_M [\sin \epsilon \sin \lambda_{eclS} \cos \phi_{eclM} - \cos \epsilon \sin \phi_{eclM}] \end{bmatrix} \quad (94)$$

The third's body effect on the satellite could be calculated using a numerical integration, but there is a potential difficulty, the distance from the Earth to the Sun and the distance from the satellite are very similar, and the cube of the difference of these distance are in the denominator.

One solution is to expand $\frac{1}{|r_* - r_{sat}|^3} = \frac{1}{r_{sat}^3}$ in a series that is the generating function for Legendre polynomials. Where r_{sat-*} is the distance from the 3th body to the satellite.

$$\frac{1}{r_{sat-*}^3} = \frac{1}{r_*} \left\{ P_0 \cos \zeta + P_1 \cos \zeta \frac{r_{sat}}{r_*} + \dots \right\} = \frac{1+B}{r_*}$$

Where $B = \sum_{j=1}^{\infty} P_j \cos \zeta \left(\frac{r_{sat}}{r_*} \right)^j$ and ζ is the angle between the third body and the satellite as seen from the Earth

Substituting the expansion in the **equation (100)** and expressing $\beta = (1+B)^3$

$$\frac{d^2 r_{sat}}{dt^2} = \sum_{k=1}^2 -\mu_* \frac{(r_{sat} - \beta_k (r_* - r_{sat}))}{r_*^3} \quad (95)$$

Finally, the perturbation potential function by expressing the third body potential in terms of the Legendre polynomials

$$R_{3-body} = \frac{\mu_*}{r_*} \sum_{l=2}^{\infty} \left(\frac{r}{r_*} \right)^l P_l \cos \zeta \quad (96)$$

By using the same development than in the gravitational field, showed in **equation (53)**, the function yields

$$R_{3-body} = \sum_{l=2}^{\infty} r_{sat}^l P_{lm} \sin \theta [A_{lm} \cos m \lambda + B_{lm} \sin m \lambda] \quad (97)$$

In this case, the coefficients take the following values

$$A_{lm} = \frac{\mu_*}{r_*^{l+1}} \frac{(l-m)!}{(l+m)!} P_{lm} \sin \theta \cos m \lambda \quad (98)$$

$$B_{lm} = \frac{\mu_*}{r_*^{l+1}} \frac{(l-m)!}{(l+m)!} P_{lm} \sin \theta \sin m \lambda \quad (99)$$

Now, using the equations of the variations of the synchronous elements of the **section 1.7.3** and assuming that

$$r_{sat} = a(1 - e_x \cos(s_s) - e_y \sin(s_s)) \quad (100)$$

$$r_{sat} = \begin{bmatrix} r_{sat}(\cos s + e_x(\cos 2s - 1) + e_y \sin 2s) \\ r_{sat}(\sin s + e_y(\cos 2s - 1) + e_x \sin 2s) \\ 0 \end{bmatrix} \quad (101)$$

Including this equations in the expressions **(35)** and **(36)** the result yields, according to P.Lagrange [7]

$$\begin{aligned} \frac{de_x}{dt} = & K_* \left(\frac{a_*}{r_*}\right)^3 \left[-\sin s - \frac{3}{4}x_*^2(\sin s + \sin 3s) + \frac{3}{4}y_*^2(5 \sin s + 3 \sin s) + \frac{3}{2}x_*y_*(3 \cos s + \cos 3s) \right] + \\ & K_* \left(\frac{a_*}{r_*}\right)^4 \left(\frac{a}{a_*}\right) \left[\frac{15}{16}y_*(1 - 5z_*) - \frac{3}{4}x_*^2 \sin 2s + \frac{3}{4}x_* \cos 2s - \frac{15}{8}x_*^3 \left(\sin 2s + \frac{1}{2} \sin 4s\right) + \frac{45}{16}x_*y_*^2 \left(\frac{10}{3} \sin 2s + \right. \right. \\ & \left. \left. \sin 4s\right) + \frac{45}{16}x_*^2y_* \left(\frac{3}{2} \sin 2s + \cos 4s\right) - \frac{15}{16}y_*^3(4 \cos 2s + \cos 4s) \right] \quad (102) \end{aligned}$$

$$\begin{aligned} \frac{de_y}{dt} = & K_* \left(\frac{a_*}{r_*}\right)^3 \left[\cos s - \frac{3}{4}x_*^2(5 \cos s - \cos 3s) + \frac{3}{4}y_*^2(\cos s - \cos 3s) + \frac{3}{2}x_*y_*(\sin 3s - 3 \sin s) \right] + \\ & K_* \left(\frac{a_*}{r_*}\right)^4 \left(\frac{a}{a_*}\right) \left[-\frac{15}{16}x_*(1 - 5z_*) + \frac{3}{4}y_*^2 \cos 2s + \frac{3}{4}y_* \sin 2s + \frac{15}{8}y_*^3 \left(\sin 2s - \frac{1}{2} \sin 4s\right) + \frac{45}{16}x_*y_*^2 \left(\frac{8}{3} \cos 2s + \right. \right. \\ & \left. \left. \cos 4s\right) - \frac{45}{16}x_*^2y_* \left(\frac{10}{3} \sin 2s - \sin 4s\right) - \frac{15}{16}x_*^3(4 \cos 2s - \cos 4s) \right] \quad (103) \end{aligned}$$

Being s the right ascension of the satellite, K_* a constant, a_* the semimajor axis, r_* the radial distance from the satellite to the Earth and x_* and y_* both components from the distance of the Earth to the centre of the third body.

Substituting the subscript $*$ by the Moon and the Sun and integrating numerically, the solution is a trigonometric series in which the coefficients are constants and known and the arguments are linear combination of parameters evolving linearly with the time.

$$e_x = e_{x0} + \sum_{j=1}^{44} \alpha_j \cos(w_j t + \gamma_j + k_j s) \quad (104)$$

$$e_y = e_{y0} + \sum_{j=1}^{44} \beta_j \sin(w_j t + \gamma_j + k_j s) \quad (105)$$

The coefficients α, β, w, γ and k have different orders of magnitude because they represent different perturbed sources, for instance, the Moon affects mainly the eccentricity in two main ways.

On one hand, the eccentricity produces loops in cycles approximately constant of 29.5 days (synodic period between the Moon and the Earth). The **figure 48** shows these loops in 56 days (3 times the period cycle T)

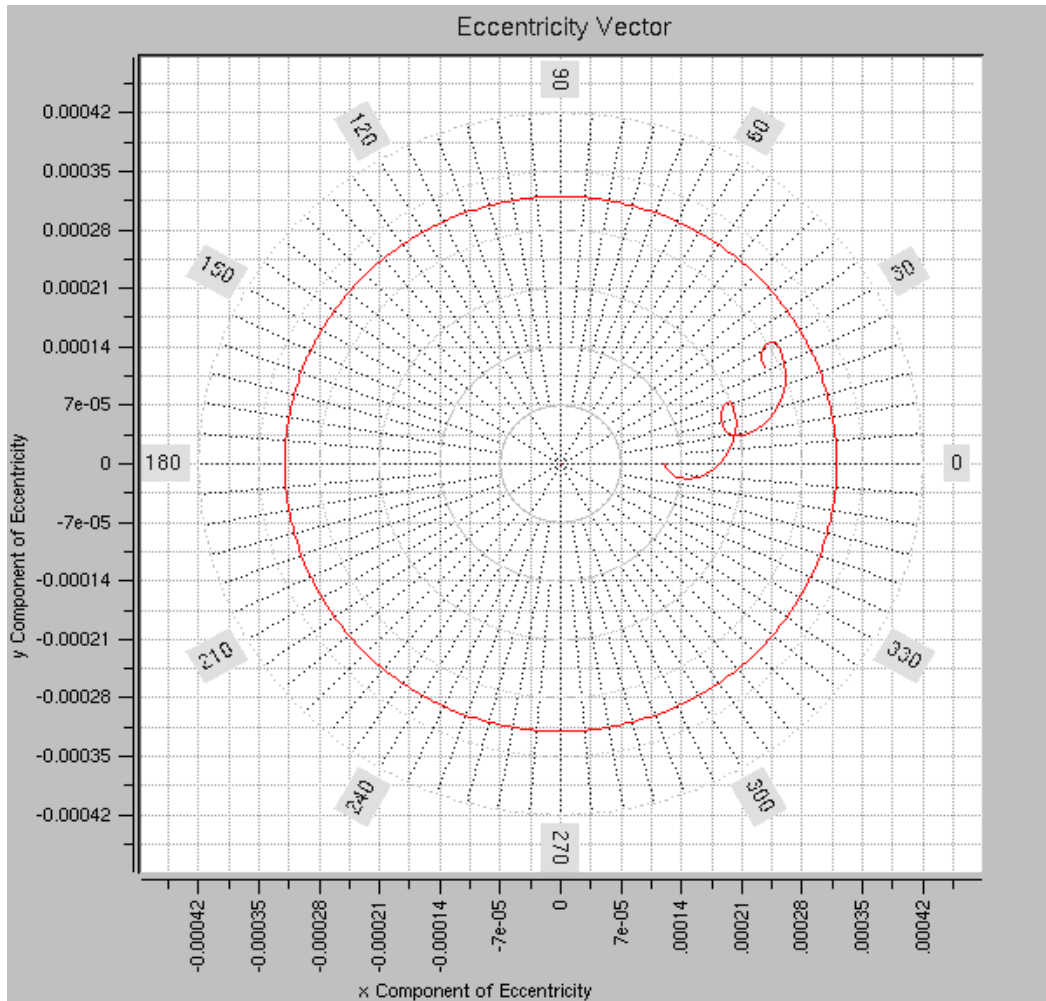


Figure 45- Loops produced by the synodic period of the Moon

On the other hand, the lunar node cycles of approximately 18.9 years produces a secular effect which moves the circle in one direction according the epoch. This effect makes that the circle does not close, as shown in the **figure 46**, where all the perturbations are included.

By the way, the effect of the gravitational field of the Sun could be considered constant and inferior to the gravitational field of the Moon.

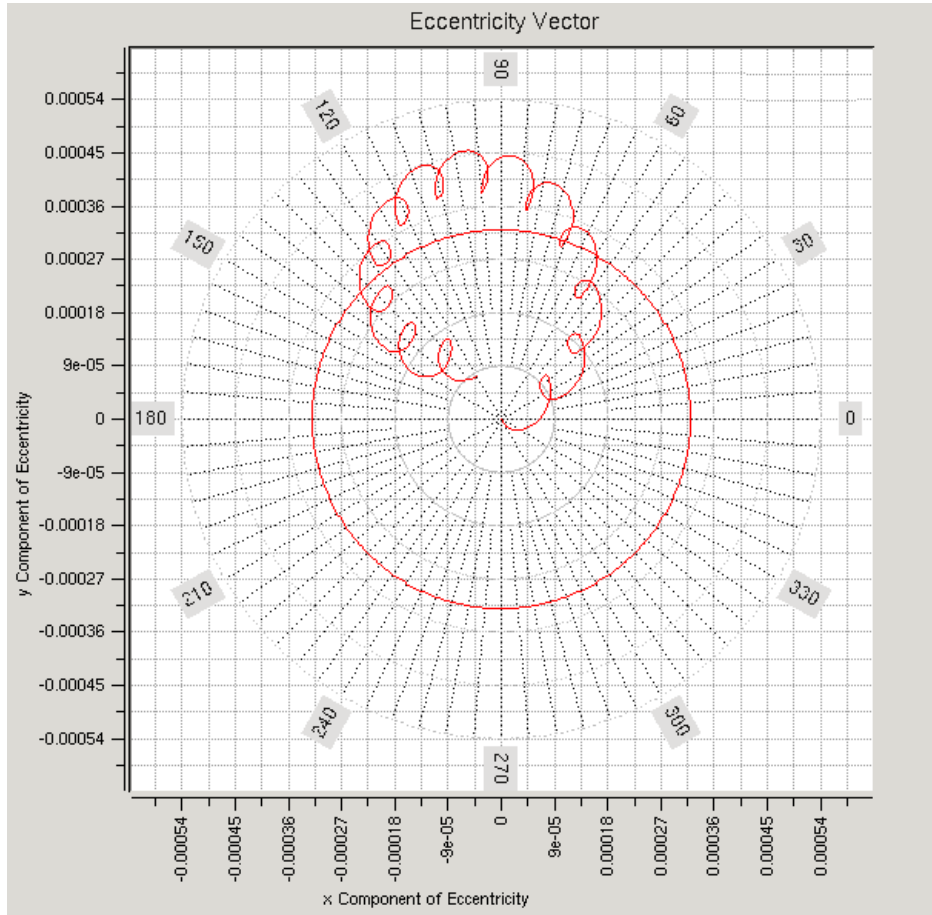


Figure 46-Free evolution of the Mean eccentricity in one year

Now that the perturbed elements are identified, it is time to know how the manoeuvres will influence the mean eccentricity.

According to the expressions of the **section 2.3** the influence of a single manoeuvre affects the eccentricity following the expression

$$\Delta e = \frac{2\Delta V}{v} \begin{pmatrix} \cos s_b \\ \sin s_b \end{pmatrix} \quad (106)$$

Where s_b is the right ascension of the satellite when the manoeuvre is applied.

$$s_b = G_0 + \psi(t - t_0) + \lambda_T \quad (107)$$

G_0 is a constant that in the year 2012 takes the value 100.06^0

$(t - t_0)$ is the difference of time from the initial epoch.

Thus, the **time of the manoeuvre**, that had been constant at 00:00:00h UTC in the longitude control will be chosen to control the eccentricity.

3.2.3. Control circle

The choice of the control circle is determined by the collocation. Collocation is the technique to place some geostationary satellites at the same longitude without danger of collision. For this reason, the eccentricity evolution has to follow with the maximum accuracy the control circle, but also with the same velocity.

In order to avoid collisions between satellites placed at same longitude, there are two parameters to consider, **the intersatellite distance and the angular separation.**

Intersatellite distance is the distance between pairs of satellites

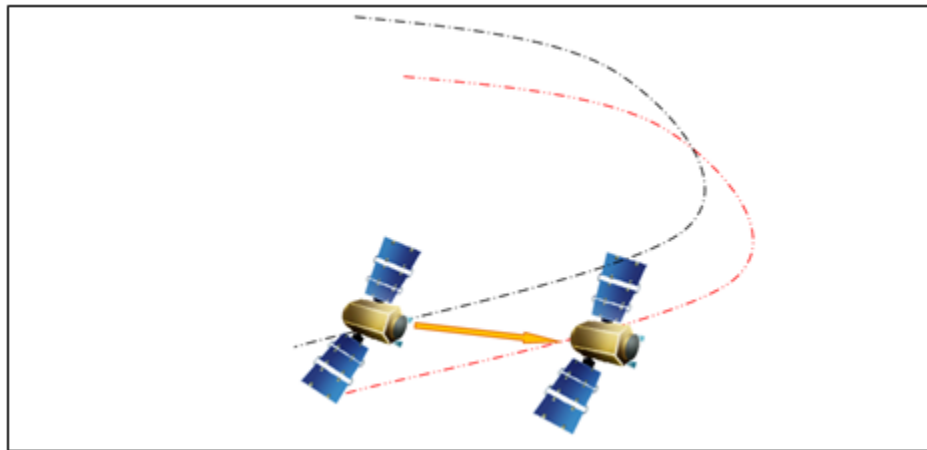


Figure 47- Intersatellite distance between two satellites placed at same longitude

Angular separation means the angle between pairs of satellites measured from a certain ground station.

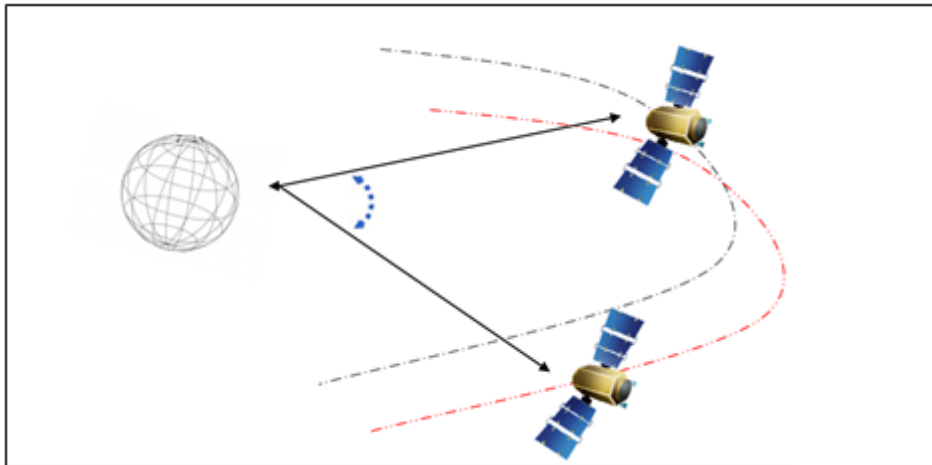


Figure 48- Angular separation between two satellites placed at same longitude

These parameters have to be approximately constant during the satellite mission. For this reason, the eccentricity vector does not have to follow any circle; the eccentricity vector must follow the circle of control, such as mentioned in the eccentricity requirements. The size of the control circle will be an input.

To preserve the intersatellite distance, the real longitude must be controlled, and for the angular separation, the real inclination.

According to these assumptions, the eccentricity must fulfil that when the satellites are placed in the intersection of their orbit planes, the separation must be longitudinal

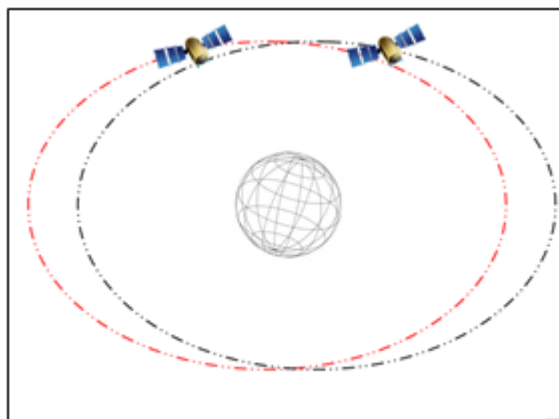


Figure 49- Pair of satellites in the intersection of their orbit planes

When the satellites are placed 90° from the intersection between their orbit planes, the separation must be radial.

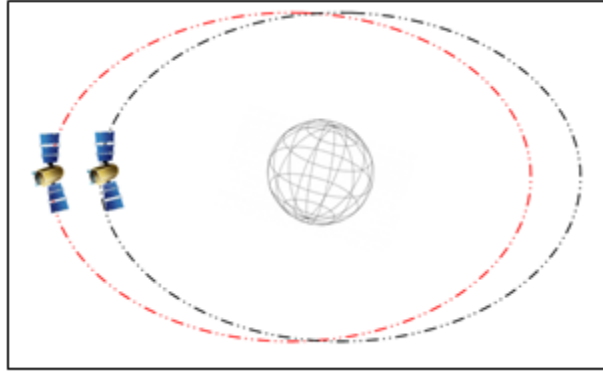


Figure 50- Pair of satellites 90° after the intersection of their orbit planes

In one year, the final and the initial eccentricity vector must be equal in order to assure that the collocation is being accomplished. The manoeuvres must correct also the perturbations that are not periodic in order to close the circle.

3.3. Sun-pointing perigee

The sun-pointing perigee strategy consists in choosing a more optimal time for the longitude drift correction thrust than apogee or perigee. It cannot prevent the eccentricity from achieving high values, however with only one manoeuvre is the strategy that provides the minimum eccentricity.

This strategy only will take into account the effects of the sun radiation pressure

The ΔV is that calculated in the previous section for the drift/longitude control, taking the **equation (62)**

$$\frac{\Delta D V}{3} = -\Delta V \rightarrow \frac{d\Delta V}{dt} \approx -\frac{\dot{\lambda} V}{3} \quad (108)$$

Thus, as was done in the **equation (87)**, the variation of eccentricity can be expressed as

$$\frac{de}{dt} \approx -\frac{2\dot{\lambda}}{3} \begin{pmatrix} \cos s_b \\ \sin s_b \end{pmatrix} \quad (109)$$

Combining the expressions of one single manoeuvre and the change of eccentricity by the Sun pressure

$$\frac{de}{dt} = \frac{3P\sigma}{2V} \begin{pmatrix} -\sin s_s \\ \cos s_s \end{pmatrix} - \frac{2}{3} \dot{\lambda} \begin{pmatrix} \cos s_b \\ \sin s_b \end{pmatrix} \quad (110)$$

Integrating

$$e(t) = e_0 + \left(\frac{3P\sigma}{2V} - \frac{2}{3}\dot{\lambda} \right) \frac{Y}{2\pi} \left(\frac{\cos s_b}{\sin s_b} \right) \quad (111)$$

The task is to select s_b to reduce the eccentricity and approach it to the circle of control.

There are two possible cases.

On one hand, if the eccentricity is near from the control circle, the manoeuvre must be done when was pointing to the Sun.

For this reason the right ascension takes the following values $s_b = s_s + \frac{\pi}{2}$ when the tesseral acceleration is positive, and $s_b = s_s - \frac{\pi}{2}$ when the tesseral acceleration is negative.

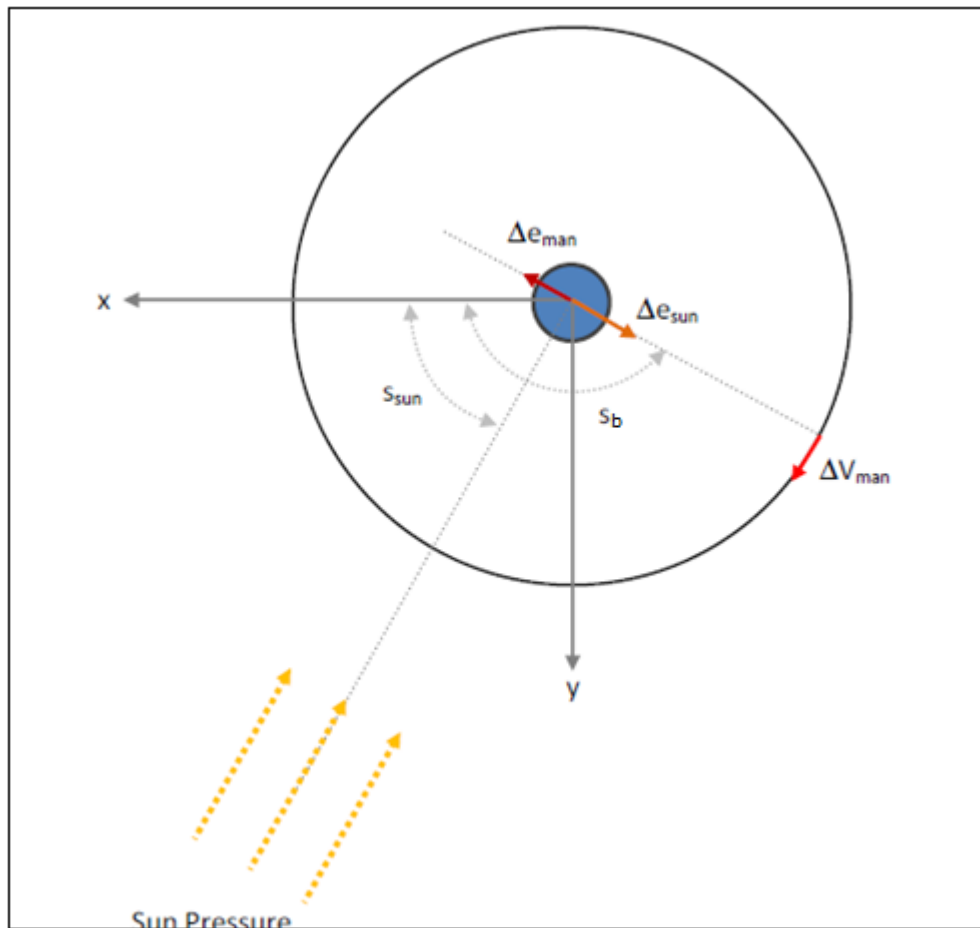


Figure 51- Eccentricity change when the manoeuvre is tangential

On the other hand, if the eccentricity has exceeded the tolerance and it is far of the control circle, the manoeuvre will have to be directly pointing to the control circle.

The targeted eccentricity at the beginning is the point of the control circle which is associated with the right ascension of the Sun. Dividing **equation (65)** by **equation (63)**

$$s_b = \text{atan} \left(\frac{e^T_y}{e^T_x} \right)$$

The super index T indicates that is the target. e^T_y and e^T_x are respectively $e_{control} \sin s_s$ and $e_{control} \cos s_s$

Pointing towards the Sun (s_s) the eccentricity vector rotates in a circle during one year and will have a constant size.

3.3.1. Algorithm

The diagram showed below represents the function **time_target** that will appear in the global algorithm at the end of the study, it shows the algorithm of the eccentricity strategy of sun-pointing.

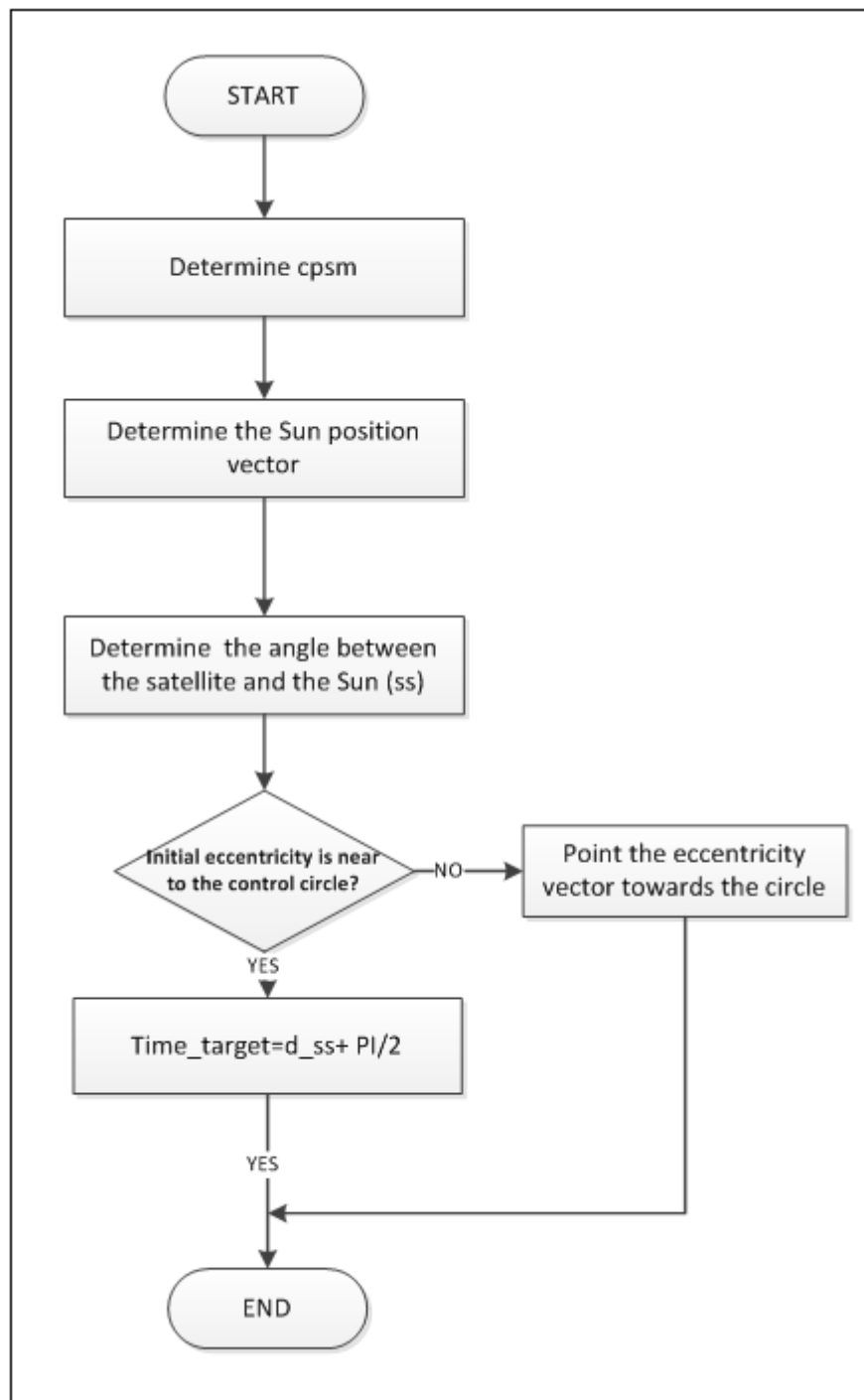


Diagram 6 – Algorithm of the eccentricity strategy of sun-pointing

The code of this strategy is quite simple. All the functions are self-explanatory.

- Calculate α (cpsm).

- Determine the Sun position vector.
- Determine the angle between the satellite and the Sun. The velocity of the Earth around the Sun is not constant, so this angle does not have a linear evolution. On 2012/04/21 at 00.00.00h UTC this angle is 0° , so this date will be used as reference to check the values.
- If the eccentricity vector is close to the control circle, the manoeuvre will be when will be pointing to the Sun. On the contrary case, the eccentricity will point directly to the control circle.

3.3.2. Results

The following results will be for $\lambda = 30^{\circ}\text{E}$

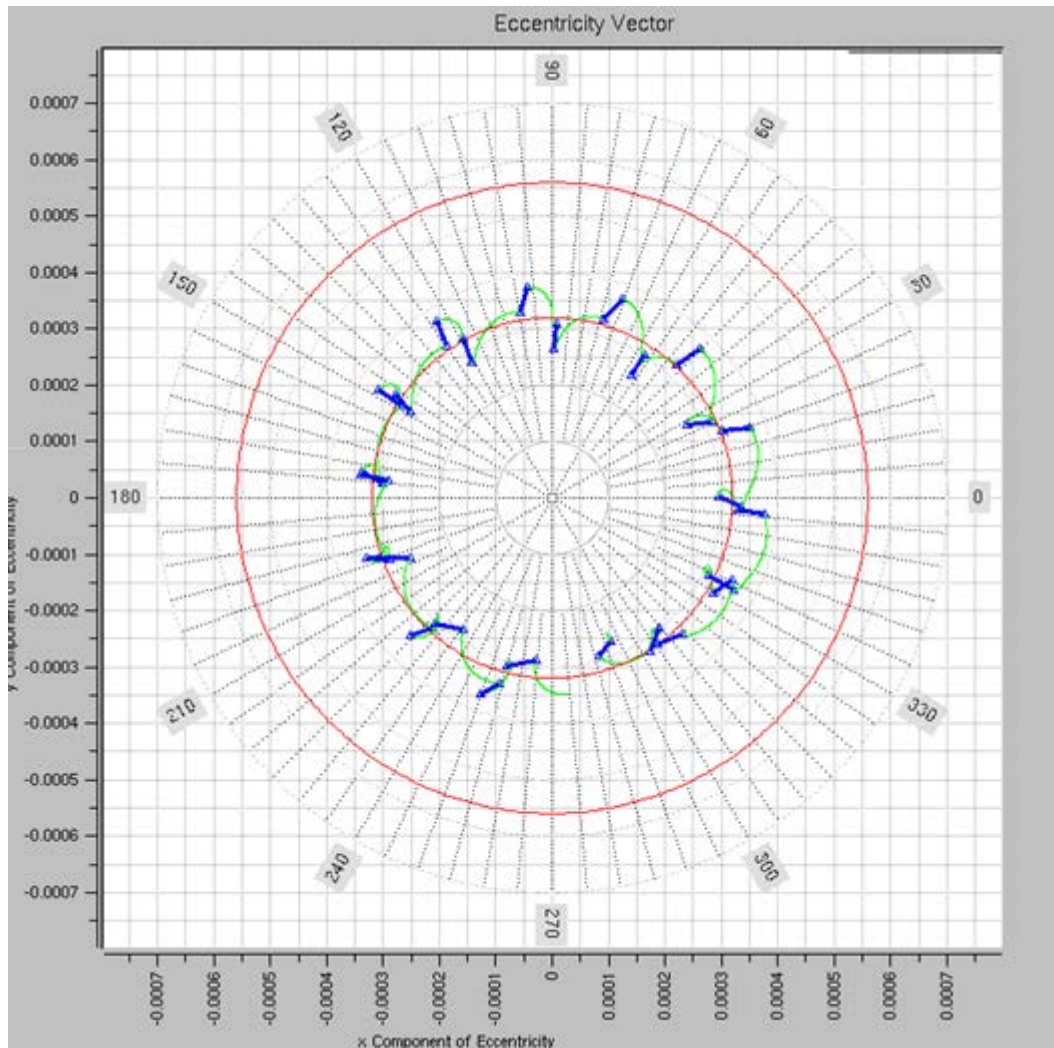


Figure 52- Mean eccentricity with sun-pointing perigee strategy

Only choosing the time of manoeuvring, the eccentricity vector can follow any circle. The sun-pointing perigee strategy does not have time restrictions, so the time of the manoeuvre can be at any hour in the day, causing problems in the drift/longitude strategy which needs to know previously when the manoeuvre will be applied.

The drift/longitude strategy puts the longitude in one point in order that the next cycle would accomplish the best parabola possible, so the time of the manoeuvre of the next cycle must be predicted approximately. If in the next cycle, the planned time changes, the algorithm has to do a process of initialization and the longitude will not repeat the same parabola.

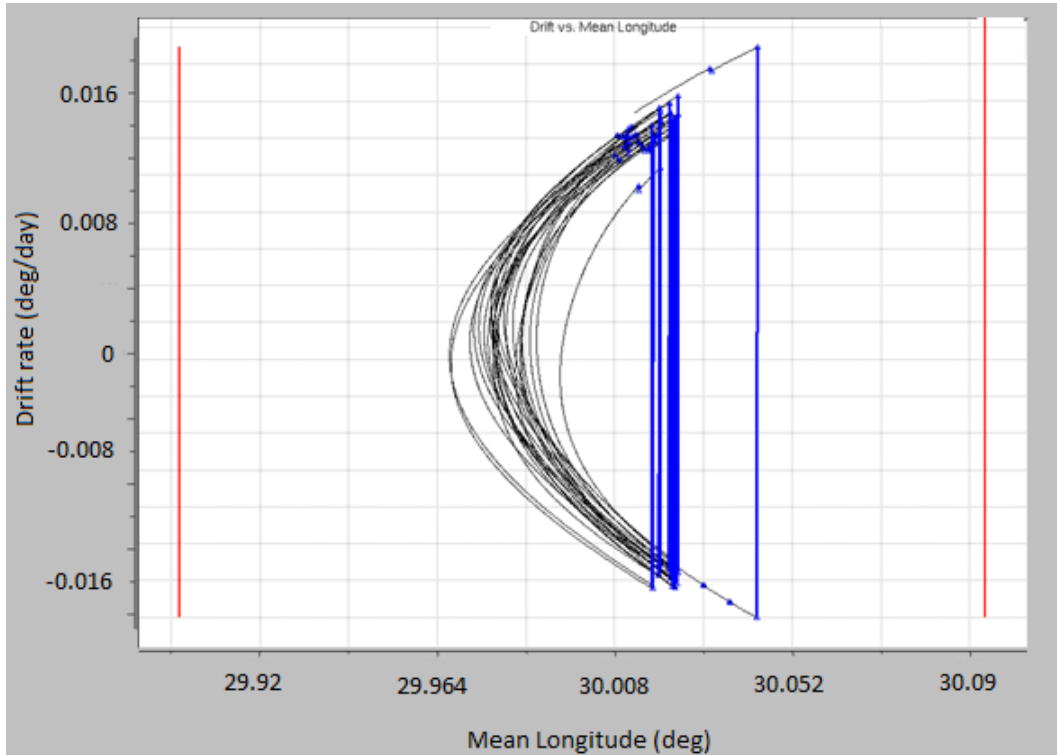


Figure 53- Drift rate vs mean longitude with sun-pointing perigee strategy.

The incompatibility with the drift/longitude strategy is not the only problem. The initial eccentricity vector does not coincide with the final eccentricity vector, because the only disturbing force considered is the sun radiation pressure.

Control cycle	ΔV (m/s)	Time when the manoeuvre is applied
01/01/2012	0.05017392	2012/01/01-06:40:42
15/01/2012	0.06936232	2012/01/15-06:54:53
29/01/2012	0.07296227	2012/01/29-14:59:18
12/02/2012	0.06376622	2012/02/12-02:50:00
26/02/2012	0.07579356	2012/02/26-09:29:39
11/03/2012	0.07128142	2012/03/11-22:02:32
25/03/2012	0.06592936	2012/03/25-08:07:00
08/04/2012	0.07650472	2012/04/08-21:15:41
22/04/2012	0.06642788	2012/04/22-08:25:50
06/05/2012	0.07585783	2012/05/06-21:22:06
20/05/2012	0.06762665	2012/05/20-09:48:39
03/06/2012	0.07417347	2012/06/03-20:24:01
17/06/2012	0.06756198	2012/06/17-09:50:00
01/07/2012	0.07345314	2012/07/01-20:07:38
15/07/2012	0.06640478	2012/07/15-09:54:52
29/07/2012	0.07381401	2012/07/29-21:02:16
12/08/2012	0.06469383	2012/08/12-09:14:07
26/08/2012	0.07556718	2012/08/26-21:20:42
09/09/2012	0.06340272	2012/09/09-08:38:05
23/09/2012	0.07817839	2012/09/23-20:53:47
07/10/2012	0.06232958	2012/10/07-08:31:45
21/10/2012	0.08032378	2012/10/21-19:58:52
04/11/2012	0.0618251	2012/11/04-08:25:56
18/11/2012	0.08066443	2012/11/18-17:20:24
02/12/2012	0.06141792	2012/12/02-07:02:33
16/12/2012	0.08033325	2012/12/16-17:07:09

Table - 3– List of manoeuvres with sun pointing and longitude/drift strategy ($\lambda = 30^\circ E$)

Analyzing the effect of the eccentricity strategy in the equilibrium points.

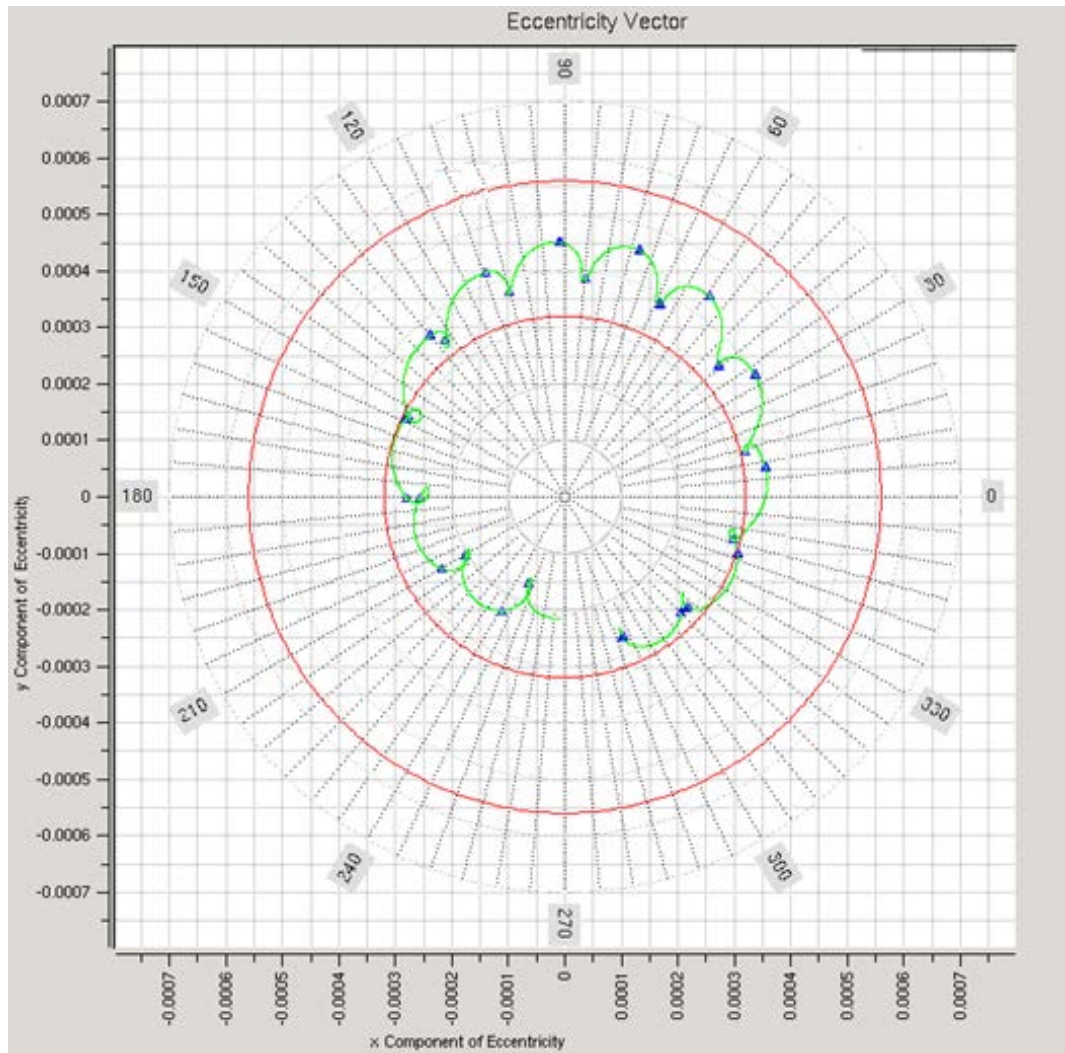


Figure 54- Eccentricity evolution with sun pointing perigee strategy at an equilibrium point

Any eccentricity strategy is difficult to apply to the equilibrium points because the ΔV will be always so small to correct any perturbation. For this reason, the only solution would be to move the eccentricity evolution the closest to the control circle.

3.4. Fixed time with variations strategy

The strategy of sun-pointing perigee has the problem that there is no connection between the times of the manoeuvres in the different cycles. The time is optimized in each cycle to get the eccentricity target. In order to solve this problem, the eccentricity strategy must be planned thinking in the eccentricity evolution in long term (one year)

In this new strategy, the objectives are to find a time (approximately constant throughout the mission) when the manoeuvres will be applied, and that the final and initial eccentricities take the same value (the eccentricity evolution closes)

The eccentricity will be propagated in one year in steps of cycles of control (14 days). The time of the manoeuvres will change in order to obtain the optimal time whose radius were the same than the control circle.

Obviously, the eccentricity evolution cannot reach all the control circles. It is limited for the time when the manoeuvres are tangential to the eccentricity (minimum control circle possible) evolution and when are normal to the eccentricity evolution (maximum control circle possible).

To develop this strategy, the orbit will be propagated considering the Sun radiation pressure, the influence of the Moon, the influence of the Sun and the manoeuvres as perturbing forces.

Once the time of the manoeuvre has been analyzed, the first step is to move the initial eccentricity to one point of the control circle in order to assure that in the next cycles the eccentricity will follow the control circle. This initial point is not any point of the control circle, it is the one which guarantee that the eccentricity will follow the circle with a fixed time in the manoeuvres.

As the initial eccentricity vector could take any value, in case that the centre of the analytical propagation does not have the same centre than the circle of the control circle, a double manoeuvre should be implemented.

3.4.1. Double manoeuvre

By applying two tangential ΔV at different times to the orbit, it is possible to produce any desired combination of the drift rate and eccentricity.

The new orbital elements can be obtained by superposition of the drift rate and eccentricity vector with the linear approximation done in the previous sections.

The two manoeuvres will be separated by half sidereal day.

$$s_{b2} = s_{b1} + \pi$$

s_{b1} is the right ascension of the satellite when the first manoeuvre is applied, and s_{b2} is when the second manoeuvre is applied.

The combination produces that

The sum $\Delta V_1 + \Delta V_2$ changes the longitude drift rate

The difference $\Delta V_1 - \Delta V_2$ changes the eccentricity

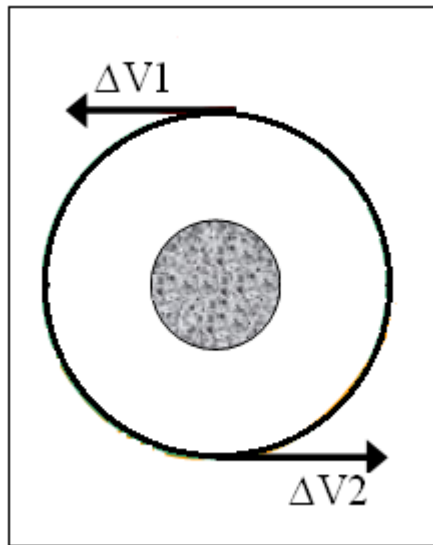


Figure 55- Double manoeuvre

The new effect in the equations is

$$\Delta a = \frac{2}{\psi} (\Delta V_1 + \Delta V_2) \quad (112)$$

$$\Delta \dot{\lambda} = -\frac{3}{v} (\Delta V_1 + \Delta V_2) \quad (113)$$

$$\Delta e = \frac{2}{v} (\Delta V_1 - \Delta V_2) \begin{pmatrix} \cos s_{b1} \\ \sin s_{b1} \end{pmatrix} = \frac{2}{v} (\Delta V_2 - \Delta V_1) \begin{pmatrix} \cos s_{b2} \\ \sin s_{b2} \end{pmatrix} \quad (114)$$

In the first interval time (between the first thrust and the second), the orbit changes under the influence of ΔV_1 . The eccentricity and the drift rate change instantaneously, however the longitude changes linearly, the velocity of longitude change depends on the value of the drift rate. Between ΔV_1 and ΔV_2 the longitude is necessary to take into account the longitude evolution to have a high accuracy.

$$\Delta\lambda = \frac{1}{v}(\Delta V_1 - \Delta V_2)[4 \sin(s - s_1) - 1.5\pi] - \frac{3}{v}(\Delta V_1 + \Delta V_2)\left(s - s_1 - \frac{\pi}{2}\right) \quad (115)$$

$$\Delta r = \frac{2}{\psi}[\Delta V_1 + \Delta V_2 - (\Delta V_1 - \Delta V_2) \cos(s - s_{b1})] \quad (116)$$

Changing the drift rate without changing the eccentricity or changing the eccentricity without changing the drift rate is possible with a double manoeuvre. In the first case both thrusts must take the same absolute value, in the second one, the addition of both must be zero.

3.4.2. Algorithm

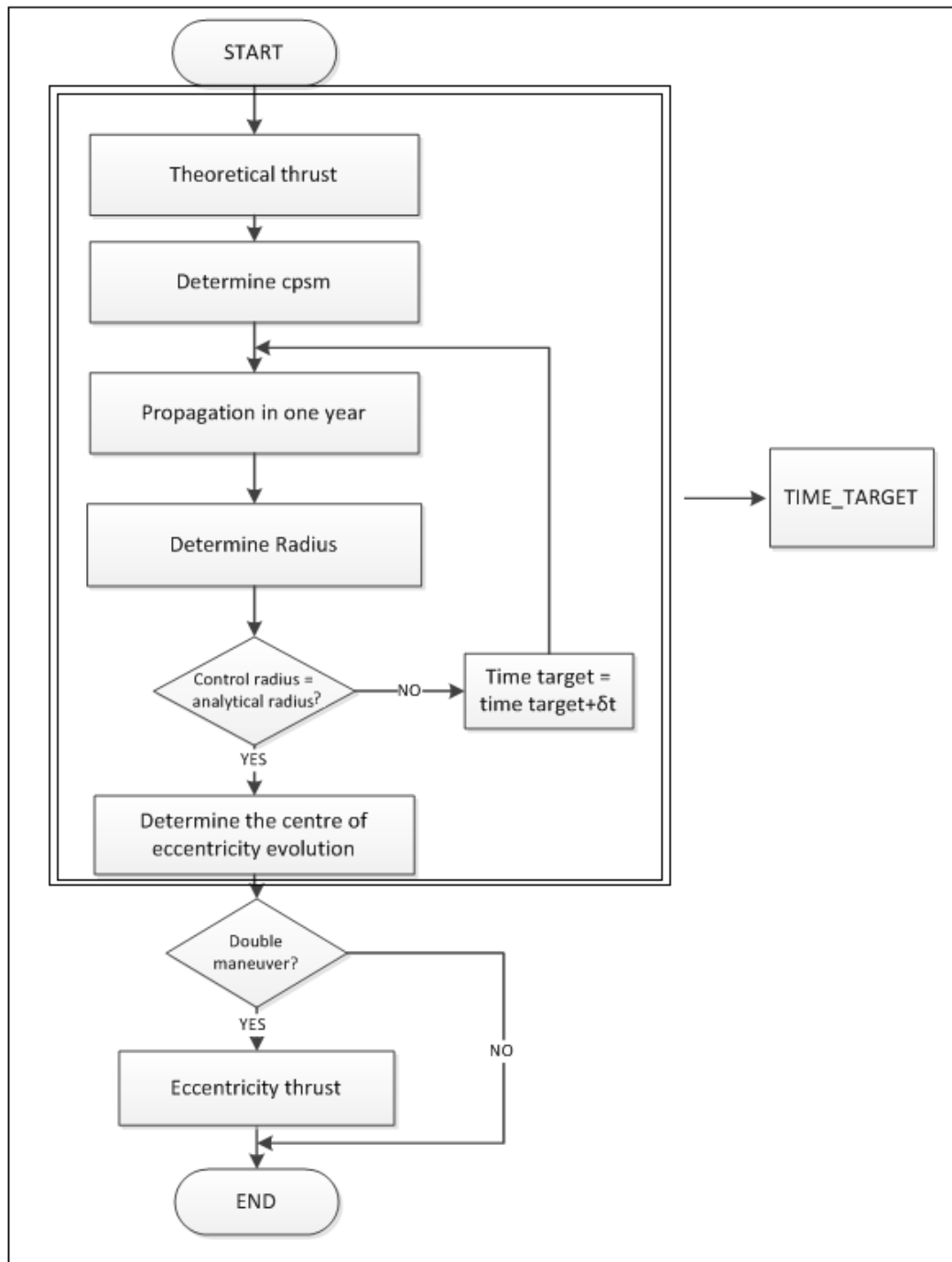


Diagram 7 – Algorithm of fixed time eccentricity strategy

- The theoretical thrust is calculated using the drift/longitude strategy. This ΔV will be considered as input to the function time_target.

- Determination of $\alpha(\mathbf{cpsm})$.
- The propagation in one year is done considering all the perturbations and the manoeuvres as perturbations that will have different influences according the time that have been chosed.

In each iteration, the eccentricity evolves following

$$e_{n+1} = e_n + \frac{3P\sigma Y}{4\pi V} \begin{pmatrix} \cos s_s^{n+1} \\ \sin s_s^{n+1} \end{pmatrix} + \frac{2\Delta V}{V} \begin{pmatrix} \cos s_b \\ \sin s_b \end{pmatrix} + \begin{pmatrix} \sum_{j=1}^{44} \alpha_j \cos(w_j t + \gamma_j + k_j s) \\ \sum_{j=1}^{44} \beta_j \sin(w_j t + \gamma_j + k_j s) \end{pmatrix} \quad (117)$$

Where s_b is fixed in a propagation of a year and s_s varies from the initial position until the end of a sidereal year, following the Sun.

- Radius is determined doing an average of the radius taken of the consecutive points.

$$R = \frac{364}{26 \cdot 14 \cdot 2\pi} \sum_{n=1}^{26} (e_{n+1} - e_n) \quad (118)$$

- Centre coordinates

$$\begin{pmatrix} C_x \\ C_y \end{pmatrix} = \frac{1}{26} \sum_{n=1}^{26} e_n - R \begin{pmatrix} \cos s_s^n \\ \sin s_s^n \end{pmatrix} \quad (119)$$

- The eccentricity target is the difference between the initial eccentricity vector and the centre of the eccentricity evolution.

$$e_0 - \begin{pmatrix} C_x \\ C_y \end{pmatrix} = e_T \quad (120)$$

3.4.3. Results

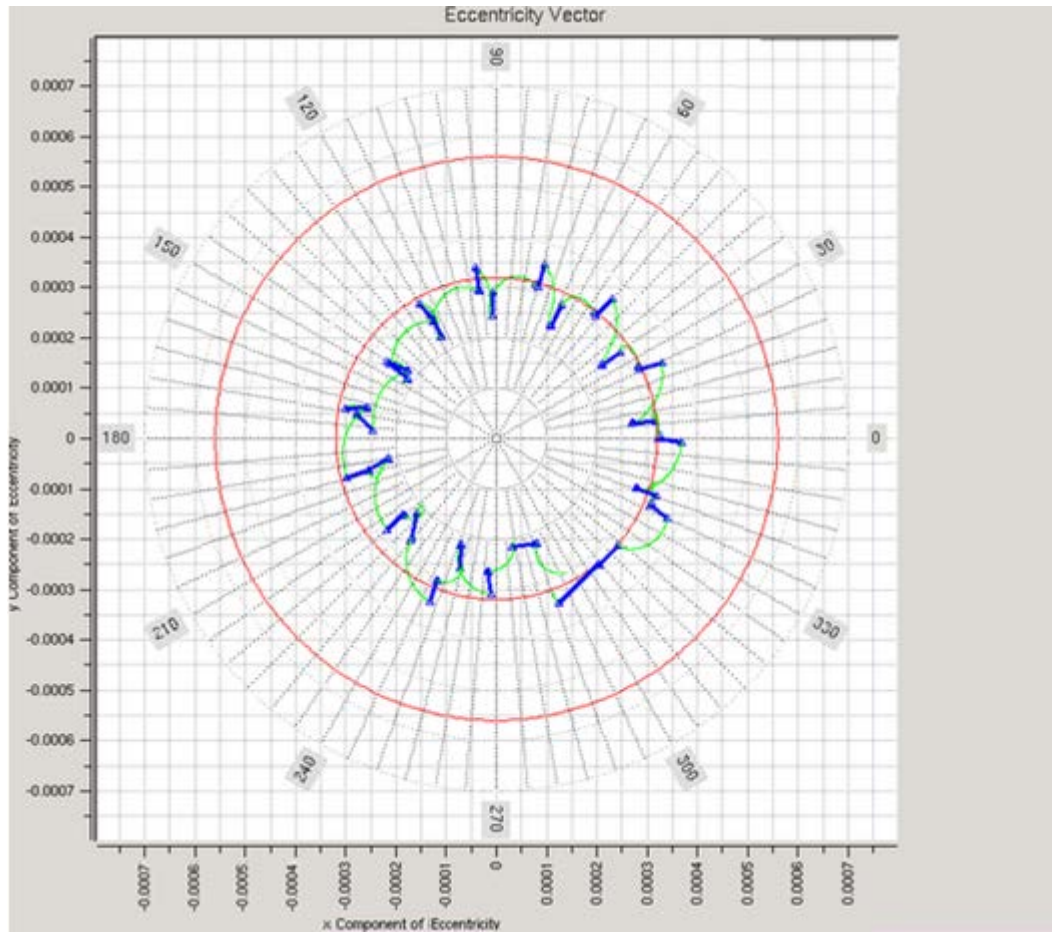


Figure 56- Eccentricity evolution with fixed time with variations strategy

The eccentricity follows the circle throughout one year with good accuracy, however, the final and the initial eccentricities do not coincide. Only fixing the time of the manoeuvre is not possible to close the eccentricity evolution. It is possible to follow the circle while not disturbing the drift/longitude strategy, but it is not possible to close it.

The optimum time of the manoeuvre to reach the control circle at longitude of 30 is 9.30h UTC local satellite. Hence, all the manoeuvres are at same time but with 14 days of difference.

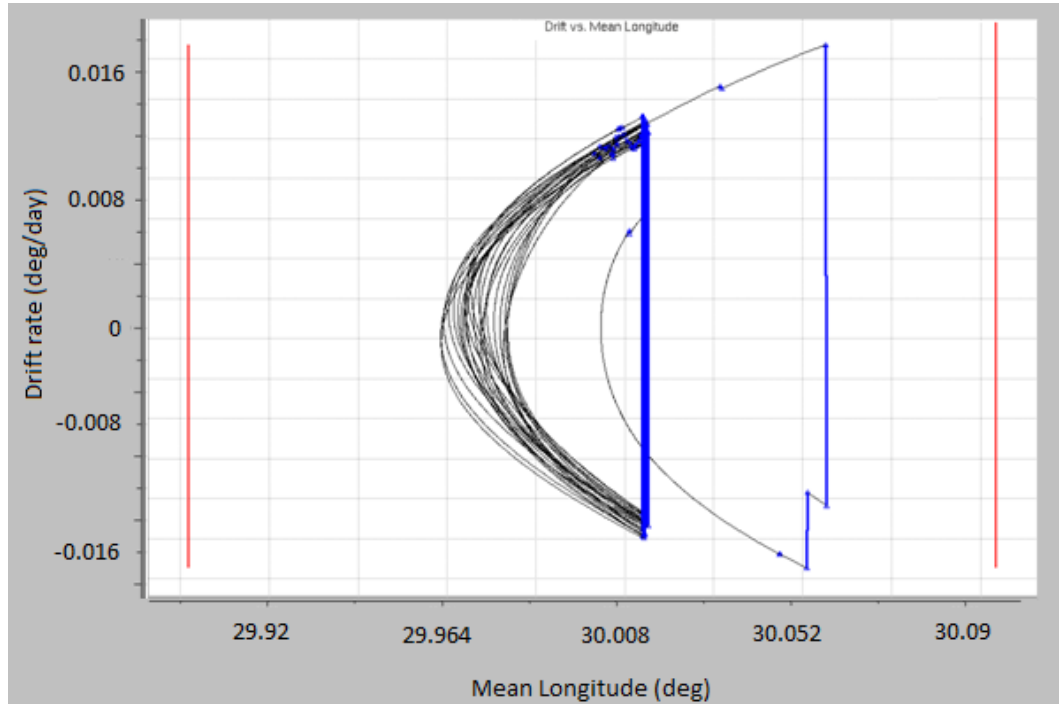


Figure 57- Drift rate vs mean longitude with fixed time with variations strategy

The eccentricity evolution can follow any circle fixing the time of the manoeuvre, so changing slightly the time of all the manoeuvres throughout a year, the initial and the final eccentricity could take the same value. Actually, this is not the best solution for the longitude control, but if the changes between two consecutive manoeuvres are small, the drift/longitude strategy will work right.

In the **section 3.2**, all the perturbing forces were analyzed; there were secular forces (Moon long terms and Sun gravity) that produce that the end and the initial of the eccentricity evolution do not close.

These perturbing forces will be omitted in the eccentricity evolution to determine the time of the manoeuvre because these contributions will be compensated for changing the time of the manoeuvre previously calculated.

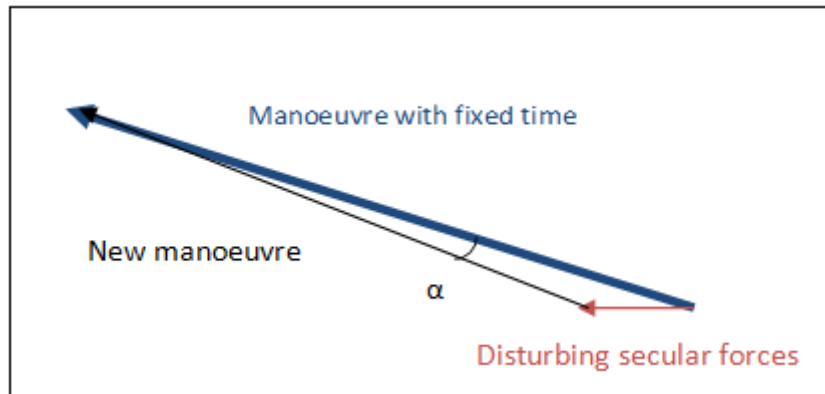


Figure 58- Variation of the direction of the thrust to compensate Moon's effect

In this way, in each control cycle (T) the contributions due to the secular disturbing forces will be cancelled changing the direction of the manoeuvre. It is possible because these contributions are small in short control cycles.

This angle α changes in each control cycle, because the position of the Sun and the Moon vary continuously. The angle is easy to find using a dot product, and the sign of the angle is determined by the cross product.

$$\alpha = \arccos\left(\frac{e_{fixed\ time} \cdot e_{disturbing\ secular\ forces}}{\|e_{fixed\ time}\| \|e_{disturbing\ secular\ forces}\|}\right) \text{sign}(e_{fixed\ time} \times e_{disturbing\ secular\ forces}) \quad (121)$$

Because the disturbing secular forces are small, this angle is also small. In case that the secular disturbing forces were higher, this strategy does not work with high accuracy.

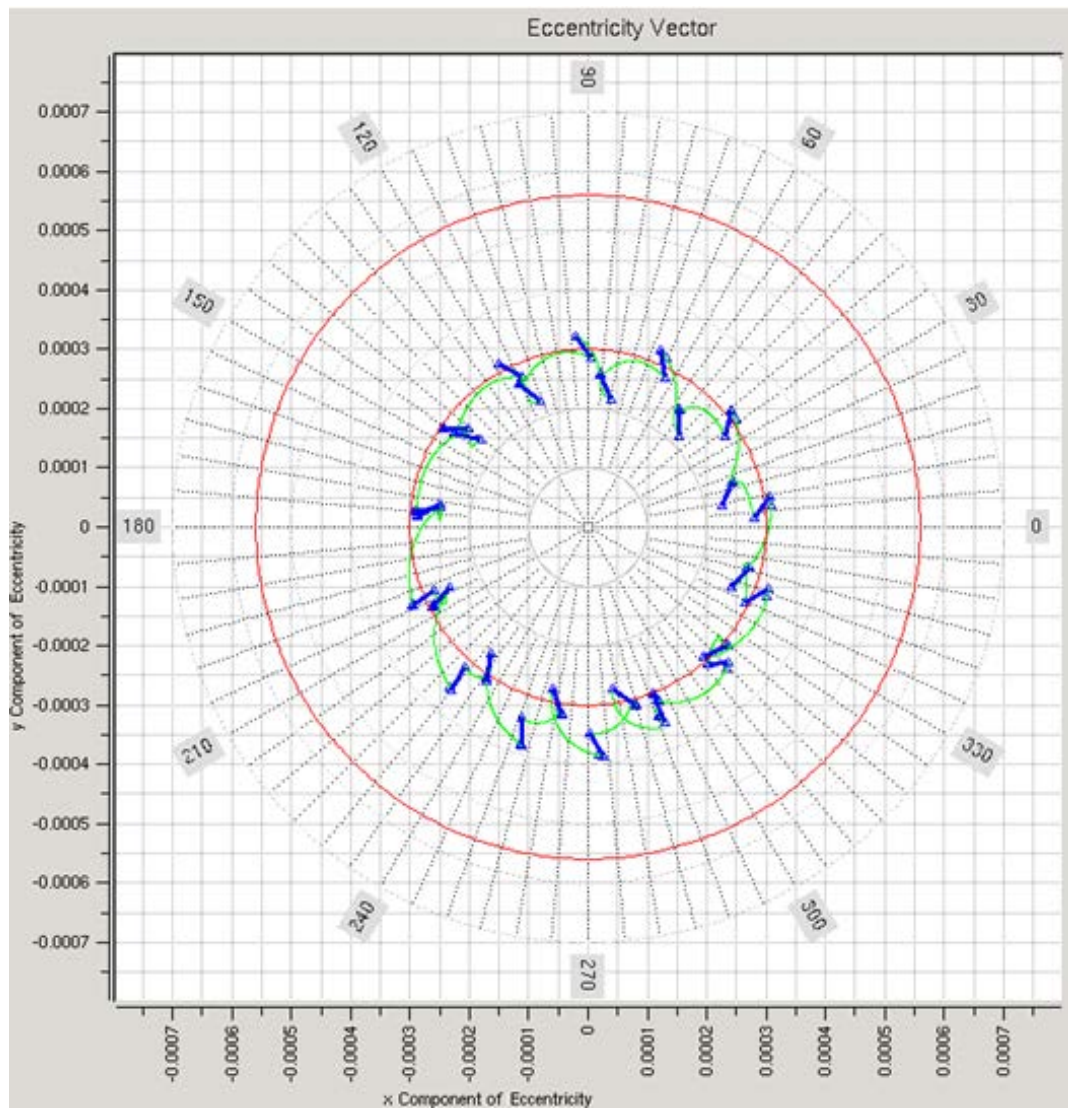


Figure 59- Mean eccentricity with the variation of the fixed time strategy

Now, the problem is solved. The times when the manoeuvres are applied are

Control cycle	ΔV (m/s)	Time when manoeuvre is applied
01/01/2012	0.07025894 0.02787545	01/01/2012 3:20:10 01/01/2012 15:20:10
15/01/2012	0.07236232	15/01/2012 9:52:30
29/01/2012	0.07096227	29/01/2012 9:59:42
12/02/2012	0.06894712	12/02/2012 9:46:44
26/02/2012	0.07054854	26/02/2012 9:43:52
11/03/2012	0.07128142	11/03/2012 9:33:47
25/03/2012	0.06892751	25/03/2012 9:40:16
08/04/2012	0.07258974	08/04/2012 9:38:49
22/04/2012	0.07468412	22/04/2012 9:36:36
06/05/2012	0.07585783	06/05/2012 9:33:43
20/05/2012	0.06968564	20/05/2012 9:27:15
03/06/2012	0.07417347	03/06/2012 9:17:10
17/06/2012	0.07158756	17/06/2012 9:11:24
01/07/2012	0.07254789	01/07/2012 9:09:58
15/07/2012	0.07058459	15/07/2012 9:08:31
29/07/2012	0.07389517	29/07/2012 9:06:22
12/08/2012	0.06859741	12/08/2012 9:09:58
26/08/2012	0.06987147	26/08/2012 9:08:14
09/09/2012	0.07258971	09/09/2012 9:06:48
23/09/2012	0.07058947	23/09/2012 9:04:42
07/10/2012	0.07459688	07/10/2012 9:07:17
21/10/2012	0.07259842	21/10/2012 9:18:48
04/11/2012	0.06741591	04/11/2012 9:22:16
18/11/2012	0.07002571	18/11/2012 9:25:17
02/12/2012	0.06587412	02/12/2012 9:26:43
16/12/2012	0.07051158	16/12/2012 9:28:44
30/12/2012	0.06748842	30/12/2012 9:35:56

Table - 4– List of manoeuvres with fixed time with variations and longitude/drift strategy ($\lambda = 30^{\circ}E$)

4. TRIPLE MANOEUVRES

Three burn manoeuvres will be considered only in extraordinary cases. These cases could be when the Operator has made a mistake or the burns have taken values really far from the expected. In these cases, the longitude, the drift rate and the eccentricity will be outside tolerance.

With only a single manoeuvre, it is possible to arrive to the targets imposed by the strategy, but the algorithm will spend many cycles (T) to get it. If the values are really far from the targets, and if the Operator wants to arrive to the targets immediately, the only solution possible is a triple manoeuvre.

Considering the linearized **equations (65)** and **(67)**, and that the time between a pair of manoeuvres is a half of a sidereal day.

The system to solve with three burns is

$$\Delta\lambda = \frac{3\pi}{v}(\Delta V_3 - \Delta V_1) - \frac{3}{v}(\Delta V_1 + \Delta V_2 + \Delta V_3)(s - s_2) \quad (122)$$

$$\Delta V_e = |\Delta V_1| + |\Delta V_2| + |\Delta V_3| \quad (123)$$

$$\Delta V_D = \Delta V_1 + \Delta V_2 + \Delta V_3 \quad (124)$$

The time of the first manoeuvre will be established by the eccentricity strategy (in order to reach the control circle), the second one, half sidereal day later, and the last manoeuvre one sidereal day later from the first one.

$$s_2 = s_1 + \pi$$

$$s_3 = s_1 + 2\pi$$

The ΔV_e will be the necessary to reach the point of the control circle that will determine strategy, according if it is sun-pointing strategy or fixed time with variations strategy, the points to reach will be different.

The parameters $\Delta\lambda$ and ΔV_D have to be performed to reach one point of the ideal parabola (drift rate with mean longitude).

In the verification process of the drift/longitude strategy, the second cycle is calculated in such a way that the drift rate with the mean longitude execute the ideal parabola. Thus, the drift rate (or semimajor axis) and the mean longitude to reach will be the point of this parabola.

Figure 60 shows that starting from a point placed wherever, in three burns the orbit achieve the control of drift eccentricity and longitude. While a double manoeuvre needed two cycles to control the three parameters.

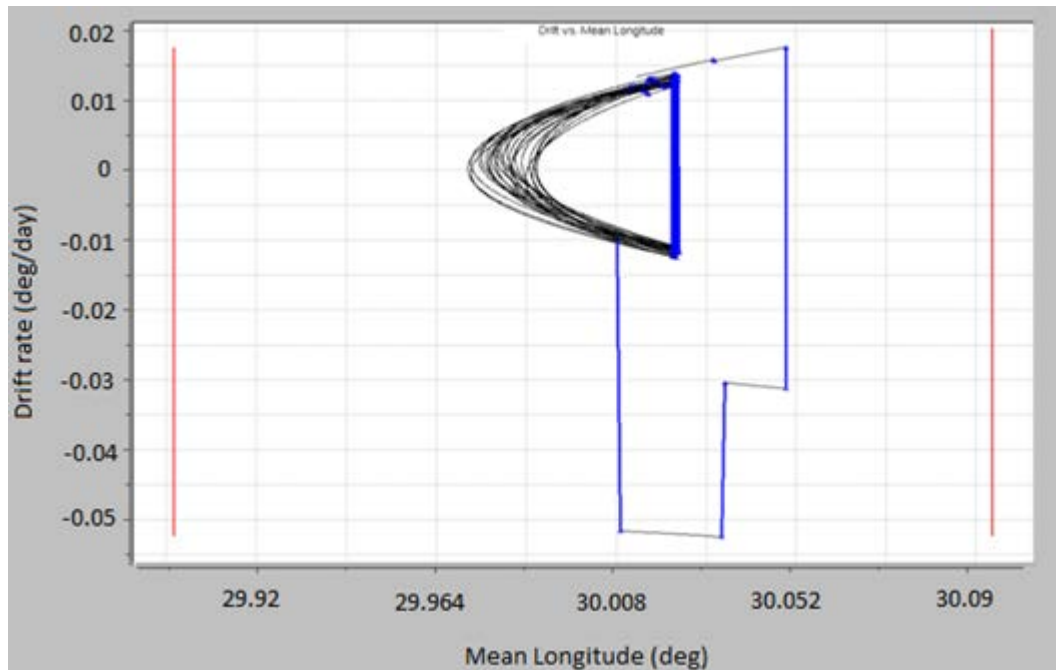


Figure 60- Three manoeuvres to reach the perfect point

Actually, the initial point cannot be placed anywhere; it must be close to the control window, because if it is really far from the control window the manoeuvre does not belong to the station keeping, it is a shift longitude. The time required to arrive at the longitude target only drifting is too much and the ΔV is also too big.

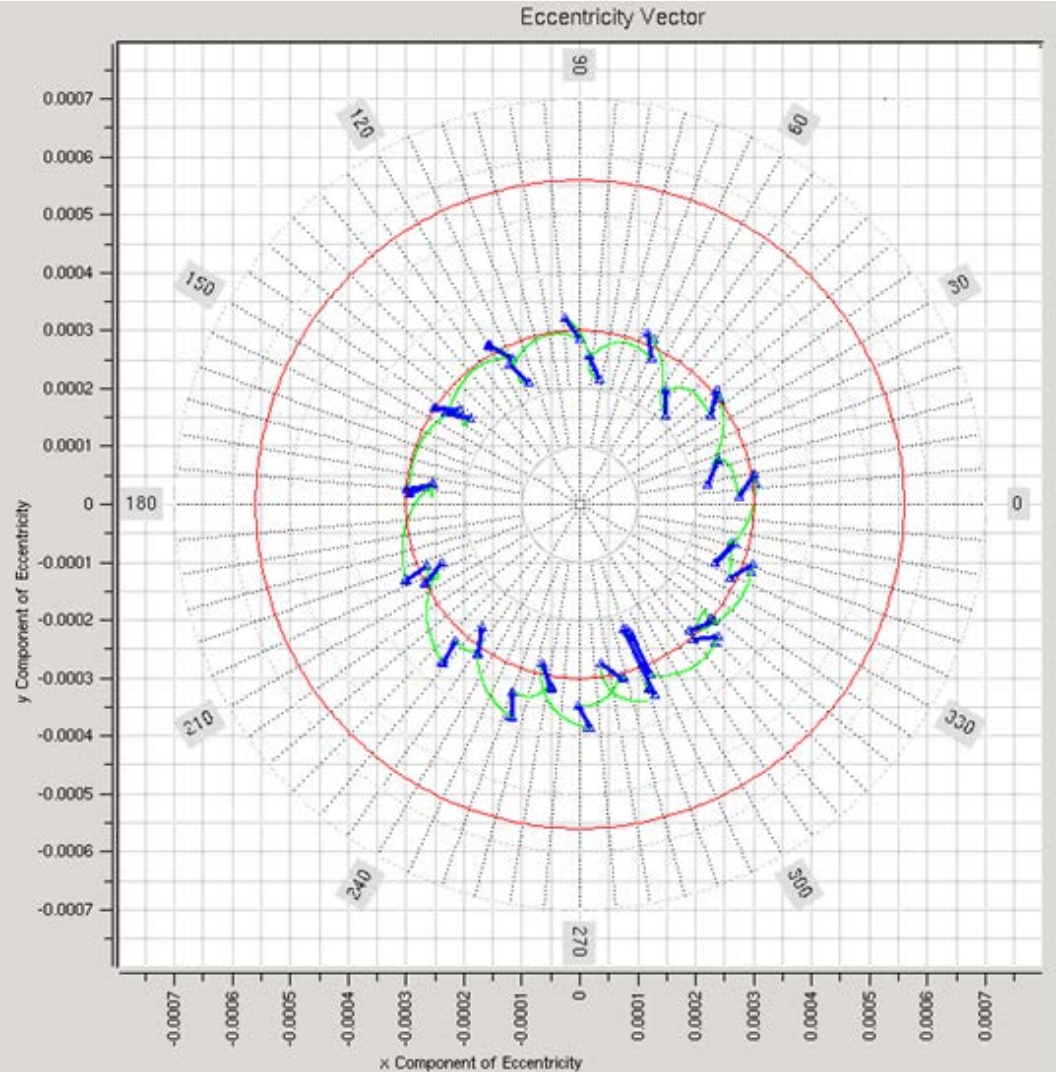


Figure 61- Eccentricity vector with three manoeuvres

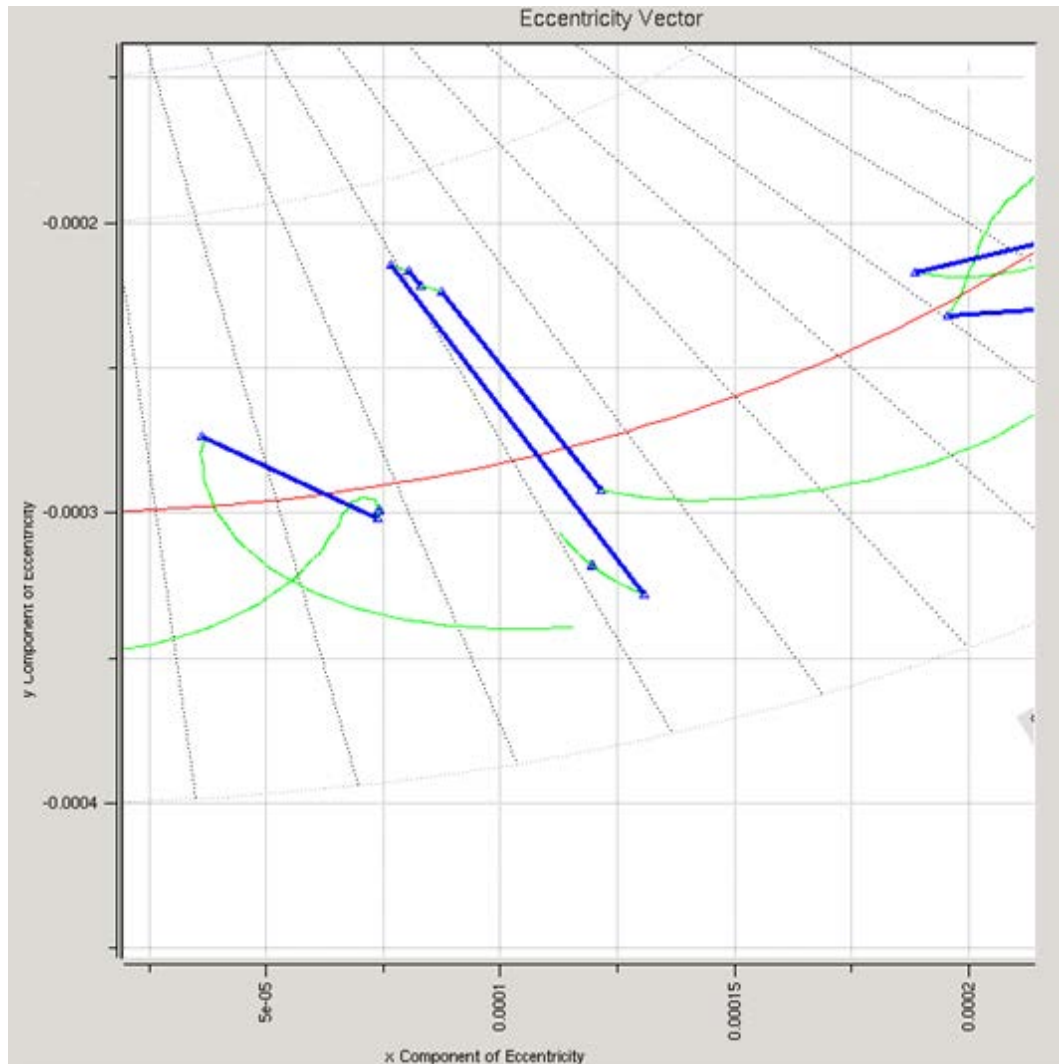


Figure 62-Zoom of the initial and final eccentricity vector

Figure 62 shows that the initial and the final eccentricity are approximately the same. Hence, the same strategy with only one burn could be applied the next year.

5. CROSS COUPLING CONTROL

Although the North/South station keeping is not studied, it is understood that a geostationary satellite will have North/South manoeuvres, and there will be a cross coupling component (tangential and radial) that will affect in the East/West direction.

Hence, cross-coupling effect means that the manoeuvres will not be considered as ideal manoeuvres. They will have components in the other directions, not only in the theoretical direction where the manoeuvre should be applied.

The aim of the cross-coupling control is to prove that the strategy is able to correct the manoeuvres even if the thrusters are not perfect. These effects are the consequence of diverse factors.

The typical configuration of thrusters consists in having two engines symmetrically positioned that theoretically would produce the same thrust each one. However, there are differences between both thrusters and they produce decompensated thrusts that have components in the other axis.

Another influence that produces cross-coupling is the effect called “**plume impingement**”. It is produced because the solar arrays are always pointing to the Sun and because of the obliquity of the ecliptic of 23.45° , the thrust that should be applied normal to the equator plane is disturbed by the solar arrays that are in the ecliptic plane.

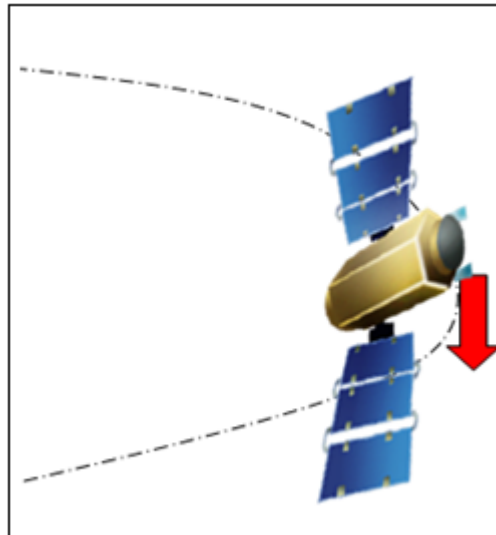


Figure 63- Interference between the thrust and the solar arrays

The cross-coupling affects to all the manoeuvres, but considering the cross-coupling of an East/West manoeuvre have no sense because normally the effect in the other components is around a 5% of the real manoeuvre. So, a 5% of a manoeuvre of 0.07m/s has no relevance.

The cross-coupling effect due to the inclination manoeuvres will be considered. Although this study does not take account the inclination manoeuvres, a typical value of an inclination manoeuvre ($\Delta V_i = 2\text{ m/s}$) will be applied two days before starting the control cycle. This the regular method applied in the inclination manoeuvres.

Inclination component	$\% \Delta V_i$	$\Delta V_{cross-coupling}(m/s)$
Radial component	2,5%	0,05
Tangential component	5,0%	0,1

Table - 5- Cross coupling effect

Although the cross-coupling is an attempt to simulate the reality, the percentages used above can vary according the satellite. Normally, a preliminary ground study must be done to estimate the percentages.

5.1. Results

As the components are previously known, the cross-coupling is considered as a perturbation which causes an instantaneous drift rate change.

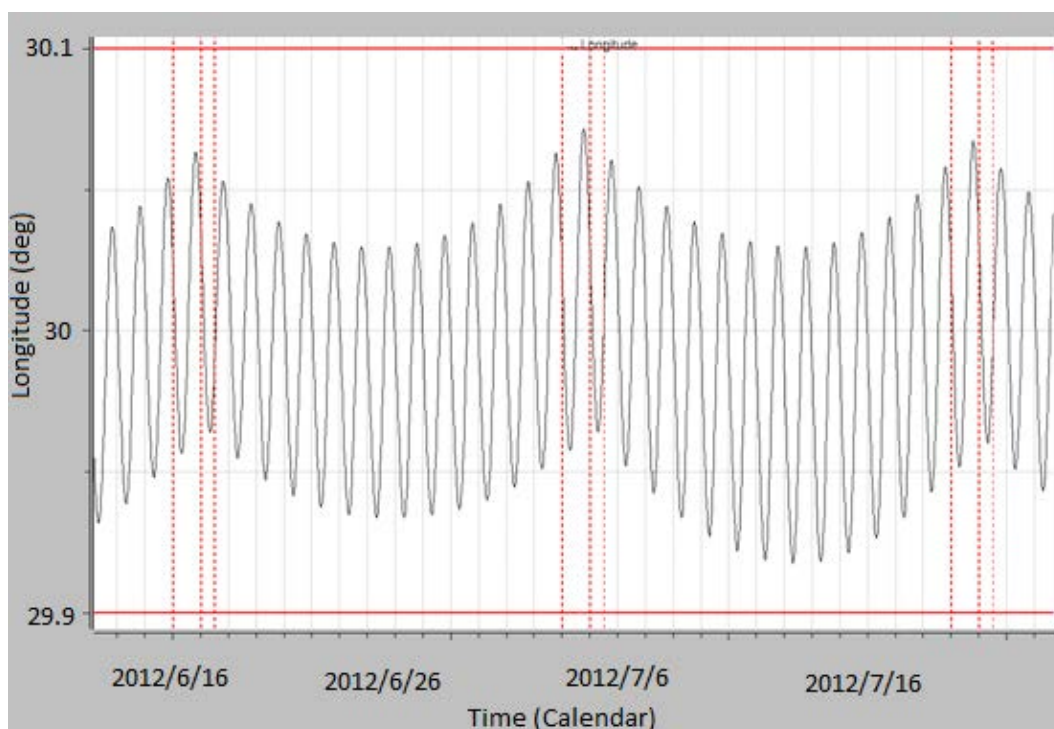


Figure 64- Longitude with cross-coupling effect

As the North/South manoeuvres take place 2 days before the control cycle, the longitude is not severely affected. The real longitude will always be confined inside the deadband. This is because the fact of having the longitude centred at the longitude window. If the real longitude was close to the boundary of the deadband, a small increment could take out the longitude from the deadband.

The North/South manoeuvres always take place at the same direction, for this reason, the longitude is slightly displaced to one side of the deadband.

The cross-coupling effect is more evident in the **figure 65**, because of the instantaneous change in the drift rate.

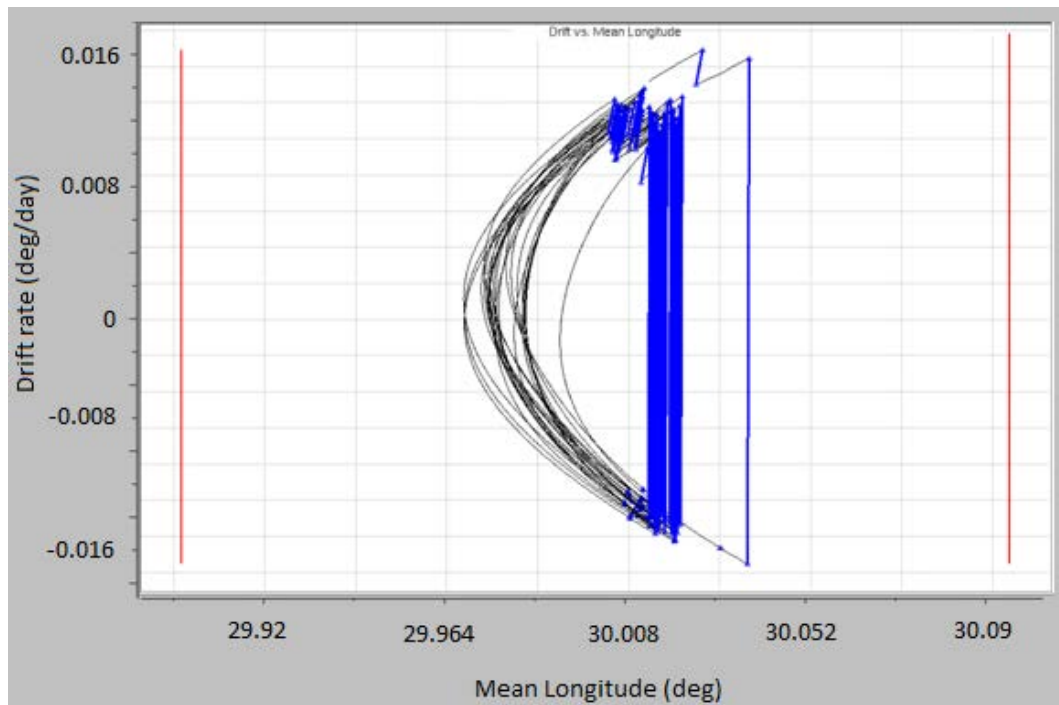


Figure 65- Drift rate vs mean longitude with cross-coupling effect

5.2. Final algorithm

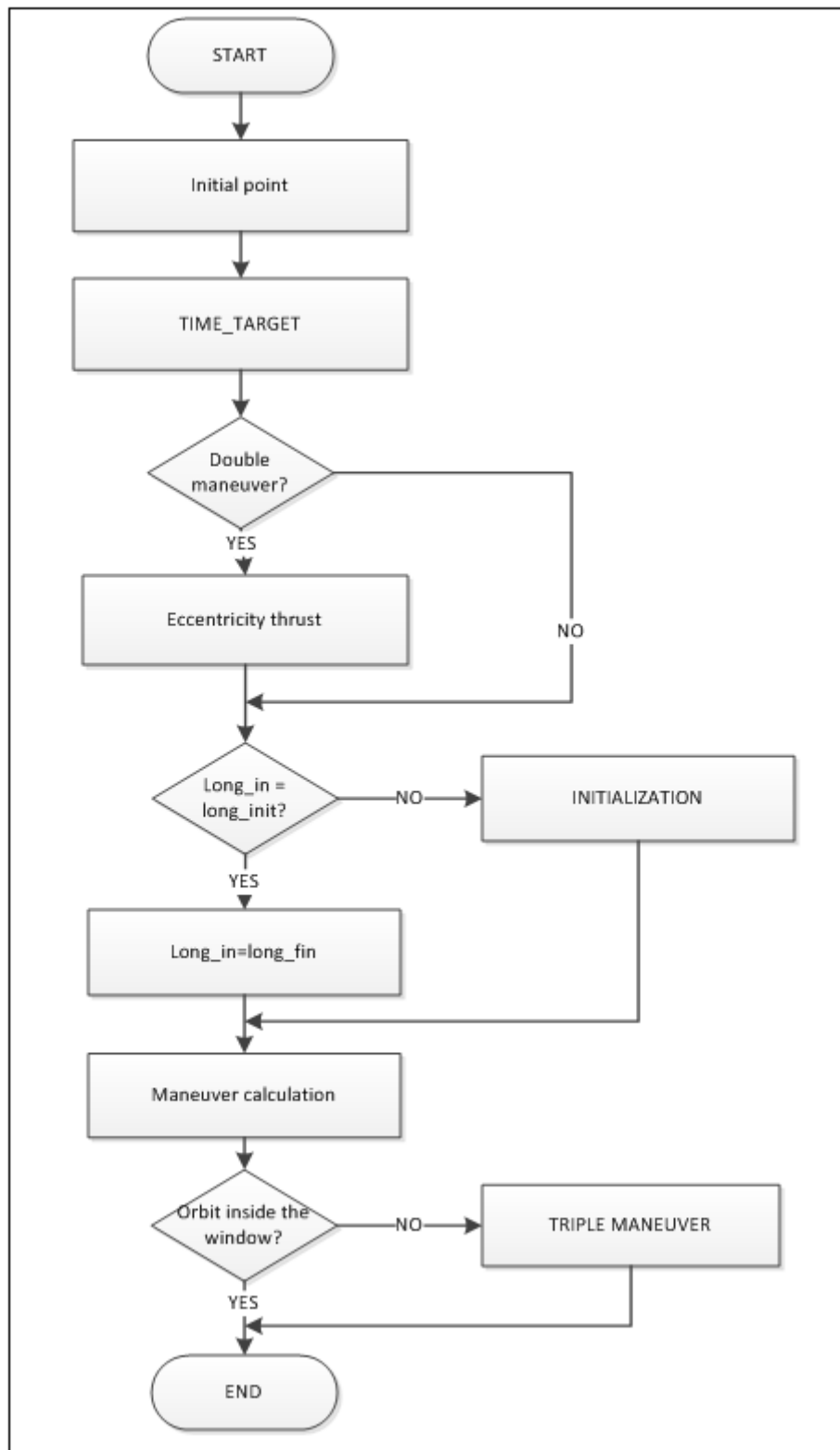


Diagram 8 – Final algorithm

6. PLANNING

This study has been realized in the company GMV Aerospace, so they had a planning ready for developing the code.

There have been tasks that have been delayed and tasks that have been realized before the required time.

Planning

	Duration	Start	Finish
Study of geostationary satellites	14 days	Wed 01/02/12	Mon 20/02/12
Introduction to the Focus environment	14 days	Wed 01/02/12	Mon 20/02/12
Development of longitude strategies	20 days	Tue 21/02/12	Sun 18/03/12
Implementation of longitude strategies	26 days	Mon 27/02/12	Sun 01/04/12
Longitude verification	3 days	Mon 02/04/12	Wed 04/04/12
Development of eccentricity strategies	12 days	Thu 05/04/12	Fri 20/04/12
Implementation of eccentricity strategies	13 days	Thu 05/04/12	Mon 23/04/12
Eccentricity verification	3 days	Tue 24/04/12	Thu 26/04/12
Implementation of double manoeuvre	7 days	Fri 27/04/12	Mon 07/05/12
Implementation of triple manoeuvre	11 days	Fri 27/04/12	Fri 11/05/12
Implementation of cross-coupling	12 days	Fri 27/04/12	Mon 14/05/12
Final conclusions	5 days	Tue 15/05/12	Mon 21/05/12

Table - 6- Planning

Reality tasks

	Duration	Start	Finish
Study of geostationary satellites	18 days	Wed 01/02/12	Fri 24/02/12
Introduction to the Focus environment	18 days	Wed 01/02/12	Fri 24/02/12
Development of longitude strategies	23 days	Mon 27/02/12	Wed 28/03/12
Implementation of longitude strategies	28 days	Fri 02/03/12	Tue 10/04/12
Longitude verification	3 days	Wed 11/04/12	Fri 13/04/12
Development of eccentricity strategies	12 days	Mon 16/04/12	Tue 01/05/12
Implementation of eccentricity strategies	15 days	Mon 16/04/12	Fri 04/05/12
Eccentricity verification	3 days	Mon 07/05/12	Wed 09/05/12
Implementation of double manoeuvre	7 days	Thu 10/05/12	Fri 18/05/12
Implementation of triple manoeuvre	11 days	Thu 10/05/12	Thu 24/05/12
Implementation of cross-coupling	12 days	Thu 10/05/12	Fri 25/05/12
Final conclusions	8 days	Sat 26/05/12	Mon 04/05/12
Revision	76 days	Thu 05/06/12	Tue 19/09/12

Table - 7- Reality tasks

Although in the planning was supposed that the study was presented in June, the report was not ready, so the rest 76 days were to write the report and verify that there were no errors in the code.

To do the planning more visual, a Gantt diagrams have been done for each planning.

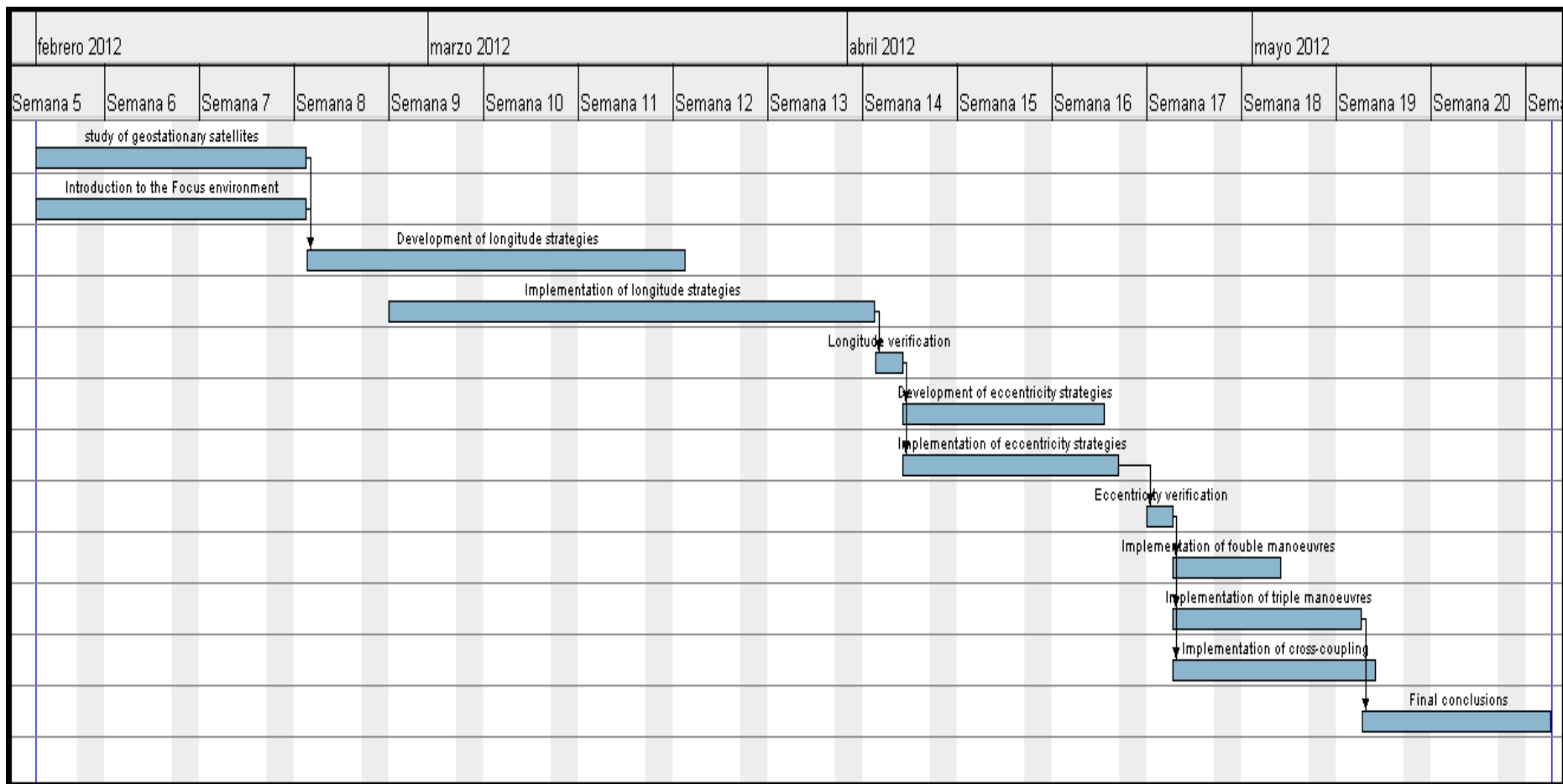


Figure 66- Gantt chart of the planning

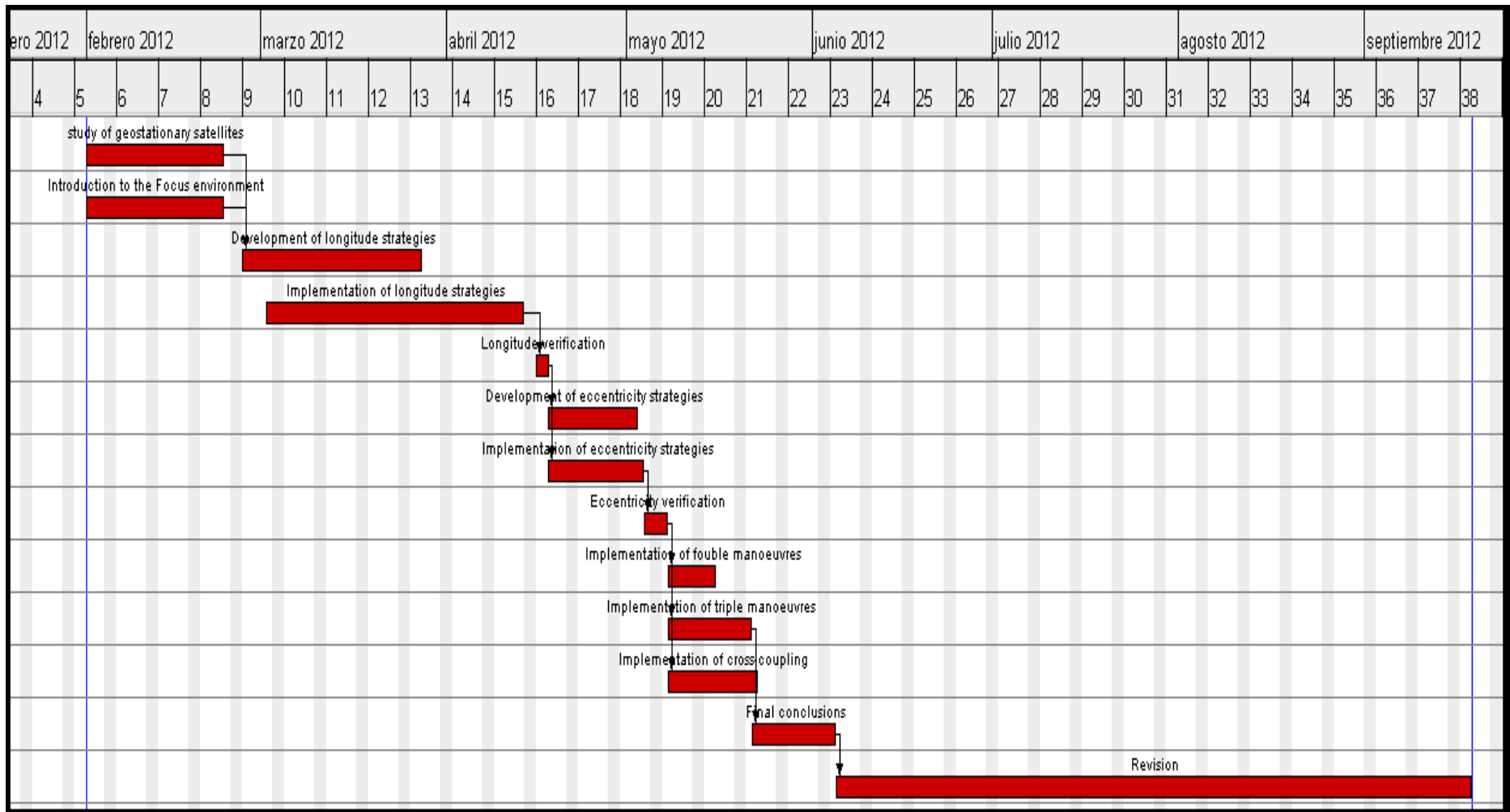


Figure 67- Gantt chart of the reality tasks

7. TECHNICAL AND ECONOMICAL VIABILITY OF THE PROPOSAL

The objective of this study was to create a code that implements the strategies preciously studied. These strategies have already been implemented in the software of GMV, **focusgeo**.

To calculate what benefits GMV could obtain from this code proves really difficult. In order to take part of the code of a product, the code should be normalized following and verified by the Operator with their satellite parameters.

Once the code is ready for sale, it is difficult to estimate the benefits of a part of one product.

8. LIFE CYCLE ENVIRONMENT EFFECT OF THE PROPOSAL

The fact of controlling the synchronous elements with a single E/W manoeuvre provides clear effects in the fuel consumption. Even through if the single thrust is big, controlling the satellite with a double or triple manoeuvre periodically means a fuel consumption of more than four times the consumption studied in this report.

Normally, station keeping software uses more than a single manoeuvre for controlling the longitude and eccentricity. This algorithm allows the control with only one.

9. CONCLUSIONS

Nowadays, the number of geostationary satellites in a single slot is increasing. Maintaining the satellites avoiding collision requires strategies that provide better solutions for any adversity. The deadbands are decreasing, and the accuracy must be better.

In order to assure the accuracy, the algorithm must be simple and fast, to do the control more automatic. For this reason, the number of manoeuvres is limited to a single manoeuvre, and the double and triple manoeuvres are only reserved for really special cases. Although the algorithm reserves the triple and double manoeuvre for when the satellite is far of the preestablished tolerance, the Operator could choose a double and a triple manoeuvre when he believes that is necessary.

Another point to be highlighted is the necessity of an algorithm that works for the whole range of longitudes. In this study, the equilibrium points represent the main problems, because they do not show the same proprieties as the other longitudes.

There have not been geostationary satellites placed in the equilibrium points, for this reason station keeping software has not been developed for these points. The fact of having an algorithm that works in all the longitude range will solve the problems for future missions.

In longitude control the proposed objectives have been accomplished. The strategy of longitude/drift control has been tested in all the adverse conditions, and it has been performed with success.

Even with cross-coupling, the longitude strategy has worked satisfactorily. The only problem is that the manoeuvres times must be scheduled and they must be taken into account in the computer process before the control cycle. In case that the manoeuvre times were unpredictable, the longitude/drift control would still work, but the accuracy obtained would degrade.

For this reason, it was important to find an eccentricity strategy in order to find another strategy that help not to lose accuracy in the longitude control. The fixed time was an idea that would facilitate the Operator work, because the operation day would be almost constant throughout a year, and an accurate schedule could be done.

Nevertheless, the algorithm should be tested in a real scenario when the errors would be greater because the satellite lifetime is around five years, whereas in this report, only one year has been considered.

To sum up, the final results obtained have been satisfactory. The code is ready for anyone who wants to implement any new feature or any improvement to the strategy, and add the N/S station keeping.

10. BIBLIOGRAPHY

10.1. Books

- [1] E.M. Soop., "Handbook of geostationary orbits" SPACE TECHNOLOGY LIBRARY Editorial Board (1994)
- [2] Larson W.J., "Space Mission Analysis and Design" 3th Microcosm Press (1992)
- [3] Agrawal B.N., "Design of Geosynchronous Spacecraft" Prentice Hall (1986)
- [4] Paluszek M., Bhatta P., Griesemer P., "Spacecraft attitude and orbit control" 2nd Ed. Princeton Satellite Systems (1996)
- [5] Mueller J. Brito M., "A Distributed Flight Software Design For Satellite Formation Flying Control," Proceedings of the AIAA Space 2003 Conference (2003)
- [6] David A. Vallado., "Fundamentals of astrodynamics and applications" 3th Ed. Microcosm Press (1997)
- [7] William M. Kaula., "Theory of satellite geodesy" 2nd Ed. Dover Publications (1966)
- [8] P.Legendre., "Analytical model of the evolution of orbit parameters of a quasi geostationary orbit" CNES (1999)
- [9] P.K. Seidelmann., "Report of the IAU Working Group on Cartographic Coordinates and Rotation Elements of the Planets and Satellites" (1982)
- [10] L.G. Taff., "Celestial mechanics" John Wiley (1985)

10.2. Websites

- [W1] Focugeo product. Last visit on May 2012
www.gmv.com/en/space/products/focusSuite/index.html
- [W2] Data from geostationary satellites. Last visit on April 2012
www.eutelsat.com/home/index.htm

11. ANNEXES

ANNEX A- Table of acceleration tesseral elements

$\ddot{\lambda}$ (0.001°/day ²)	0	1	2	3	4	5	6	7	8	9
1	0.65	0.70	0.76	0.81	0.87	0.92	0.97	1.02	1.07	1.12
2	1.17	1.21	1.26	1.30	1.34	1.38	1.42	1.46	1.50	1.53
3	1.56	1.59	1.62	1.65	1.67	1.70	1.72	1.73	1.75	1.76
4	1.77	1.78	1.79	1.79	1.80	1.80	1.79	1.79	1.78	1.77
5	1.76	1.74	1.72	1.70	1.68	1.65	1.63	1.60	1.56	1.53
6	1.49	1.45	1.41	1.37	1.32	1.27	1.22	1.17	1.12	1.06
7	1.01	0.95	0.89	0.82	0.76	0.80	0.61	0.56	0.50	0.43
8	0.36	0.29	0.22	0.14	0.07	0.00	-0.07	-0.15	-0.22	-0.29
9	-0.36	-0.44	-0.51	-0.58	-0.65	-0.72	-0.79	-0.85	-0.91	-0.99
10	-1.05	-1.11	-1.17	-1.23	-1.29	-1.35	-1.40	-1.45	-1.50	-1.55
11	-1.60	-1.64	-1.68	-1.72	-1.76	-1.79	-1.82	-1.85	-1.88	-1.90
12	-1.92	-1.94	-1.96	-1.97	-1.98	-1.99	-1.99	-2.00	-2.00	-1.99
13	-1.99	-1.98	-1.97	-1.95	-1.93	-1.92	-1.89	-1.87	-1.84	-1.81
14	-1.78	-1.75	-1.71	-1.67	-1.63	-1.59	-1.55	-1.50	-1.45	-1.40
15	-1.35	-1.30	-1.25	-1.19	-1.13	-1.08	-1.02	-0.96	-0.90	-0.83
16	-0.77	-0.71	-0.64	-0.58	-0.51	-0.45	-0.38	-0.32	-0.25	-0.19
17	-0.12	-0.06	0.01	0.07	0.14	0.20	0.26	0.33	0.39	0.45
18	0.51	0.57	0.62	0.68	0.74	0.79	0.84	0.89	0.94	0.99
19	1.04	1.09	1.13	1.17	1.21	1.25	1.29	1.33	1.36	1.39
20	1.42	1.45	1.48	1.50	1.53	1.55	1.56	1.58	1.60	1.61
21	1.62	1.63	1.64	1.64	1.65	1.65	1.65	1.64	1.64	1.63
22	1.63	1.62	1.60	1.59	1.58	1.56	1.54	1.52	1.50	1.48
23	1.45	1.43	1.40	1.37	1.34	1.31	1.27	1.24	1.21	1.17
24	1.13	1.09	1.05	1.01	0.97	0.93	0.89	0.94	0.80	0.75
25	0.71	0.66	0.62	0.57	0.52	0.47	0.43	0.38	0.33	0.28
26	0.23	0.18	0.14	0.09	0.04	-0.01	-0.06	-0.10	-0.15	-0.20
27	-0.24	-0.29	-0.34	-0.38	-0.43	-0.47	-0.51	-0.56	-0.60	-0.64
28	-0.68	-0.72	-0.76	-0.80	-0.83	-0.87	-0.91	-0.94	-0.97	-1.01
29	-1.04	-1.07	-1.10	-1.13	-1.15	-1.18	-1.20	-1.23	-1.25	-1.27
30	-1.29	-1.31	-1.33	-1.34	-1.36	-1.37	-1.38	-1.39	-1.40	-1.41
31	-1.42	-1.42	-1.42	-1.43	-1.43	-1.42	-1.42	-1.42	-1.40	-1.40
32	-1.40	-1.39	-1.37	-1.36	-1.35	-1.33	-1.31	-1.29	-1.27	-1.25
33	-1.22	-1.20	-1.17	-1.14	-1.11	-1.08	-1.05	-1.01	-0.98	-0.94
34	-0.90	-0.86	-0.82	-0.78	-0.74	-0.69	-0.64	-0.60	-0.55	-0.50
35	-0.45	-0.40	-0.35	-0.30	-0.24	-0.19	-0.14	-0.08	-0.03	0.03
36	0.09	0.14	0.20	0.25	0.31	0.37	0.42	0.48	0.54	0.59

Table - 8- Tangential acceleration due to tesseral Earth's terms.



Study of different strategies of control for geostationary satellites

BUDGET

by

Angel Frutos Jurado

September 2012

Tutors: Diogo Silva Ribeiro (GMV)

Roberto Maurice Flores Le Roux (ETSEIAT)

BUDGET

This is a software project, so the budget consists of the list below and the work hours.

Hardware	Computer	700 €
	Microsoft Office	500 €
Software	focus environment	0 €
Engineer salary	10 €/h (700h)	7.000 €
TOTAL		8.200,00 €